MOLECULAR INTERACTIONS BETWEEN '*CANDIDATUS* LIBERIBACTER SOLANACEARUM' AND THE POTATO PSYLLID, *BACTERICERA COCKERELLI*, AT THE GUT INTERFACE

A Dissertation

by

XIAOTIAN TANG

Submitted to the Office of Graduate and Professional Studies of
Texas A&M University
in partial fulfillment of the requirements for the degree of

DOCTOR OF PHILOSOPHY

Chair of Committee,	Cecilia Tamborindeguy
Committee Members,	Rodolfo Aramayo
	Patricia V. Pietrantonio
	Keyan Zhu-Salzman
Head of Department,	Pete Teel

May 2020

Major Subject: Entomology

ABSTRACT

'*Candidatus* Liberibacter solanacearum' (Lso), is an emerging and serious bacterial pathogen of solanaceous crops, and it can cause very damaging plant diseases (e.g., zebra chip in potatoes). Presently, two haplotypes of Lso (LsoA and LsoB) are present in North America; both are transmitted by potato psyllid, *Bactericera cockerelli* (Šulc), in a circulative and persistent manner. The psyllid gut is the first organ Lso encounters and could be a barrier for its transmission. However, the molecular mechanisms involved in Lso acquisition and transmission by the potato psyllid are largely unknown. This dissertation aims to understand the molecular interactions between Lso and the potato psyllid at the gut interface. First, the acquisition and transmission of LsoA or LsoB by potato psyllid were investigated. Second, I investigated the global transcriptional responses of the adult psyllid gut upon infection of the two Lso haplotypes using Illumina sequencing. Third, I explored whether any of these two Lso haplotypes triggered an apoptotic or autophagic response in the gut of the adult potato psyllid. The results indicated that LsoB relative abundance increased faster in the psyllid gut than that of LsoA, and LsoB had a shorter latent period than LsoA. In addition, the transcriptome analyses showed that each haplotype triggers a unique transcriptional response, with most of the distinct gene expression changes being elicited by the highly virulent LsoB. Furthermore, Lso might repress the apoptotic response in the adult psyllid gut by inducing the anti-apoptotic gene IAPP5.2 at the early stage of the infection, which may favor Lso acquisition and colonization of the psyllid gut cells. However, Lso might induce an

autophagic response in the adult psyllid gut since the majority of autophagy-related genes (ATGs) are sensitive and responsive to the exposure or infection of both LsoA and LsoB. Further investigation needs to be conducted to deepen the study of autophagic response of potato psyllid to Lso infection. This dissertation is therefore an important contribution to a mechanistic understanding of Lso transmission, provides insights into understanding the adaptive significance of the immune response and has the potential to create new approaches for disrupting Lso transmission.

ACKNOWLEDGEMENTS

I would like to thank my advisor, Dr. Cecilia Tamborindeguy for her support and mentorship during my Ph.D. studies. I also thank my committee members, Dr. Patricia V. Pietrantonio, Dr. Keyan Zhu-Salzman, and Dr. Rodolfo Aramayo for their guidance throughout my Ph.D. program.

Thanks to current and previous members of Dr. Tamborindeguy's lab that I overlapped with during my stay here: Dr. Julien Levy, Dr. Azucena Mendoza, Dr. Ordom Huot, Dr. Freddy Ibanez, Dr. Chloe Hawkings, Dr. Kyle Harrison, Dr. Angelica Tomilhero Frias, Dr. Zafarullah Khan, Kelsy Fortuna, Brenda Leal and Jesse Starkey. Many thanks for their encouragement and help.

I would also like to thank friends, colleagues, department faculty and staff for making my time at Texas A&M University a great experience.

Finally, I would like to thank my mother and father for their tremendous support through this long academic journey.

CONTRIBUTORS AND FUNDING SOURCES

Contributors

This work was supervised by a dissertation committee consisting of Professors Cecilia Tamborindeguy [advisor], Patricia V. Pietrantonio and Keyan Zhu-Salzman of the Department of Entomology, as well as Professor Rodolfo Aramayo of the Department of Biology.

All work for the dissertation was completed independently by the student, under the advisement of Dr. Cecilia Tamborindeguy of the Department of Entomology.

Funding sources

This work was supported by Texas A&M University and Texas A&M AgriLife Research (Controlling Exotic and Invasive Insect-Transmitted Pathogens) and Hatch project TEX0-1-9381 Accession Number 1015773. Xiaotian Tang received the Herb Dean ’40 Endowed Scholarship from the Department of Entomology at Texas A&M University.

TABLE OF CONTENTS

Page

LIST OF FIGURES

FIGURE Page

FIGURE Page

LIST OF TABLES

CHAPTER I

INTRODUCTION AND LITERATURE REVIEW

1.1 HEMIPTERANS AND THEIR ASSOCIATIONS WITH PLANT PATHOGENS

1.1.1 Overview of hemipterans and plant pathogens

Hemiptera is the fifth largest insect order after Coleoptera, Diptera, Hymenoptera, and Lepidoptera (Grimaldi et al., 2005). It is composed of three main suborders of Sternorrhyncha (e.g., whiteflies, aphids, mealybugs, and psyllids), Auchenorrhyncha (e.g., planthoppers, leafhoppers, and cicadas), and Heteroptera (e.g., stink bugs and bedbugs, Fig. 1.1) (Gullan & Cranston, 2014). Hemipteran insects are damaging pests because of their wide host range, rapid reproduction, and ability to transmit numerous pathogens as vectors.

Plant pathogens have evolved numerous strategies that enable their movement from plant to plant. One of the strategies is to exploit the feeding mechanisms of a diverse range of insect vector species. Hemipteran insects are by far the most important vectors of plant-infecting pathogens (Perilla-Henao & Casteel, 2016). Hemipteran insects are abundant and have evolved a diverse range of plant feeding and colonization strategies that enable pathogens including viruses and bacteria to adapt in various ways to utilize these herbivores as vectors for transmission (Orlovskis et al., 2015).

The transmission of plant viruses by insects was first described in 1920s. However, it was not until 1967 that insect transmission of plant bacterial pathogens was reported (Purcell, 1982). Aphids and whiteflies, both from the suborder Sternorrhyncha, are the

most important vectors of plant viruses, transmitting ~46% of the known plant-infecting viruses (Gilbertson et al., 2015; Hogenhout et al., 2008a). By contrast, psyllids, leafhoppers and planthoppers mainly transmit bacterial pathogens (Fig. 1.1).

In the past decades, plant disease outbreaks caused by viral and bacterial pathogens have posed serious threats to crop production and caused great economic losses all over the world. For example, a loss of around one billion dollars has been calculated due to one viral disease (tomato spotted wilt disease) collectively in tomato, pepper, peanut and tobacco crops globally in 1990s (Prins & Goldbach, 1998).

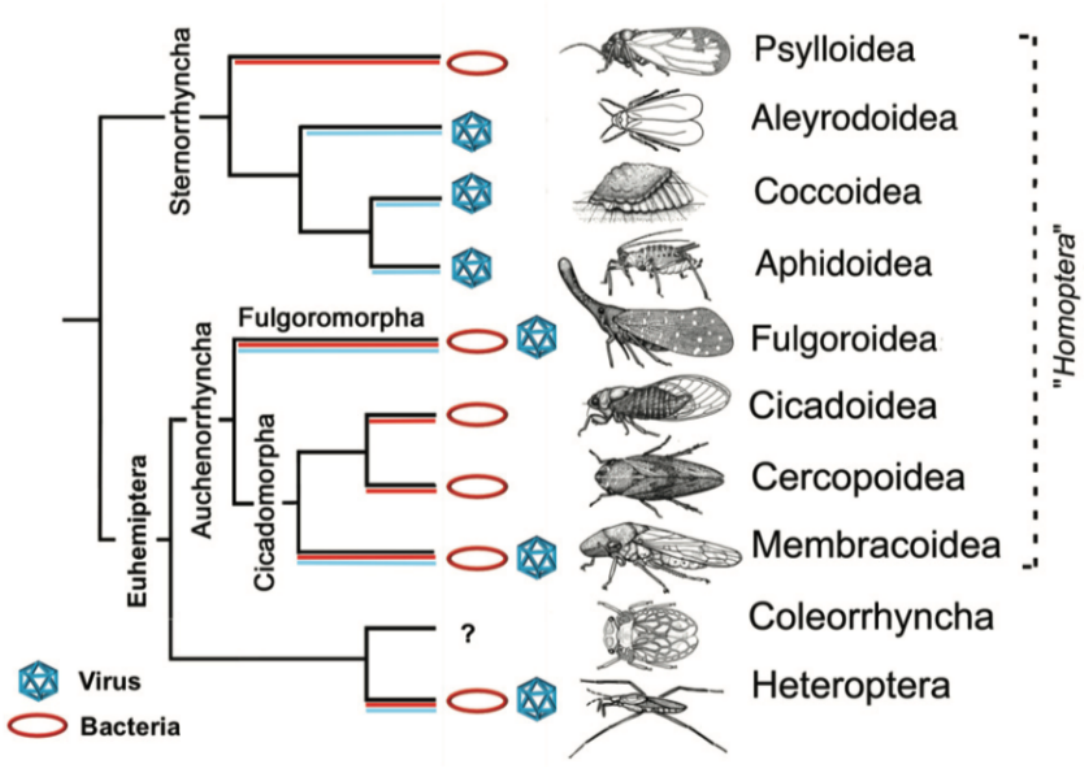

Figure 1.1 Hemiptera taxa: reported vectors and groups of plant pathogens. "Homoptera" in quotes refers to such previous classification of the groups encompassed by the dashed line. The image is reprinted from Gullan & Cranston (2014) and Perilla-Henao & Casteel (2016).

1.1.2 Vector-borne bacterial plant pathogens

In this review, I mainly summarize the interactions between bacterial plant pathogens and their hemipteran vectors. Recently, there has been a leap in our understanding of vector-borne bacterial plant pathogens due to devastating outbreaks of diseases such as citrus greening, Pierce's disease in vineards, and zebra chip in potatoes. Importantly, the emergence of vector-borne bacterial plant pathogens has recently become a major threat to food security. The current understanding of the pathogenicity mechanisms of vector-borne bacteria is largely influenced by our ability to culture those bacteria. To date only *Spiroplasma* spp. and the xylem-restricted *Xyllela fastidiosa* have been cultured *in vitro* and both require very specific conditions (Dourado et al., 2015; Renaudin et al., 2015). Because of this limitation, much of the biology and mechanisms of host colonization and transmission of other vector-borne plant bacterial pathogens are still largely unknown.

Phytoplasmas, spiroplasmas, and liberibacters are three well-known phloem-limited vector-borne bacteria groups. Phytoplasmas and spiroplasmas are plant pathogens of the class Mollicutes, which are cell wall-less obligate parasites that have evolved from Gram-positive bacteria (Gasparich, 2010). Liberibacters are Gram-negative bacteria that depend on psyllids for transmission (Tamborindeguy et al., 2017). All these phloem-limited vector-borne bacteria appear to colonize both the insect vector and the plant host intracellularly (Orlovskis et al., 2015).

Phytoplasma is a genus of the class Mollicutes and forms a large discrete monophyletic group with more than 30 *Candidatus* Phytoplasma species described. They

have a wide host range, infecting hundreds of different plant species worldwide including many economically important crops (Hogenhout et al., 2008b). Numerous plant diseases such as many different yellows, dwarf and witches' broom diseases are caused by phytoplasmas that are transmitted by leafhoppers and a few other hemipterans (Perilla-Henao & Casteel, 2016). Phytoplasmas encode translocase SecA protein, part of the secretion system for bacteria (Kakizawa et al., 2001). Proteins secreted through this secretion system are characterized by the presence of a signal peptide in their N-terminus which targets them for secretion. After the signal peptide is cleaved, the protein is released into the host environment where it can alter host functions and act as a virulence effector (Bai et al., 2009).

Spiroplasma is another genus of Mollicutes that contains vector-borne plant pathogens. In fact, only three *Spiroplasma* species are known to cause plant diseases and are transmitted by leafhoppers. The best studied species of spiroplasmas are *Spiroplasma citri*, the causative agent of citrus stubborn disease, and *S. kunkelii*, the causative agent of corn stunt disease (Bové et al., 2003; Carpane et al., 2013). After acquisition, spiroplasmas adhere to receptors in the lumen of the insect midgut, and probably enter the epithelial cell by receptor-mediated endocytosis (see below). Once in the gut cell, they migrate by intracellular vesicular transport towards the hemolymph, from where they eventually reach the salivary glands (Fletcher et al., 1998). Currently, the specific insect receptors and factors mediating the bacterial journey inside the vector remain unknown. However, several candidate proteins such as P58 and the plasmid-borne protein P32 have been identified (Wayadande & Fletcher, 1998).

Liberibacter bacteria have been associated mainly with psyllid vectors. In this review, I will focus on the associations and interactions between *Liberibacter* bacteria and psyllids (see below).

1.2 HEMIPTERAN TRANSMISSION OF PLANT PATHOGENS

1.2.1 Transmission mechanisms of plant pathogens

Transmission by insect vectors is critical for the infection cycle of a great number of plant pathogens. The transmission of plant pathogens by insect vectors involves a combination of coevolving biological traits of plant hosts, insect vectors and plant pathogens (Heck, 2018). In addition, the bacterial endosymbionts harbored by the insect vector can be involved also in the transmission mechanism in some cases. For example, the chaperonin GroEL protein of the secondary symbiont *Hamiltonella* in whitefly (biotype B) facilitates *Tomato yellow leaf curl virus* (TYLCV) transmission (Gottlieb et al., 2010).

There are three closely interrelated phases in the transmission of pathogens by vectors: acquisition, inoculation, and latent period. Acquisition access period (**AAP**) represents the length of time that a pathogen-free vector needs to have access to an infected source to acquire the pathogen. Inoculation access period (**IAP**) represents the length of time that a vector carrying a pathogen needs to have access to an uninfected host to inoculate the pathogen. **Latent period** is the time required between the pathogen is acquired and the vector is able to inoculate it.

The transmission of insect-borne plant pathogens can be classified as (1) non-persistent, (2) semi-persistent, (3) circulative and non-propagative, and (4) circulative and propagative (Fig. 1.2) (Dietzgen et al., 2016; Gray & Banerjee, 1999). Plant viruses usually exhibit one of the above four transmission mechanisms. For non-persistent viruses (e.g., *cucumber mosaic virus*, CMV), transmission can occur within minutes of acquiring the viral particles (virions) and particles are retained in the stylet or in the alimentary canal of the insect (Ng & Falk, 2006). For the majority of semi-persistent viruses (e.g., *cauliflower mosaic virus*, CaMV and *Lettuce infectious yellows virus*, LIYV), the retention of virions can last for days and the retention sites are found in the alimentary canal or gut lumen of the insect. Current evidence suggests that non-persistent and semi-persistent plant viruses can employ one of two mechanisms of transmission: capsid or helper strategy. In the capsid strategy, the virus coat protein interacts directly with binding sites (receptors) in the vector mouthparts, whereas additional nonstructural viral proteins, designated helper component (HC), are required in the helper strategy. The HC creates a reversible bridge between virus and vector (Froissart et al., 2002; Ng & Falk, 2006). Conversely, circulative viruses circulate through the body of the vector. In this case, the virus which is acquired from an infected host during feeding, is transported from the gut lumen into the hemocoel, and it circulates until it reaches the salivary gland. The virus is then transported through the salivary system and delivered to a new host during salivation. Circulative viruses can either circulate through the insect vector's body without replicating, those are referred to as non-propagative, or they can circulate and multiply within the insect vector, in which case their transmission is classified as propagative. Luteoviruses (e.g., *Barley*

yellow dwarf virus, BYDV) are an example of viruses transmitted by aphid vectors in a circulative and non-propagative manner (Gray & Gildow, 2003). However, only a few families of vector-borne plant viruses have propagative transmission within vectors, those include the families of *Rhabdoviridae* (e.g., rhabdoviruses), *Reoviridae* (e.g., reoviruses), and *Bunyaviridae* (e.g., tospoviruses) (Ammar et al., 2009; Hogenhout et al., 2008a; Whitfield et al., 2015).

Bacterial pathogens usually adopt a circulative and propagative transmission. Some exceptions, such as the vector-borne xylem specialist, *Xylella fastidiosa*, which is foregut-borne and has a semi-persistent association with its vectors (see below) exist (Hill & Purcell, 1995).

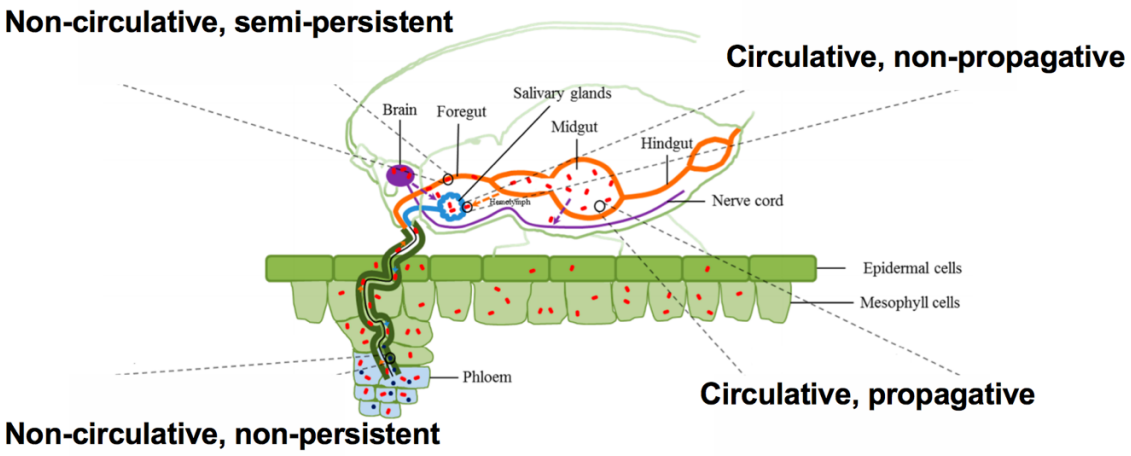

Figure 1.2 Four plant pathogen transmission strategies in insect vectors. The image is modified and reprinted from Dietzgen et al. (2016).

1.2.2 The gut as a barrier for pathogen transmission

The transmission of circulative pathogens by their insect vector requires specific interactions between pathogen and vector components which allow the pathogen to be transported across vector tissues. Those tissues are therefore considered potential transmission barriers. Four different barriers to successful infection or transmission of pathogens have been identified: (1) midgut infection barrier, (2) midgut escape barrier, (3) salivary gland infection barrier, and (4) salivary gland escape barrier (Agarwal et al., 2017). In this review, I mainly focus on the gut barriers.

After being acquired from infected plants, the circulative pathogens first must cross the vector gut. The gut is not only vital for biological process for insects, but also could be a barrier for pathogen transmission. Indeed, circulative transmitted pathogens must escape the insect gut and spread to neighboring organs for transmission. For example, viruses injected directly into the hemocoel are transmitted at higher rates than orally acquired viruses, because movement of the virus across the insect gut is often a significant barrier to transmission (Ammar & Hogenhout, 2008; Ammar et al., 2005). Therefore, the ability of the pathogen to cross and/or infect the gut from the alimentary canal into the hemocoel can determine its transmission efficiency.

The midgut of hemipterans is usually composed of a single layer of epithelial cells. It has been demonstrated that in general, viruses attach to receptors present on midgut or hindgut epithelial cells. In the case of luteoviruses, the transmission process usually involves receptor-mediated endocytosis (Gildow, 1993). Specifically, invaginated pits containing the virus bud into the cytoplasm forming ligand containing coated vesicles,

which migrate in the cytoplasm delivering the ligand (the virus) to a larger vesicle (called an endosome). The coated vesicle fuses with the endosome releasing the virus particle into the vesicle lumen. The viruses accumulate in the endosome and may be repackaged into tubular vesicles and delivered to the basal membrane, therefore releasing the virus into the aphid hemocoel (Gray & Gildow, 2003).

However, mechanisms involved in the transmission of plant bacterial pathogens are less well studied. Usually, intracellular bacteria are larger than viruses, and they are too large to be taken up by receptor-mediated endocytosis, and other mechanisms are involved in the bacterial entry into the eukaryotic cell. For example, some bacteria enter their mammal host intestinal cells through phagocytosis (Ribet & Cossart, 2015).

1.2.3 The immune responses of hemipterans and their roles in pathogen transmission

The innate immune response plays a key role in the defense against microbial infections and affects microbial transmission in invertebrates. Insects such as *Drosophila* rely on four major immune pathways: Toll, Immune deficiency (IMD), Janus Kinase and Signal Transducer and Activator of Transcription (JAK/STAT), and c-Jun N-terminal kinase (JNK) (Hoffmann & Reichhart, 2002; Leclerc & Reichhart, 2004). The Toll pathway is activated by the detection of fungi and Gram-positive lysine-type peptidoglycan (Lys-PGN)-containing bacteria by circulating receptors (e.g., PGRP-SA) (Michel et al., 2001), which then initiate a proteolytic cascade leading to the activation of the cytokine Spatzle (Spz) and its recognition by the receptor Toll (Valanne et al., 2011). The IMD pathway is activated following the detection of products from Gram-negative

bacteria diaminopimelic acid-type peptidoglycan (DAP-PGN) by the membrane-bound peptidoglycan recognition protein LC (PGRP-LC) (Myllymäki et al., 2014). The Toll and IMD pathways are responsible for the immune response that is mediated by the production of antimicrobial peptides (AMPs) (Charroux & Royet, 2010). These mechanisms are more or less conserved in other insects. Although the IMD pathway regulates immune responses in epithelia, hemocytes, and the fat body, supporting an important and ancestral role of this pathway in antimicrobial defenses (Buchon et al., 2009), the absence of the complete IMD pathway appears to be common in hemipterans, especially in phloem feeders. For example, the genome of pea aphid *Acyrthosiphon pisum* has been sequenced and shown to lack genes in the IMD pathway (Gerardo et al., 2010) (Fig. 1.3), and the IMD pathway gene transcripts were also not found in the transcriptome of the Asian citrus psyllid (*Diaphorina citri*) and potato psyllid (*Bactericera cockerelli*) (Kruse et al., 2017; Nachappa et al., 2012a).

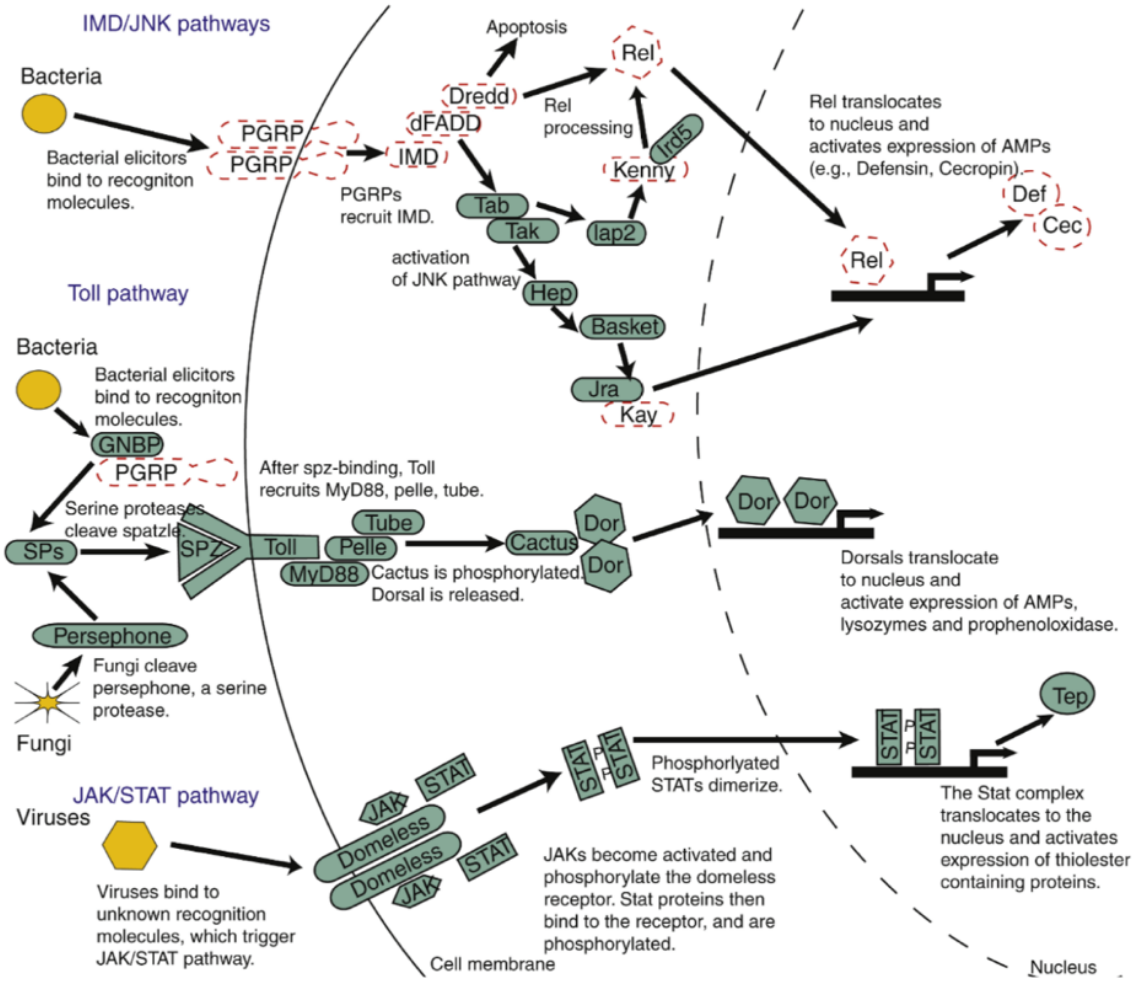

Figure 1.3 The immune pathways in pea aphid. Some key insect recognition, signaling and response genes (dashed lines) are missing in the pea aphid. The image is reprinted from Gerardo et al. (2010).

In addition, several genes thought central to arthropod innate immunity are missing in aphids and other hemipteran insects. For example, AMPs, which are mainly produced by the fat body and then secreted into the hemolymph, can destroy invading microbes by disrupting the microbial cell membranes, leading to cell lysis (Hoffmann & Reichhart, 2002). However, many of the AMPs (e.g., defensins) common to other insects appear to be missing in the pea aphid. In addition, PGRP, as one of the pathogen recognition

receptors (PRRs), mainly recognizes peptidoglycans present in cell walls of Gram-positive and Gram-negative bacteria. However, in contrast to other insects, the pea aphid appears to have no PGRPs. It seems that hemipteran insects (especially phloem feeders) might have a reduced immunity system compared to other insects (Gerardo et al., 2010). However, it cannot be excluded that these different components of the immune pathways are not missing, but rather that they were not identified, maybe because of sequence divergence between hemipterans and other well-studied insects or that the endosymbionts provide some of these components.

The RNA interference (RNAi) antiviral pathway, another immune pathway, may play a crucial role in controlling viral transmission by preventing the excessive accumulation of plant viruses in insect vectors, thereby protecting them from the negative impact of these viruses (Chen et al., 2016b). For example, knockdown of the expression of core components of the RNAi antiviral pathways Dicer2 and Argonaute2 reduced the survival rate and lifespan of white-backed planthopper (*Sogatella furcifera*) infected with *Southern rice black-streaked dwarf virus* (SRBSDV) (Lan et al., 2015).

Recently, it has been demonstrated that plant pathogens could induce or manipulate insect immunity, including programmed cell death (PCD) in the tissue cells (e.g., gut and salivary gland cells) of their vectors. Furthermore, the induced PCD plays a critical role in the regulation of transmission of plant pathogens. Indeed, PCD is known to play a major role in the development and/or the stress responses of organisms (Green, 2011; Hengartner, 2000). Two common types of PCD, apoptosis and autophagy, have been identified. These mechanisms are important components of an organism defense

because they can be used to destroy or neutralize pathogens. These mechanisms are particular important to destroy intracellular pathogens that depend on the host cell for their multiplication and survival. Generally, apoptosis is called "self-killing", and key regulators such as caspases, inhibitors of apoptosis (IAPs) and apoptosis-inducing factors (AIFs) play a central role in this process (Candé et al., 2002; Kornbluth & White, 2005). Autophagy is a cellular mechanism of "self-eating". Previous studies have identified series of autophagy-related genes (ATGs) that can regulate auto-phagosome formation and other functions (Klionsky et al., 2003). In most cases, there are interplays between the autophagy and apoptosis processes (Lalaoui et al., 2015; Marino et al., 2014). In insects, the PCD is not only vital to defend against pathogens (Clarke & Clem, 2003; Clem, 2005), but also is involved in the transmission efficiency of pathogens within their insect vectors. Indeed, these mechanisms could be triggered by the pathogens as a mechanism to exit specific cells. For example, apoptosis and autophagy have been shown to affect the efficiency of virus transmission in whiteflies, planthoppers and leafhoppers (Chen et al., 2017; Huang et al., 2015; Wang et al., 2016). For instance, Huang et al. (2015) found that *Rice ragged stunt virus* (RRSV) could induce apoptosis in the salivary glands of its insect vector, the brown planthopper (*Nilaparvata lugens*), and the induced apoptosis probably promotes the virus transmission. Interestingly, Chen et al. (2017) found that autophagy is induced by *Rice gall dwarf virus* (RGDV) in the intestine of its vector, the rice leafhopper (*Recilia dorsalis*); further investigation demonstrated that the activation of autophagy improves the transmission of RGDV, whereas inhibiting the autophagy pathway blocks viral transmission. In addition, TYLCV also activates the autophagy pathway in its vector,

the whitefly, and the induction of autophagy results in decreased transmission while the inhibition of this response facilitates virus transmission (Wang et al., 2016). Therefore, it is clear that different pathogens may elicit different responses in their vector, and whether those responses are to the advantage of the pathogen or the vector needs to be evaluated.

1.3 PSYLLIDS AND *LIBERIBACTER* BACTERIA

1.3.1 Overview of psyllid and *Liberibacter* bacteria

Several plant diseases previously thought to be caused by viruses, phytoplasmas or insect feeding damage have been found to be associated with species of phloem-limited, nonculturable, Gram-negative bacteria. These bacteria were named *Liberibacter* (Jagoueix et al., 1994), and include '*Candidatus* (*Ca*.) Liberibacter (L.) asiaticus' (CLas), '*Ca*. L. americanus' (CLam), '*Ca*. L. africanus' (CLaf), '*Ca*. L. europaeus', '*Ca*. L. brunswickensis', and '*Ca*. L. solanacearum' (Lso) (Tamborindeguy et al., 2017). In addition, there is another *Liberibacter* bacteria, *L. crescens*, which can be cultured *in vitro*, but it is not considered phytopathogenic and presently it is unknown if it is associated with insects (Leonard et al., 2012).

CLam, CLaf and CLas are causative agents associated with citrus greening disease, also referred as Huanglongbing (HLB) in different regions around the globe such as America, Africa and Asia. HLB is the most devastating disease of citrus. In Florida, HLB caused a total estimated loss of $4.5 billion between 2006 and 2011 (Hodges & Spreen, 2012). The above three *Liberibacter* bacteria are transmitted by *D. citri* (Asian citrus psyllid) in Asia and America, and *Trioza erytreae* (African citrus psyllid) in Africa.

Importantly, because the global distribution and catastrophic impact of Asian citrus psyllid and CLas on the citrus industry, CLas is the most studied *Liberibacter* pathogen.

Lso is phytopathogenic to members of the Apiaceae and Solanaceae plant families and also causes great economic loss in agriculture production. Presently, seven Lso haplotypes (LsoA, LsoB, LsoC, LsoD, LsoE, LsoF, and LsoU) have been identified in the world (Glynn et al., 2012; Haapalainen et al., 2018; Lin et al., 2012; Nelson et al., 2013; Swisher Grimm & Garczynski, 2019). Haplotypes LsoA and LsoB are transmitted by the potato psyllid (also known as tomato psyllid), *B. cockerelli*, and infect solanaceous plants (e.g., potato and tomato) in North America, while only haplotype A is present in New Zealand (Liefting et al., 2009a). These two haplotypes are associated with potato Zebra Chip (ZC) disease, which has been responsible for millions dollars of losses in potato producing regions (Munyaneza, 2012). LsoF was recently found in a symptomatic potato in the USA; however, it has not been determined yet whether this is a psyllid-borne pathogen. LsoC, LsoD and LsoE are transmitted by carrot psyllids, *T. apicalis* and *B. trigonica*, and infect some apiaceous crops (e.g., carrot and celery) in Europe, North Africa and Middle East (Alfaro-Fernández et al., 2012; Munyaneza et al., 2010; Tahzima et al., 2014; Teresani et al., 2014). LsoU was found in the psyllid *T. urticae* and the plant host stinging nettle, *Urtica dioica*.

1.3.2 Effects of *Liberibacter* bacteria on their vectors

Symbionts play a critical role in the physiology, ecology and evolution of a diverse range of insects. They can increase (mutualism), decrease (parasitism), or have no

influence (commensalism) on insect hosts fitness (Klepzig et al., 2009). Similarly, the presence of bacterial plant pathogens can have a positive, negative, or neutral impact on the vectors. The interaction between vector-borne plant pathogens and their vector should be under selection to influence the vector and result in enhanced transmission. This influence could be directly, after acquisition of the pathogen the fitness and/or behavior of the vector is modified, or indirectly, through modifications the host plant by the infection which enhance the vector fitness and/or modify its behavior (Eigenbrode et al., 2018). The Asian citrus psyllid nymphal developmental rate and adult survival are reduced in CLas-infected insects compared to uninfected. However, both the finite rate of population increase and net reproductive rate are greater among CLas-infected Asian citrus psyllids as compared with uninfected ones, indicating that the overall population fitness of infected psyllids is improved given the greater number of offspring produced (Pelz-Stelinski & Killiny, 2016). This may suggest that there may be a fitness trade-off in response to CLas infection. In addition, CLas-infected Asian citrus psyllids have increased propensity for dispersal as compared with uninfected psyllids (Martini et al., 2015). A beneficial effect of a plant pathogen on vector fitness may suggest that the pathogen developed a relationship with the insect before secondarily moving to plants (Pelz-Stelinski & Killiny, 2016). However, in potato psyllid, infection with either Lso haplotype LsoA or LsoB results in decreased potato psyllid fecundity, and infection with haplotype LsoB results in lower nymphal survival (Yao et al., 2016). Therefore, it appears that LsoB is more pathogenic than LsoA for the vector. Differences of pathogenicity of these two haplotypes in association with their host plants also exist, in association with tomato LsoB

is more pathogenic than LsoA (Mendoza Herrera et al., 2018). The effects of the other Lso haplotypes on the fitness of their psyllid vectors have not been determined yet.

1.3.3 Acquisition and transmission of *Liberibacter* bacteria

Acquisition and transmission of CLas by Asian citrus psyllids has been well determined. It is interesting that Asian citrus psyllid exhibits developmentally regulated vectoring efficiency. Specifically, Inoue et al. (2009) found that after adult psyllids fed on CLas-infected plants at 5-day intervals for a period of 20 days, the concentration of the bacterium did not increase significantly and the pathogen was not transmitted to any citrus seedlings. In contrast, when psyllids fed on infected plant as nymphs, the concentration of the pathogen significantly increased and CLas was successfully transmitted to 67% of citrus seedlings by emerging adults. This phenomenon was consistent with the observation from subsequent studies (Ammar et al., 2016; Canale et al., 2016; Pelz-Stelinski et al., 2010). For example, Ammar et al. (2016) observed that following 1- or 7-day acquisition access periods (AAPs) as nymphs, 49-59% of CLas-exposed psyllids became CLas-infected (qPCR-positive), whereas only 8-29% of the psyllids were infected following 1-14-day AAP as adults. Therefore, it seems that CLas titer increases at a much faster rate when the bacterium is acquired by nymphs compared to adults, and adults mainly transmit CLas if they acquired it as nymphs. Recent reports indicate that CLas induces apoptotic immune response in the gut of Asian citrus psyllid adults, while no evidence of apoptosis was found in the nymphal guts (Ghanim et al., 2016; Mann et al., 2018). Therefore, the induction of apoptosis in the gut of adults may lead to elimination of the pathogen from

the gut, which could be a factor explaining the developmental differences of CLas acquisition by the vector.

In contrast to CLas, potato psyllids can acquire and transmit Lso efficiently as both nymphs and adults, and in fact adults are more efficient vectors than nymphs. For example, Buchman et al. (2011) assessed the transmission efficiency of Lso and the inoculation access period (IAP), the time needed to inoculate the pathogen, required for potato psyllid nymphs and adults. They found that nymphs were less efficient than adults at transmitting Lso; in addition, exposure of a plant to 20 adult potato psyllids for a period as short as 1 h resulted in ZC symptom development. Furthermore, it was shown that a single adult potato psyllid was capable of inoculating Lso to potato plants within a period as short as 6 h. Sengoda et al. (2013) investigated Lso acquisition rate by adult psyllids following different AAPs on potato and tomato plants. They found that the increase of Lso titer in the insects reached a plateau after an average of 15 days following 24 and 72 h AAP on potato or tomato. In 2014, the same research group found that Lso relative abundances in psyllids peaked two weeks after the initial pathogen acquisition and psyllids were capable of transmitting Lso to non-infected host plants only after a two-week incubation period even with a short AAP of 24 h (Sengoda et al., 2014). However, all these studies utilized double infected (LsoA and LsoB) psyllids, and it remains to be investigated the acquisition or transmission of individual Lso haplotypes.

1.3.4 Genome and transcriptome of psyllid and *Liberibacter* bacteria

Approaches combining genomics, bioinformatics and transcriptomics have contributed to recent advances in the understanding of how bacterial pathogens colonize their host environments. Recently, genome sequencing of psyllids and *Liberibacter* bacteria has enabled a deeper understanding of their interactions. The genome of Asian citrus psyllid has been sequenced (Arp et al., 2016), and it suggested that this insect has a reduced immune capability, and the absence of immune-related genes from the Asian citrus psyllid genome may facilitate CLas infection. To date, the genome of potato psyllid, however, is not available. The complete genome sequences for several *Liberibacter* strains are available and both CLas and Lso genomes have been sequenced (Duan et al., 2009; Katsir et al., 2018; Kunta et al., 2017; Lin et al., 2011; Thompson et al., 2015). Overall, liberibacters have a small genome of around 1.2 Mb. Similar to phytoplasmas, they lack some of the genes responsible for the biosynthesis of amino acids, sugars, and nitrogenated bases, which implies that they obtain those metabolic products from their hosts (Thompson et al., 2015). Indeed, host dependence is likely a result of genome degradation, where essential biosynthetic pathways from the bacterial ancestor have been lost when the same resources can be obtained from the host environment (Lo et al., 2016). The comparison of the different Lso genome sequences available as well as of other liberibacters could help identify proteins present in all genomes that could be involved in the successful colonization of the host or the vector. Proteins only present in LsoA and LsoB compared to other Lso haplotypes could be involved in the host and vector specificity, while proteins that differ between the two haplotypes could be responsible for

the differences in symptomatology associated with these haplotypes. One potential contribution to differences in pathology between LsoA and LsoB is the presence of a shorter coding domain predicted to encode serralysin (hemolysin-related protein) in the LsoB genome compared with that in the LsoA genome; hemolysin-related protein is also required for virulence of animal pathogens (Ravindran et al., 2018; Thompson et al., 2015).

The fastidious nature of *Liberibacter* bacteria has hindered the study of the interactions with their psyllid hosts. However, RNA-seq or transcriptome provides a way to understand the interactions between liberibacters and psyllids and the strategies used by these pathogens to infect their vectors. In response to Lso infecting tomato, several genes involved in different metabolic processes were regulated in infected psyllids. Among those, were vitellogenin, heat shock proteins, phenoloxidase, as well as a few other genes involved in immune and stress response (Nachappa et al., 2012a). The Asian citrus psyllid expression profiles suggested the existence of a CLas-mediated alteration of the adult nutrition and metabolism, and of nymphal development and immunity (Vyas et al., 2015). Furthermore, CLas exposure resulted in changes in pathways involving the tricarboxylic acid cycle (TCA) cycle, iron metabolism, insecticide resistance and the insect's immune system in the psyllid gut (Kruse et al., 2017). Fisher et al. (2014) compared potato psyllid and Asian citrus psyllid transcripts in response to *Liberibacter* bacteria, and found that the responses of these two vectors to the respective *Liberibacter* infection was different. Specifically, the Asian citrus psyllid response was characterized by the regulation of a greater proportion of immune-related transcripts than the potato psyllid. In addition, a greater proportion of immune-related differentially expressed genes

were down-regulated in the Asian citrus psyllid than in the potato psyllid. As expected, the most expressed *Liberibacter* genes in association with the insect vector were cold and heat shock proteins, outer membrane protein, ferroxidase, GroES and hypothetical proteins (Ibanez et al., 2014b). In addition, differences in the expression of key candidate genes between LsoA and LsoB were found. Among the 16 putative type IV effector genes tested, four of them were differentially expressed between Lso haplotypes (Yao et al., 2016). Overall, the above transcriptome studies may provide evidence of conserved mechanisms in psyllid-*Liberibacter* interactions.

1.4 CONTROL OF *LIBERIBACTER* BACTERIA AND SIGNIFICANCE

Control of plant diseases caused by vector-borne pathogens commonly relies on chemical control of the insect vector populations. However, this strategy promotes the development of insecticide resistant insect populations and is not effective (Kanga et al., 2015; Prager et al., 2013). In most cases, insecticidal applications are not sufficient to control the spread of the pathogens and the associated diseases (Rivero et al., 2010). Furthermore, insect resistance and environmental regulations have limited the viability of long-term application of insecticides. Given the limited success of this classic strategy, novel approaches such as pathogen transmission disruption are urgently needed.

In regards to the control of diseases caused by *Liberibacter* bacteria, the major limitations to develop these novel strategies are the complexity of the pathosystems, the lack of fundamental knowledge of the biology of the vector and the fastidious nature of the pathogens. In particular, these limitations hamper our ability to study the mechanisms

involved in *Liberibacter* acquisition and transmission by the vector. In the absence of such knowledge, the development of effective transmission disruption strategies to help control these devastating diseases is impossible.

Increasing our understanding of the liberibacters circulative and propagative transmission pathway at the molecular and cellular levels is of interest to enable the discovery of psyllid-*Liberibacter* interactions that can be targeted using new technologies such as RNAi (Wuriyanghan & Falk, 2013; Wuriyanghan et al., 2011). Indeed, RNAi is very promising technology to block the transmission of vector-borne pathogens within vectors. But the first step towards the development of this strategy is to understand the biology and interactions between liberibacters and psyllids, and identify suitable and stable targets to manipulate.

In the potato psyllid and *Liberibacter* bacteria system, the psyllid gut represents the first barrier to transmission. Obviously, the ability of Lso to infect the gut or to cross from the alimentary canal into the hemocoel could determine its transmission efficiency. Thus, disruption of this process could be an effective way to control the spread of diseases. Therefore, in this study, my goal is to investigate the molecular interactions between the potato psyllid and Lso at the gut interface, and identify key factors and mechanisms underpinning the interactions between the vector and pathogen, so that sustainable control approaches for the damaging plant diseases caused by these pathogens based on the disruption of these interactions can be developed. Toward this end, I propose three objectives:

(1) Characterize the acquisition and transmission of Lso within the potato psyllid;

(2) Identify genes involved in the interactions between the potato psyllid gut and Lso based on transcriptome analyses and other molecular tools;

(3) Investigate the intracellular immune response (apoptosis and autophagy) of potato psyllids to Lso at the gut interface, and manipulate the immune response to inhibit the pathogen transmission in the laboratory.

This dissertation is therefore an important contribution to a mechanistic understanding of Lso transmission. It provides insights into understanding the adaptive significance of the immune response and has the potential to create new approaches for disrupting Lso transmission.

CHAPTER II

ACQUISITION AND TRANSMISSION OF TWO '*CANDIDATUS* LIBERIBACTER SOLANACEARUM' HAPLOTYPES BY THE POTATO PSYLLID *BACTERICERA COCKERELLI*

2.1 INTRODUCTION

'*Candidatus* Liberibacter solanacearum' (Lso) is a phloem-limited, Gram-negative and unculturable bacterium associated with severe plant diseases. To date, seven haplotypes (LsoA, LsoB, LsoC, LsoD, LsoE, LsoF, and LsoU) of this pathogen have been identified (Glynn et al., 2012; Haapalainen, 2014; Lin et al., 2012; Nelson et al., 2013; Swisher Grimm & Garczynski, 2019). Haplotypes A and B infect solanaceous crops in North America and cause damaging diseases such as zebra chip in potatoes (Liefting et al., 2009a; Tamborindeguy et al., 2017). These two haplotypes are transmitted by the potato psyllid (also known as the tomato psyllid), *Bactericera cockerelli* (Šulc) (Hemiptera: Triozidae). Currently, the major control strategy deployed to control Lso is the use of pesticides to control the psyllid vector populations because no commercially acceptable genetic resistance has been identified in the affected crops. However, the success of this strategy is limited and novel control approaches such as pathogen transmission disruption are urgently needed. The major limitations to develop these novel strategies are the complexity of the pathogen-vector systems, the lack of fundamental knowledge of the vector biology, and the fastidious nature of the pathogens.

Lso is transmitted by psyllids in a circulative and propagative manner (Cicero et al., 2017; Cooper et al., 2014; Sengoda et al., 2013; Sengoda et al., 2014). Therefore, the gut is the first psyllid organ that the bacterial pathogen colonizes. The gut is indeed the first organ involved in pathogen transmission, and therefore provides an essential link for understanding the biology of Lso acquisition or transmission within the potato psyllid. More importantly, a gut barrier is a promising way to disrupt Lso transmission. However, little is known about the acquisition or transmission of Lso at the gut interface.

Some studies focused on Lso acquisition and transmission by the potato psyllid. For example, the transmission efficiency of Lso and the inoculation access period (IAP), the time needed to inoculate the pathogen, required for potato psyllid nymphs and adults to inoculate potato plants were assessed (Buchman et al., 2011). It was found that nymphs were less efficient than adults at transmitting Lso; in addition, exposure of a plant to 20 adult infected potato psyllids for a period as short as 1 h resulted in zebra chip symptom development in potatoes. It was also shown that a single potato psyllid adult was capable of inoculating Lso to potato plants within a period as short as 6 h. Lso acquisition rate by adult psyllids following different acquisition access periods (AAPs) on potato and tomato plants was also investigated (Sengoda et al., 2013). It was determined that the increase of Lso titer in whole insects reached a plateau after an average of 15 days following 24- and 72-h AAPs on potato or tomato. Later, the same research group found that Lso relative abundances in adult psyllids peaked two weeks after the initial pathogen acquisition, and psyllids were capable of transmitting Lso to non-infected host plants only after a two-week incubation period even with a short AAP of 24 h (Sengoda et al., 2014).

However, the main limitation of the studies described above is that they were carried out using double infected (LsoA and LsoB) psyllids, and importantly, distinct acquisition or transmission profiles could exist between the Lso haplotypes A and B. Indeed, results from our previous studies indicate that there are differences of pathogenicity between these two haplotypes in association with their host plants and insect vector, in all cases LsoB was found to be more pathogenic (Harrison et al., 2019; Mendoza Herrera et al., 2018; Yao et al., 2016).

Therefore, it is imperative to understand the biology and mode of acquisition and transmission of these two haplotypes by their psyllid vector. In the present study, our primary goal was to investigate the acquisition and transmission of Lso haplotype A and haplotype B by potato psyllids. Toward this end, first, the accumulation of LsoA and LsoB in the gut of adult psyllids over time was quantified by quantitative real-time PCR (qPCR) and observed by immunolocalization. Second, we determined the transmission rate of each Lso haplotype and their respective latent periods. Therefore, in this study we assessed whether differences in the acquisition, latent period (the time between acquiring being able to transmit a pathogen) or transmission efficiency between the two Lso haplotypes existed. The data from this study will be the foundation to investigate the molecular interactions that occur between the insect vector and the bacterial pathogen during acquisition resulting in the development of novel strategies to disrupt Lso transmission.

2.2 MATERIALS AND METHODS

2.2.1 Insect colonies and tomato plants

Lso-free, LsoA-, and LsoB-infected psyllid colonies (psyllids of western haplotype) were maintained separately on tomato plants in insect cages (24 × 13.5 × 13.5 cm, BioQuip®, Compton, CA) at room temperature 24 ± 1°C and photoperiod of 16: 8 h (L: D) (Nachappa et al., 2012b).

To obtain Lso-infected tomato plants, tomato plants of the variety "Moneymaker", were grown from seeds (Victory seed company, Molalla, OR). Six-week-old tomato plants were infected as described previously (Nachappa et al., 2014) using three male psyllids harboring LsoA or LsoB, respectively. After one week, all psyllids were removed from the tomato plants. Three weeks after Lso inoculation, the plants were tested for Lso infection using the LsoF/OI2 primers (Li et al., 2009) and the Lso haplotype in the plants was confirmed using the Lso SSR-1 primers (Lin et al., 2012).

2.2.2 Psyllid exposure to Lso and gut dissection

Young Lso-free adult psyllids (less than 7 days old) were transferred to LsoA- or LsoB-infected tomato plants. To minimize the effect of differences in Lso titer within infected plants (Mendoza Herrera et al., 2018), the adult psyllids were caged on leaves at the same level of the tomato plants using organza bags. Fifty insects were collected every two days in order to obtain 2-, 4-, 6-, 8-, 10-, 12-, 14-, and 16-day Lso-exposed psyllids. The experiments were stopped after 16 days of AAP because adult potato psyllids live on average one month and high mortality of psyllids started to be observed.

Guts from the LsoA- or LsoB-exposed psyllids were dissected under the dissecting microscope (Ibanez et al., 2014a). DNA from pools of 50 guts was purified following the protocol of blood/tissue DNA extraction kit (Qiagen, Hilden, Germany); each pool was used as an individual template for qPCR analysis. Thus, each pool of 50 guts represented one replicate, and there were three replicates for each combination of exposure time point and haplotype. Each replicate was obtained by using independent LsoA- or LsoB-infected plants as Lso inoculum. All the experiments were conducted at 24 ± 1°C.

2.2.3 Quantification of Lso

The Lso 16S rDNA specific primers (LsoF: 5'-CGAGCGCTTATTTTTAATAGGAGC-3' and HLBR: 5'-GCGTTATCCCGTAGAAAAAGGTAG-3') (Li et al., 2009; Li et al., 2006) were used for Lso quantification in the guts of adult psyllids, and the psyllid 28S rDNA primers (28S rDNAF: 5'-AGTTTCGTGTCGGGTGGAC -3' and 28S rDNAR: 5'-AACATCACGCCCGAAGAC-3') (Nachappa et al., 2014) were used as internal control. qPCR was performed using SYBR Green Supermix Kit (Bioline, Taunton, MA) according to manufacturer's instructions. Each reaction contained 25 ng of DNA, 250 nM of each primer, and 1X of SYBR Green Master Mix; the volume was adjusted with nuclease-free water to 10 µL. The qPCR program was 95 °C for 2 min followed by 40 cycles at 95 °C for 5 sec and 60 °C for 30 sec. The qPCR assays were performed using a QuantStudio™ 6 Flex Real-Time PCR System (Applied Biosystems, Foster City, CA). Reactions for all samples were performed in triplicates with a negative control in each run. In order to

standardize the amount of Lso in psyllid guts, data are reported as delta Ct = (Ct of Lso gene) - (Ct of psyllid 28S gene). The biological replicates were analyzed and the average delta Ct value was used to quantify the levels of Lso. A standard curve was prepared for quantification of Lso in psyllid guts using a plasmid containing the Lso 16S rDNA target. For the standard curve, 10-fold serial dilutions of the plasmid were performed. The procedure for the standard curve preparation and the calculations of molecules (relative abundances) followed the methods described in Levy et al. (2011) and Nachappa et al. (2014). The Lso relative abundance in each sample was estimated by comparing delta Ct values of each sample to the standard curve.

2.2.4 Immunolocalization of Lso in psyllid guts

Immunolocalization was used to visualize Lso in the Lso-exposed psyllid gut tissues. The psyllid guts were dissected in 1X phosphate buffered saline (PBS) (Sigma-Aldrich, St. Louis, MO) from adults at four-day-infection intervals. Then, the guts were fixed in 4% paraformaldehyde for 30 min at room temperature. After fixation, the guts were incubated with Sudan Black B (SBB) (Sigma-Aldrich) for 20 min to quench autofluorescence as described in Tang et al. (2019). Next, the guts were permeabilized by adding 0.1% Triton X-100 (Calbiochem/EMD Chemicals, Gibbstown, NJ) for 30 min at room temperature, and washed three times with PBS containing 0.05% Tween 20 (PBST) prior to a 1-h blocking incubation at room temperature with blocking buffer (PBST with 1% [w/v] bovine serum albumin). Lso immunolocalization was performed using a rabbit-derived polyclonal antibody (GenScript Corp, Piscataway, NJ) directed against Lso OMP-

B (Ab-OMP-B) which detects both Lso haplotypes (Tang & Tamborindeguy, 2019). The guts were incubated with the antibody (diluted 1: 500) overnight at 4 °C. The guts were then washed three times with PBST and incubated with an Alexa Fluor 594 goat anti-rabbit IgG secondary antibody (diluted 1: 2000; Invitrogen, Carlsbad, CA) for 1 h at room temperature. The guts were washed again three times with PBST, and mounted with one drop of Vectashield mounting medium with 4′,6-diamidino-2-phenylindole (Vector Laboratories Inc., Burlingame, CA) on a microscope slide. The slide was covered with a glass coverslip and sealed with nail polish. The guts were examined using Axioimager A1 microscope (Carl Zeiss microimaging, Thornwood, NY, USA) and the images were collected and analyzed with the Axiovision Release 4.8 software (Carl Zeiss).

2.2.5 Lso transmission assay

Fifty young adult psyllids were exposed to LsoA- or LsoB-infected plants for a 7-day AAP as described above. Then, groups of five LsoA- or LsoB- exposed psyllids were transferred to ten four-week-old non-infected recipient tomato plants for a 10-day IAP. Then every four days, the same batch of LsoA- or LsoB-exposed psyllids were continuously transferred to new set of ten non-infected recipient tomato plants. In total, four rounds of transfer were conducted. As a positive control, we also transferred adult psyllids from the LsoA- or LsoB-infected colonies, which acquire Lso as nymphs, to six four-week-old non-infected recipient tomato plants. Four weeks after the end of the IAP, the plants were tested for Lso infection as described above. The transmission assays were performed three times.

2.2.6 Data analysis

The data were analyzed using spss statistical software (IBM SPSS Statistics V22.0) and R (https://www.r-project.org/). For analysis of Lso relative abundance in the gut of psyllid, the raw data were first log10-transformed and analyzed using a two-way ANOVA with Tukey's *post hoc* test. Homogeneity of variance was assessed with the Levene's Test, residuals normal distribution was tested by Shapiro-Wilk normality test. The comparison of percentage of infected plants were determined with Chi-square test.

2.3 RESULTS AND DISCUSSION

2.3.1 LsoA and LsoB quantification in the gut of adult psyllid

Previously, differences in the interaction of LsoA and LsoB with the potato psyllid were reported (Yao et al., 2016). However, the transmission cycles of the different haplotypes were not compared. The psyllid gut is the first organ Lso encounter once ingested from an infected plant. Therefore, colonization of this organ is essential for Lso transmission by the psyllid vector. We first examined the acquisition of Lso haplotypes A and B by adult potato psyllids at the gut interface.

Quantification of each Lso haplotype following different exposure times to infected plants revealed that both LsoA and LsoB populations increased regularly in the potato psyllid guts, albeit at different rates. LsoA and LsoB were detectable by qPCR in the gut of adult potato psyllids after a 2-day AAP (Fig. 2.1). LsoB titer increased rapidly; there were an average of 99,205 equivalent genomes after six days of AAP, and on average a maximum of 326,214 equivalent genomes was reached after 14 days of AAP. There

were significantly more LsoB equivalent genomes after 8 days of AAP than after a 2- or 4-day AAP ($P < 0.05$). In contrast, the increase in LsoA relative abundance was slower, reaching on average a maximum of 135,328 equivalent genomes after 16 days of AAP. After 12 days of AAP, there were significantly more LsoA bacteria than after a 2- or 4-day AAP ($P < 0.05$). In addition, between 4- and 10-day AAP, there were significantly more LsoB equivalent genomes than LsoA ($P < 0.05$), while after 12-day AAP, there is no significance difference between them ($P > 0.05$). However, we observed that until a 12-day AAP, LsoA had the similar relative abundances with LsoB at day4. Therefore, it is likely that there is an approximately 8 day-lag for LsoA accumulation in the gut of the potato psyllid compared to LsoB.

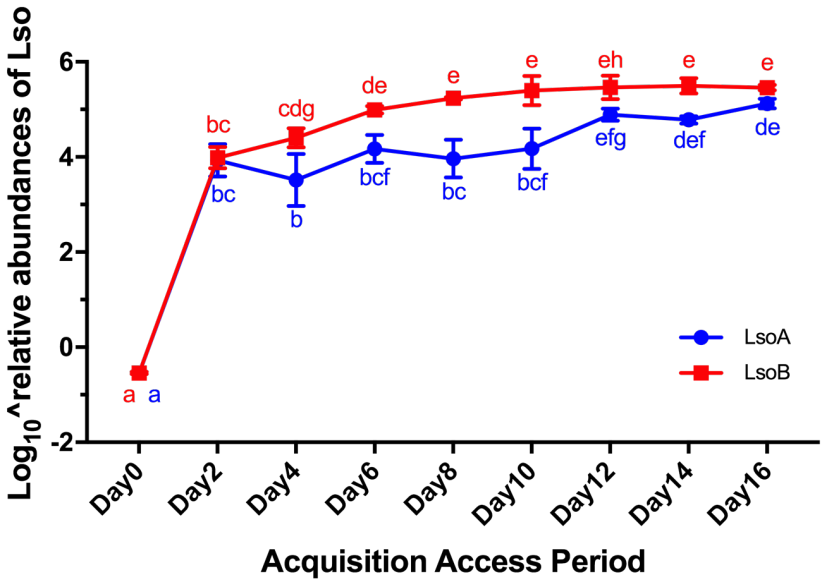

Figure 2.1 Quantification analysis of Lso relative abundance in the gut of potato psyllids following Lso acquisition. LsoA (blue) and LsoB (red) titer in pools of 50 guts following a 0- to 16-day acquisition access period (AAP). Data represent means ± SD of three independent experiments. Different letters indicate statistical differences at $P < 0.05$ using two-way ANOVA with Tukey's *post hoc* test.

Immunofluorescence of Lso further confirmed the progressive accumulation of the bacteria in the gut. In accordance with the quantification analysis by qPCR, weak LsoA-derived signal was observed in the psyllid gut within ten days of AAP (Figs. 2.2 A1 to C2), while more LsoA-derived signal was observed after 14 days of AAP (Fig. 2.2 D1 and D2). A greater amount of LsoB-derived signal was observed shortly after the beginning of the AAP, although the signal was low until six days of AAP (Figs. 2.2 A3 to B4). However, the LsoB-derived signal was strong and more widespread after ten days of AAP (Figs. 2.2 C3 and D4). Therefore, although both Lso haplotypes A and B are transmitted by the same vector, distinct acquisition profiles were identified in the gut of adult potato psyllids.

Overall, the infection of the adult gut by LsoA or LsoB can be divided into two stages. LsoB titer in the gut of psyllids increases rapidly and plateaus after 6 days, while LsoA accumulation is slower between days 2 and 12. Overall, these findings are consistent with the previous report (Sengoda et al., 2014), which determined that the relative abundances of Lso (co-infections of LsoA and LsoB) in psyllids increased from week 0 to week 2 of the incubation period before reaching a plateau. In addition, similar propagative accumulation patterns have been reported in other plant-pathogen-insect systems; for instance, the *Rice gall dwarf virus* (RGDV) exhibits a progressive accumulation in the gut of the rice leafhopper *Recilia dorsalis* with a peak around 12 days following the initial infection (Chen et al., 2017).

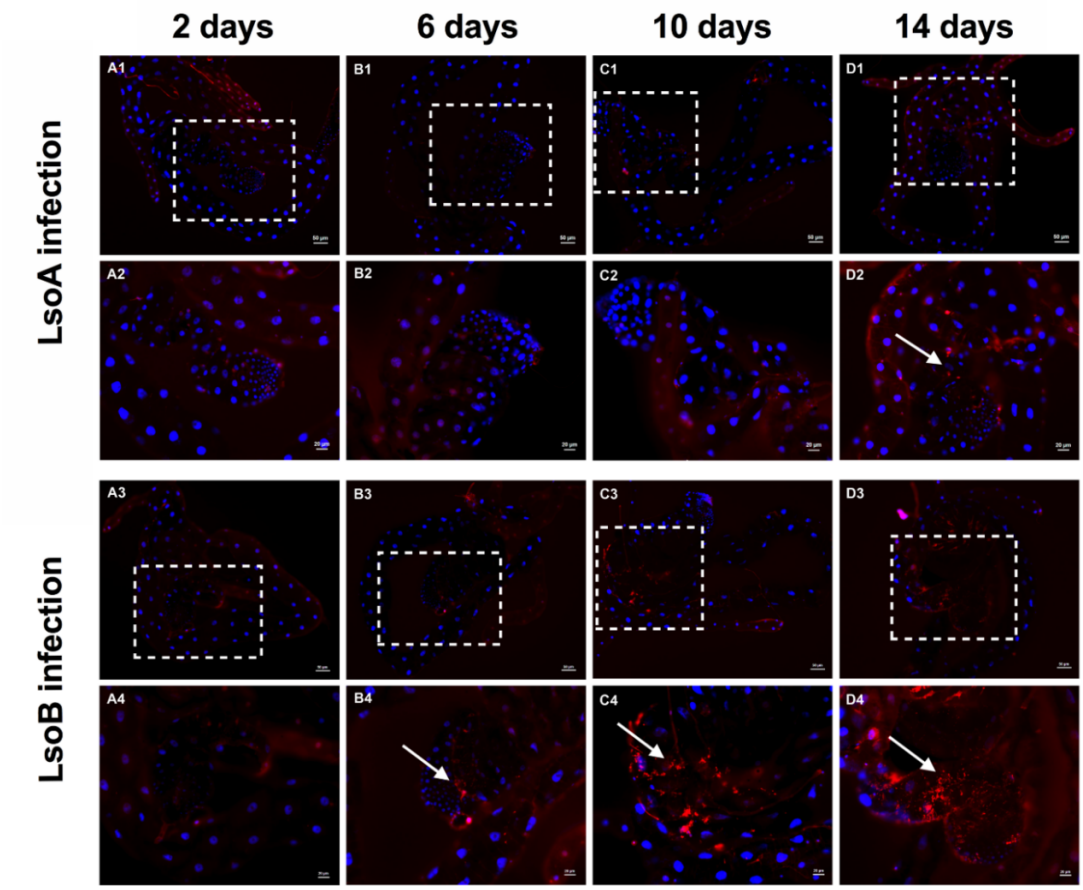

Figure 2.2 Immuno-staining of LsoA and LsoB in the guts of potato psyllids following continuous acquisition. (A1-A4) 2 days acquisition; (B1-B4) 6 days acquisition; (C1-C4) 10 days acquisition; (D1-D4) 14 days acquisition. The white dashed rectangle indicates the enlargement region (A2-D2 and A4-D4) of the filter chamber and midgut. White arrows indicated the Lso signals.

Previously, it was demonstrated that differences in Lso titer in inoculum plants do not result in differences in Lso titer in psyllids (Sengoda et al., 2013). Furthermore, we have previously investigated the distribution of LsoA and LsoB titers in tomato plants (Mendoza Herrera et al., 2018). The results presented here were obtained from three independent replicates, and all plants used had high Lso titers. Therefore, it is unlikely that

differences in Lso titer in the infected plants significantly affected the LsoA and LsoB accumulation in psyllids. However, the differences of LsoA and LsoB titer in the gut of adult psyllids could be the result of differences of bacterial pathogenicity or the elicited psyllid immune responses. Indeed, we have previously shown that LsoB is more pathogenic than LsoA (Harrison et al., 2019; Mendoza Herrera et al., 2018; Yao et al., 2016). Similarly, the vector immune response could be one factor explaining the different Lso accumulation profiles. For instance, autophagy is induced by RGDV in the gut of its vector, the rice leafhopper *R. dorsalis* (Chen et al., 2017). Further investigation demonstrated that autophagy activation improves the acquisition of RGDV, whereas inhibiting the autophagy pathway reduces viral titers in the leafhopper gut. Indeed, one potential explanation for the different acquisition of LsoA or LsoB could be that distinct immune responses are elicited by each haplotype. These immune responses could affect the replication rates of Lso in the potato psyllid gut. If indeed, different responses are elicited by each haplotype, it is possible that the response only affects Lso accumulation upon infection or in adult psyllids, because, adults that acquired Lso as nymphs have similar LsoA or LsoB titers in their guts (Chapter IV) (Tang & Tamborindeguy, 2019).

2.3.2 Transmission of LsoA and LsoB

Because the colonization of the psyllid gut by LsoA and the increase of its titer were slower than LsoB, we hypothesized that the circulation of LsoA within the vector could also take longer than that of LsoB. Therefore, we performed sequential inoculation of tomato plants with adults following a 7-day AAP. All the recipient tomato plants were

Lso-negative at day 17 post acquisition. LsoB was detectable in plants as early as 21 days post acquisition with an average transmission rate to tomato plants of 43.3%. This rate increased and remained around 90% after day 25 post acquisition. In contrast, LsoA could not be detected until 25 days post acquisition, when an average of 20% of the plants tested positive for Lso infection. At 29 days post acquisition, only 30% of plants were infected by LsoA (Fig. 2.3). The sequential transmissions were stopped at day 29 because of adult psyllid mortality. As a control, on average 94.4% and 100% of the tested plants were infected by insects from the LsoA- and LsoB-infected colonies, respectively. Overall, LsoB was transmitted with a significant higher rate than LsoA after 21 days (Chi-square test, $P < 0.001$). We also observed a lag between LsoA and LsoB transmission, which is consistent the differences of Lso accumulation in the gut obtained by quantification. Therefore, LsoB had a shorter latent period than LsoA. Specifically, the latent period of LsoB was between 17 and 21 days, while LsoA took between 21 and 25 days to be transmitted. The latent period for Lso transmission observed here is consistent with the previous study which determined that a two-week latent period was required for adult potato psyllids to transmit Lso following a 24- or 72-h AAP (Sengoda et al., 2014). While the authors did not test transmission of each Lso haplotype separately, they did not observe significant differences of latent period between the two Lso haplotypes (Sengoda et al., 2014). The discrepancies between those results and ours could result from the analysis of the transmission of each Lso haplotype separately. Indeed, it is possible that competition or cooperation between the Lso haplotypes occurs within the insect or the host plant. Another difference between the two studies was the use of tomato as source and recipient

hosts in the present study, while before potato as used for the acquisition and transmission analyses (Sengoda et al., 2014). Additionally, there are four potato psyllid haplotypes in North America (Swisher et al., 2014; Swisher et al., 2012), and the previous study used central haplotype psyllids (Sengoda et al., 2014), our study was performed with western haplotype psyllids. Therefore, it is possible that genetic differences among the potato psyllid populations or even the endosymbionts associated with each population (Cilia et al., 2011) result in different capacity for Lso transmission. Indeed, it appears that the inoculation rates of the bacterial pathogen '*Candidatus* Liberibacter asiaticus' by adult Asian citrus psyllid populations in North America might be less efficient than those previously reported by the vector Chinese populations (Pelz-Stelinski et al., 2010; Xu et al., 1988).

Several factors could potentially account for the difference of LsoA or LsoB transmission rates by potato psyllids. First, the ability of Lso to infect the gut or to cross from the gut into the hemocoel can determine its transmission efficiency. Indeed, as discussed above the insect immune system may prevent or delay the pathogen circulation through the vector. Consequently, future analyses should focus on the immune responses elicited by each Lso haplotype on the psyllid vector. In addition, LsoB was found to be more pathogenic in association with their host plant and insect vector (Harrison et al., 2019; Mendoza Herrera et al., 2018; Yao et al., 2016). It is therefore possible that LsoB is able to better defend itself against the psyllid immunity, or even manipulate those defenses to its advantage (Levy et al., 2019). As a consequence, LsoB could be acquired and transmitted with higher efficiency than LsoA. Second, the salivary gland is another

potential barrier for Lso transmission. It was established that over 10,000 Lso genomes were required in the salivary glands for potato psyllids to effectively transmit the bacterium (Sengoda et al., 2014). Based on our results, it appears that LsoB reaches that threshold earlier than LsoA. This could be because LsoB is able cross the gut barrier faster than LsoA, or that LsoB required less time to colonize the salivary glands and multiply, reaching the transmission threshold earlier.

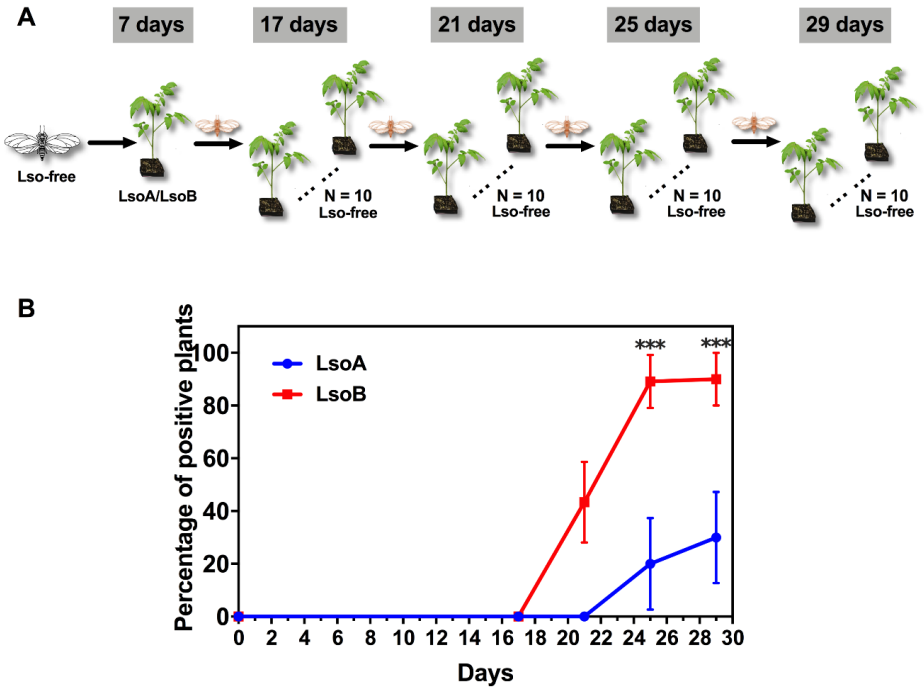

Figure 2.3 Sequential transmission test of LsoA and LsoB to tomato by psyllids after a 7-day acquisition access period (AAP). (A) Adult psyllids were given a 7-day AAP on LsoA or LsoB infected tomato plants. Then, groups of five adult psyllids were transferred to 10 recipient non-infected tomato plants for a 10-day inoculation access period, and each group was sequentially transferred to a new uninfected recipient plant every four days as shown in the schematic representation. The days showed in the figure indicate the days post acquisition. After four weeks, the presence of Lso was tested in each plant by PCR. (B) Comparison of transmission between LsoA and LsoB. The latent period for LsoB in adult potato psyllids is between 17 and 21 days, while for LsoA is between 21 and 25 days. *** $P < 0.001$ based on Chi-square test.

Interestingly, LsoB can be efficiently transmitted by adult potato psyllids, however, LsoA can be transmitted efficiently by adults only if it was acquired during the nymphal stage. The epidemiological implications if any, of this difference in transmission efficiency between the two Lso haplotypes need to be investigated.

In summary, we suggest that the Lso haplotypes A and B have distinct acquisition and transmission profiles. LsoB titer increased more rapidly in the adult psyllid gut than LsoA. Furthermore, LsoB had a significantly higher transmission efficiency by adult psyllids than LsoA and a shorter latent period between acquisition and inoculation. The information in the present study could be of significance for disease epidemiology and to develop strategies to disrupt pathogen transmission. Additional studies are needed to explore the accumulation of the two Lso haplotypes in the salivary glands and determine the Lso transmission in other psyllid haplotypes.

CHAPTER III

POTATO PSYLLID GUTS MOUNT DISTINCT RESPONSES UPON INFECTION WITH EACH OF THE TWO '*CANDIDATUS* LIBERIBACTER SOLANACEARUM' HAPLOTYPES

3.1 INTRODUCTION

'*Candidatus* Liberibacter solanacearum' (Lso), is a Gram-negative phloem-limited bacterium infecting crops worldwide. Presently, seven Lso haplotypes (LsoA, LsoB, LsoC, LsoD, LsoE, LsoF, and LsoU) of this pathogen exist in the world (Glynn et al., 2012; Haapalainen et al., 2018; Lin et al., 2012; Nelson et al., 2013; Swisher Grimm & Garczynski, 2019). They are transmitted by distinct psyllid species, and they infect different crops. For instance, haplotypes LsoA and LsoB are vectored by the potato psyllid (also known as the tomato psyllid), *Bactericera cockerelli* (Šulc) (Hemiptera: Triozidae) and infect solanaceous crops. By contrast, haplotypes LsoC and LsoD/E are vectored by carrot psyllids *Trioza apicalis* Förster and *B. trigonica* Hodkinson, respectively, and have been reported infecting the crops in the family Apiacea (Katsir et al., 2018).

Haplotypes LsoA and LsoB are associated with potato zebra chip (ZC) disease, which has been responsible for millions of dollars of losses in potato producing regions of the United States, Central America, and New Zealand (Munyaneza, 2012). Apart from potato, LsoA and LsoB also affect the production of a wide range of other important solanaceous crops such as tomato (Liefting et al., 2009b). Differences of virulence between these two haplotypes were determined in association with their host plants and

their insect vector: in both cases LsoB was found to be more pathogenic (Harrison et al., 2019; Mendoza Herrera et al., 2018; Yao et al., 2016). Currently, the only control strategy available for the diseases caused by these pathogens is based on controlling the psyllid populations by regular pesticide applications, thus, limiting the spread of Lso. However, frequent chemical applications would not only have negative impacts on the environment and human health, but also could contribute to the development of resistance in vector populations (Prager et al., 2013). Therefore, there is an urgent need to develop environmentally friendly and more sustainable strategies to control the diseases rather than rely exclusively on vector control.

Disrupting the pathogen transmission cycle within the insect vector is a promising approach to control diseases. Lso is transmitted in a circulative and persistent manner within potato psyllid (Cicero et al., 2016; Cicero et al., 2017; Cooper et al., 2014). Once ingested by the psyllid, Lso moves from the gut lumen into the hemocoel where it circulates. Once the pathogen reaches the salivary gland, it can be disseminated to new host plants during psyllid feeding. In this process, the gut represents the first barrier for transmission by the psyllid. Indeed, the ability of Lso to infect the gut or to cross from the alimentary canal into the hemocoel could determine its transmission efficiency. Thus, disruption of this process could be an effective way to control the spread of these pathogens. However, despite our adequate understanding of the invasion route of Lso within the potato psyllid, the molecular mechanisms underpinning the transmission process remain largely unknown. Therefore, as a first step, it is essential to understand the interactions that occur between the pathogen and the insect vector.

RNA sequencing (RNA-seq) or transcriptome analysis is a powerful methodology to quantify global gene expression patterns in various contexts from single cell to whole tissues (Wang et al., 2009). The objective of our earlier transcriptome studies was to develop genomic tools for this non-model organism. They were also analyzed to assess the potato psyllid responses to Lso at the whole-body level. These analyses identified genes such as vitellogenin and heat shock protein as differentially expressed (Nachappa et al., 2012a). This analysis, however, failed to identify immune genes commonly induced in response to Gram-negative bacteria in other insects (Nachappa et al., 2012a). Similar results were found by another study in the Asian citrus psyllid (Vyas et al., 2015). In addition, Ghosh et al. (2019) found genes from the endoplasmic reticulum associated degradation (ERAD) and the unfolded protein response (UPR) pathway were overexpressed after Lso haplotype D infection in the gut of carrot psyllid *B. trigonica*. Although the above studies have contributed to our understanding of the molecular basis of interactions of Lso and its insect vectors, the transcriptional responses of potato psyllid to the infection of LsoA and LsoB at the gut interface remain largely unknown.

In the present study, we took advantage of the existence of two bacterial haplotypes with different pathogenicity to identify key components involved in the interactions at the gut interface based on transcriptome analyses. Transmission of pathogens in persistent and propagative manner involves host-pathogen interactions at multiple stages. We examined changes in gene transcription of potato psyllid gut after feeding on LsoA- or LsoB-infected tomato plants for acquisition access periods (AAPs) of 2 days and 7 days, which correspond to early and late gut colonization time in adults, respectively. Our two

objectives in this study were to: (1) compare adult psyllid gut responses to two haplotypes LsoA or LsoB to identify the similarities and differences between these responses, and (2) provide insights into how the potato psyllid gut responds in a temporally manner to LsoA or LsoB infection. Further, I wanted to explore if I could compare the transcriptomes of LsoA and LsoB during their interaction with the gut to identify the molecular basis of the difference of pathogenicity between these haplotypes. Therefore, our study will not only uncover Lso haplotypes effects, but also reveal temporal profiles of psyllid gut responses to Lso infection. The data from this study will contribute to the knowledge of the mechanisms underpinning the interactions between potato psyllid and Lso at the gut interface, which can serve as a basis for developing new strategies to control vector-borne diseases based on pathogen transmission disruption.

3.2 MATERIALS AND METHODS

3.2.1 Insects and plants

Lso-infected and -uninfected psyllid colonies were maintained separately on tomato plants in insect cages (24 × 13.5 × 13.5 cm, BioQuip®, Compton, CA) at room temperature 24 ± 1°C and photoperiod of 16: 8 h (L: D). To obtain Lso-infected tomato plants, 6-week-old tomato plants were infected as described in Nachappa et al. (2014) using psyllids harboring LsoA or LsoB. After one week, psyllids were removed from the plants. Three weeks after Lso inoculation, the plants were tested for Lso infection using LsoF/OI2 primers (Li et al., 2009) and for Lso haplotype using Lso SSR-1 primers (Lin et al., 2012).

3.2.2 Lso infection, RNA purification and sequencing

Cohorts of 7-day-old female adult psyllids from the Lso-uninfected colony were transferred to uninfected (control), LsoA- or LsoB-infected tomato plants for 2 and 7 days AAPs, respectively. For each AAP and haplotype there were 200 psyllids use and three biological replicates performed for a total of 1,200 psyllids used per haplotype. After infection, psyllid guts were dissected under the stereomicroscope (Olympus) as described in Ibanez et al. (2014a). RNA samples for Illumina sequencing were purified using RNeasy Mini Kit (Qiagen, Hilden, Germany) followed by DNase I treatment with Turbo DNase (Ambion, Invitrogen, CA). Each RNA sample was ribo-depleted to remove bacterial and psyllid rRNA using RiboMinus Transcriptome Isolation kit (Life Technologies, Carlsbad, CA) combined with 100 pmol of each psyllid specific probes and 100 pmol of bacterial rRNA specific probes from the kit as described in Ibanez et al. (2014b). The psyllid mRNA (poly (A) + RNA, hereafter called "mRNA") was further purified using Dynabeads mRNA Purification kit (Life Technologies, Carlsbad, CA), the remaining RNA after rRNA depletion and mRNA purification is hereafter called "depleted RNA".

Based on the low number of Lso genomes previously measured 2 days after infection and the low percentage of bacterial reads obtained from our previous transcriptome analyses (Ibanez et al., 2014b; Yao et al., 2016), the mRNA for the 2-day-infection samples was used for library production and sequencing without ribodepletion for the psyllid rRNA (Fig. 3.1). However, for the 7-day-infection samples, a time point in which there is a greater amount of Lso, the mRNA and the depleted RNA sample which

contains the bacterial mRNA (Fig. 3.1) were submitted for library preparation and sequencing. For the control treatments, total RNA was subjected to the same procedurs but only the mRNA samples (which contains the insect mRNA) were used for library production. Both samples, the insect mRNA and the depleted RNA libraries were sequenced by the Texas A&M AgriLife Genomics and Bioinformatics.

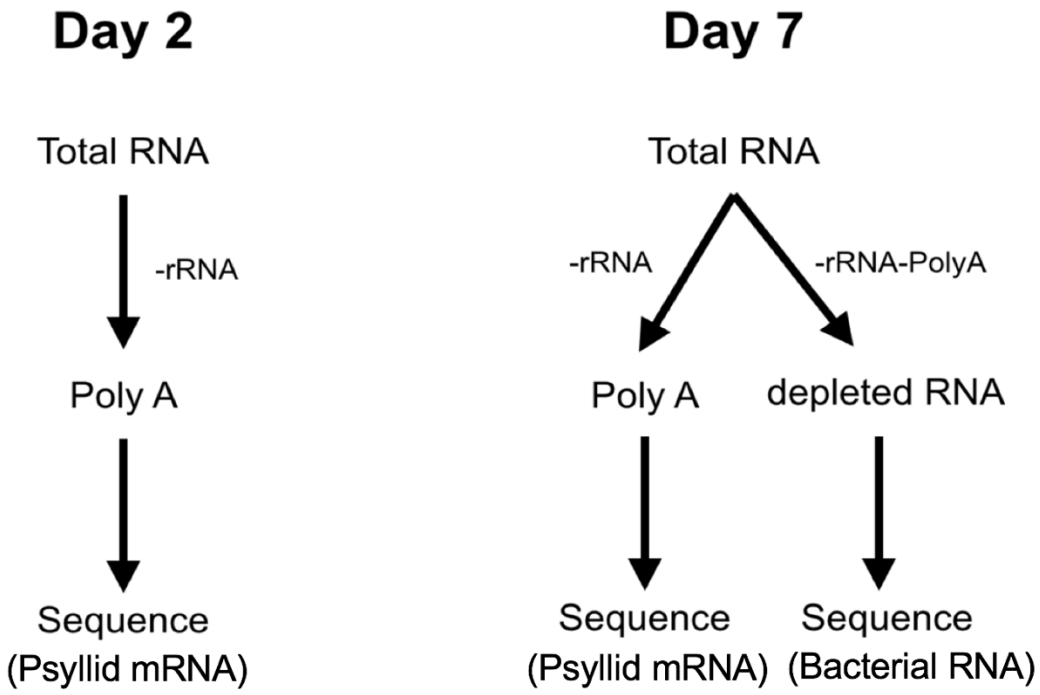

Fig. 3.1 Diagram depicting the purification steps to obtain RNA for sequencing. Total RNA was purified and subjected to Lso and psyllid rRNA depletion (-rRNA). Then, poly (A) + RNA (RNA with a poly A tail) was purified. For samples at day 2, only the psyllid mRNA (polyA RNA) was sequenced, while for day 7 samples, both the psyllid mRNA (PolyA RNA) and the bacterial RNA (depleted RNA) were sequenced.

3.2.3 Bioinformatic analyses

The Illumina pipeline programs for sequence processing were used to produce FASTQ files, sort libraries and remove barcodes and adaptors. The high quality reads were analyzed in Discovery Environment web interface and platform at CyVerse (http://www.cyverse.org/) using the Tuxedo suite (Trapnell et al., 2012). The RNA-seq reads from the mRNA samples that passed the quality filters were mapped to the global transcriptome developed in our previous study (Nachappa et al., 2012a). The RNA-seq reads from the depleted RNA samples were mapped to the genomes of bacterial species associated with potato psyllids: the primary endosymbiont *Carsonella* ruddii, the bacteria pathogen Lso, and the facultative endosymbiont *Wolbachia* (Thompson et al., 2015). The expression levels were calculated by using the Fragments Per Kilobase of transcript per Million mapped reads (FPKM) method. Genes with an adjusted *p* value (false discovery rate, FDR) less than 0.01 and fold change greater than or equal to 2.0 were considered as significantly differentially expressed genes (DEGs). RStudio (https://rstudio.com) was used for cluster dendrogram and multidimensional scaling (MDS) plot. DEGs were annotated by BLASTx searches against NCBI's non-redundant (nr) database (E-value cut off 1e-3) and UniProt database (https://www.uniprot.org/) using BLAST+ tools in Galaxy (Cock et al., 2015). To further obtain an overview of the biological functions of genes, all DEGs were subjected to Gene Ontology (GO) functional annotation using WEGO 2.0 (http://wego.genomics.org.cn/) (Ye et al., 2006; Ye et al., 2018) and mapped to terms in Kyoto Encyclopedia of Genes and Genomes (KEGG) pathway database using KOBAS 3.0 (http://kobas.cbi.pku.edu.cn/) and KEGG Mapper

(https://www.genome.jp/kegg/tool/map_pathway2.html). Enrichment analysis was used to identify the GO terms and significantly regulated KEGG pathways.

3.2.4 Real-time quantitative PCR (RT-qPCR) validation

Ten genes related to the representative category were selected to validate the bioinformatic expression analyses by RT-qPCR. For this validation, female adult psyllids from the Lso-uninfected colony were allowed to feed for 2 and 7 days on uninfected, LsoA-, and LsoB-infected tomato plants as previously described to obtain additional independent samples from the ones used for the sequencing (three replicates). The total RNA was purified from pools of psyllid guts as previously described in section 3.2.2. cDNA synthesis reactions were performed from each total RNA pool (independent from those for sequencing). Five hundred nanograms of total RNA was reverse-transcribed into cDNA using Verso cDNA Synthesis kit (Thermo, Waltham, MA) and anchored-Oligo (dT) primers following the manufacturer's instructions. The RT-qPCR reactions were performed using SensiFAST SYBR Hi-ROX Kit (Bioline, Taunton, MA) according to manufacturer's instructions. Each reaction contained 5 ng of cDNA, 250 nM of each primer (Table A.1) and 1X of SYBR Green Master Mix; the volume was adjusted with nuclease-free water to 10 µL. The RT-qPCR program was 95 °C for 2 min followed by 40 cycles at 95 °C for 5 sec and 60 °C for 30 sec. RT-qPCR assays were performed using an Applied Biosystems™ QuantStudio™ 6 Flex Real-Time PCR System (Applied Biosystems). Reactions for all samples were performed in triplicates with a negative control (water) in each run. The relative expression of the candidate genes were estimated

with the delta delta CT method (Schmittgen & Livak, 2008), using two reference genes of elongation factor-1a (GenBank KT185020) and ribosomal protein subunit 18 (GenBank KT279693) (Ibanez & Tamborindeguy, 2016).

3.3 RESULTS AND DISCUSSION

3.3.1 Overview of the transcriptome dataset

The potato psyllid gut is the first barrier that Lso have to overcome for their successful transmission. The transcriptome of gut can provide us with the potential mechanisms underlying the molecular interactions between the potato psyllid and Lso. In this study, we examined changes in gene transcription of potato psyllid gut after feeding on Lso-free, LsoA- or LsoB-infected tomato plants for AAPs of 2 days and 7 days. These treatments represent no infection, and early (2d) and later infection (7d). Transcriptome sequences from six treatments were generated in this study: (1) 2 days Lso-free, (2) 7 days Lso-free, (3) 2 days LsoA-infection, (4) 7 days LsoA-infection, (5) 2 days LsoB-infection, and (6) 7 days LsoB-infection. Three biological replicates were analyzed per treatment, and therefore a total of 18 independent libraries were constructed for the mRNA samples and 9 for the depleted samples. After sequencing, each mRNA library generated between 36 and 54 million reads and between 39.3 to 44.1% (Table A.2) of the reads in each library mapped to the global transcriptome developed in our previous study (Nachappa et al., 2012a). And, for the depleted RNA, libraries generated between 57 and 84 million reads (Table A.3). A very low number of reads in depleted library mapped to the Lso genome

(0.00-0.08%) (Table A.3); therefore, in this study, we only focused on the mRNA libraries and the transcriptome of the potato psyllid.

Multidimensional scaling (MDS) plot and cluster dendrogram of samples from the 18 libraries showed the mixture of non-infected and Lso-infected psyllids. However, there was a clear separation between the non-infected and 2-day Lso infected psyllids, and the 7-day Lso-infected psyllids based on the analysis of six treatments (Figs. A.1 and A.2).

The following of comparisons were made. The response to LsoA and LsoB at 2 and 7 days was assessed by comparing for each time point the transmcriptome of the LsoA-infected or LsoB-infected treatments to the Lso-free transcriptomes. These comparisons permit to identify common and specific responses to Lso haplotypes. In addition, the gut response to each haplotype was compared at day 2 and 7 to assess the temporal responses to the infection with each haplotype. A total of 1,698 DEGs were identified with an adjusted *p* value (FDR) less than 0.01 and fold change greater than or equal to 2.0.

For the first objective of evaluating the haplotype effect, there were 15 DEGs when comparing guts from LsoA-infected and Lso-uninfected psyllids at day 2; while at day 7, 109 DEGs were differentially expressed between LsoA- and Lso-uninfected guts. However, there were 41 DEGs identified by comparing the Lso-uninfected and LsoB-infected gut transcriptomes at day 2, and 867 DEGs were identified when comparing at day 7. Only 2 and 23 DEGs were regulated in common in response to both LsoA and LsoB at days 2 and 7, respectively, those could be considered as the general psyllid response to Lso (Fig. 3.2).

The comparison of the Lso-free guts at days 2 and 7 indentified only 9 DEGs. These genes could be linked to the normal aging of the tissue. The temporal comparison (from 2 to 7 days' infection) of the gut transcriptomic profiles showed that there were 210 DEGs when comparing the guts of LsoA-infected psyllids, and 1,369 DEGs when comparing the guts of LsoB-infected psyllids. Of those, 46 DEGs were identified in response to both LsoA and LsoB (Fig. 3.2C).

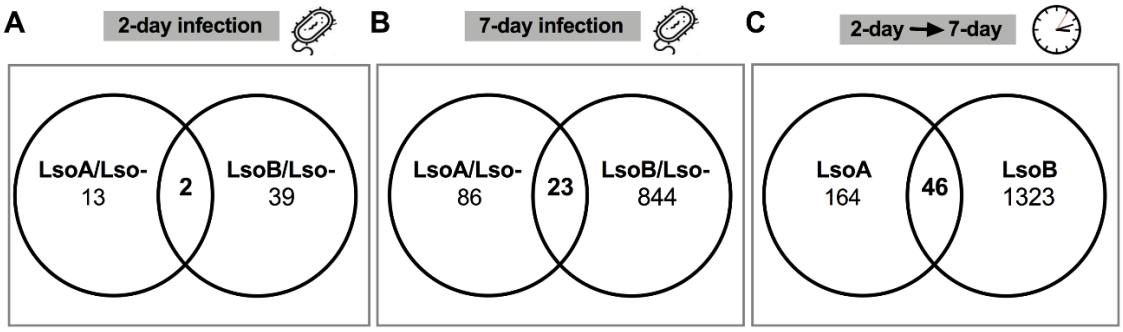

Figure 3.2 Venn diagram depicting unique and common differentially expressed genes (DEGs) in response to infection with LsoA or LsoB. (A) DEGs identified when comparing the responses to Lso after an AAP of 2 days; (B) DEGs identified when comparing the responses to Lso after an AAP of 7 days; (C) DEGs identified when comparing the guts after 2- and 7-day AAP for Lso treatment. LsoA/Lso- indicates the comparison between LsoA-infected and Lso-uninfected psyllids. LsoB/Lso- indicates the comparison between LsoB-infected and Lso-uninfected psyllids.

3.3.2 Response to LsoA

Of the 15 DEGs identified in response to LsoA at day 2, nine were upregulated and six were downregulated. The function of ten of those genes remains unknown (either they are hypothetical proteins or without similarities to other proteins). Among the genes with a putative function, a predicted HIG1 domain family member 2A, which is a mitochondrial gene involved in cellular respiration, and a 26S proteasome regulatory

subunit 6A, which is involved in the degradation of ubiquitinated proteins, were up-regulated. While a beta-ureidopropionase, the E3 ubiquitin-protein ligase TRIP12, and a reversion-inducing cysteine-rich protein with Kazal motifs were down-regulated. This latter gene was found up-regulated in *Tribolium* upon septic injury.

At day 7, 82 genes were up-regulated and 27 were down-regulated. These DEGs included 12 of the DEGs that were identified at day 2, all of which had the same expression pattern except for the 26S protease regulatory subunit 6A which was up-regulated in response to LsoA at day 7 while it was down-regulated at day 2. Twenty-six (31.7%) of the up-regulated genes encoded genes with a putative function. They were potentially involved in cell division or microtubule organization (spindle assembly abnormal protein 6 homolog, mitotic spindle assembly checkpoint protein MAD2, cyclin-dependent kinase 11B-like, Lipoma-preferred partner homolog, wiskott-Aldrich syndrome protein family member 3, TPPP family member), peptidase activity or other lysosomic acitivity (legumain-like, E3 ubiquitin-protein ligase TRIP12, E3 UFM1-protein ligase 1, LMBR1 domain-containing protein, 26S protease regulatory subunit 6A, GTP-binding protein ypt7), gene expression (THO complex, 60S ribosomal protein L37a, chromatin-remodeling ATPase INO80, histone H1-I-1), and metabolism and detoxification (HIG1 domain family member 2A, phospholipid hydroperoxide glutathione peroxidase, phosphoenolpyruvate carboxykinase). Among the down-regulated genes, 11 (40.7%) had a putative function, some of those genes could be involved in attachement and organization of cells into tissues (laminin subunit alpha, reversion-inducing cysteine-rich protein with Kazal motifs), and endocytosis and cell trafficking (huntingtin, golgin

subfamily B member 1). Other down-regulated genes had similarities with putative low-density lipoprotein receptor-related protein 1, beta-ureidopropionase, RNA pseudouridylate synthase domain-containing protein 3, probable small nuclear ribonucleoprotein E, REST corepressor 2, UNC93-like protein MFSD11, tudor domain-containing protein 1.

3.3.3 Response to LsoB

The response to LsoB was characterized by a greater number of DEGs at each time point compared to LsoA. At day 2, there were 17 up-regulated and 24 down-regulated genes. None of the up-regulated genes encoded proteins of known function except for putative phosphatidylinositol-glycan biosynthesis class X protein, which transfers the first of the 4 mannoses in the GPI-anchor precursors during GPI-anchor biosynthesis. Nine of the 24 down-regulated genes (37.5%) encoded putative proteins with a known function. These genes were involved in endocytosis and cell trafficking (protein wntless-like, huntingtin, golgin subfamily B member 1, pleckstrin-like proteiny domain-containing family J member 1, and conserved oligomeric Golgi complex subunit 3). Other down-regulated genes were RNA pseudouridylate synthase domain-containing protein 4-like, beta-ureidopropionase, tudor domain-containing protein 1, alanine aminotransferase 2, and N-alpha-acetyltransferase 35, NatC auxiliary subunit.

Only a tudor domain-containing protein 1 and a beta-ureidopropionase genes were regulated in response to both LsoA and LsoB at day 2, in both cases these genes were down-regulated in the infected samples. However, the tudor domain-containing protein 1

and the beta-ureidopropionase as well as the RNA pseudouridylate synthase domain-containing protein 3, hungtintin, golgin subfamily B member 1 were also down-regulated at day 7 in the LsoA samples compared to the Lso-free.

At day 7, there were 847 genes up-regulated in response to LsoB while 19 were down-regulated. Nine of the down-regulated genes (47.4%) had similarities to genes of known function: shootin-1, pleckstrin-like proteiny domain-containing family J member 1, mitotic spindle assembly checkpoint protein MAD2, conserved oligomeric Golgi complex subunit 3, beta-ureidopropionase, metallophosphoesterase 1 homolog, lipid storage droplets surface-binding protein 1, probable phospholipid hydroperoxide glutathione peroxidase, and RNA pseudouridylate synthase domain-containing protein 4. Among the up-regulated genes were several genes encoding for enzymes such as carboxypeptidases, maltases, trehalases, lipases, aminopeptidases and proteases and different transporters. There were also genes involved in ubiquitination, stress response, immunity, and detoxification.

3.3.4 DEGs associated with stress response, immunity, and detoxification

Potato psyllid gut is the first organ Lso encounter. Despite the simplicity of this tissue, the gut epithelium plays vital roles in response of stimuli. A number of stress response, immunity and detoxification related genes were regulated in response to both LsoA and LsoB but especially to LsoB, after an AAP of 7 days rather than 2 days. First, heat shock proteins (HSPs) have been shown to be up-regulated after septic injury and microbial infection (Gerardo et al., 2010). We found that the gene encoding HSP70 was

up-regulated in response to LsoB. Our data also demonstrated that ingestion of LsoB triggers a stress response that includes the production of enzymes such as glutathione S-transferases (GSTs) (Table 3.1). HSPs and GSTs are also involved in immunity or detoxification (see below). For example, HSPs may serve as signaling proteins during immune responses to pathogens (Götz et al., 2012; Kruse et al., 2017). In addition, genes related to response to stress stimulus such as tribbles homolog 2, ras-related proteins, short neuropeptide F, GTP-binding protein, atrial natriuretic peptide receptor, and glutathione peroxidase were also highly up-regulated (Table 3.1).

Second, the innate immune response plays a key role in defense against microbial infections in invertebrates (Hoffmann & Reichhart, 2002). Our data showed that following Lso infection, immune responses of potato psyllid including humoral and cellular were activated. The activation of immune responses is probably the evolved strategy of the potato psyllid to protect itself to some extent from the deleterious effects of Lso. It is interesting that LsoA and LsoB seem to induce distinct immune pathways (Fig. 3.3) in the potato psyllid gut. Specifically, we found that whether from the infection type or the temporal perspective, after an AAP of 7 days, LsoA down-regulated laminin subunit alpha, which is involved in phosphatidylinositol 3-kinase (PI3K) - protein kinase B (Akt) signaling pathway; while LsoA up-regulated phosphoenolpyruvate carboxykinase, which is involved in forkhead box O (FoxO) signaling pathway (Table 3.1). In fact, the FoxO transcription factors are negatively regulated by the PI3K/Akt signaling pathway and are considered to have inhibitory effect on cell proliferation and survival (Hay, 2011; Zhang et al., 2011). In mammals, Akt phosphorylation of FoxOs promotes cell survival since the

FoxOs regulate the pro-apoptotic protein TNF-related apoptosis-inducing ligand (TRAIL) (Zhang et al., 2011). Therefore, it is most likely that LsoA promotes gut cell death by inhibiting PI3K-Akt pathway and then activating the downstream pathway, FoxO signaling pathway. In contrast, we observed that two inhibitors of apoptosis were up-regulated by LsoB after an AAP of 7 days. The programmed cell death (apoptosis and autophagy) have been shown to be important in affecting transmission of plant pathogens in phloem feeders such as whitefly, planthopper and leafhopper (Chen et al., 2017; Huang et al., 2015; Wang et al., 2016). For example, Huang et al. (2015) found that *rice ragged stunt virus* (RRSV) could induce apoptosis in salivary gland of the insect vector, brown planthopper, and the apoptotic response probably promotes the virus transmission. We hypothesize that the regulation of the cell death pathways could be a psyllid adaptation to limit Lso invasion or a strategy used by the bacterial pathogen Lso to enhance their transmission. Indeed, recent reports indicated that the occurrence of apoptosis in the gut of CLas-infected Asian citrus psyllid adults which could be a factor explaining the developmental differences of CLas acquisition by the vector; in particular, no evidence of apoptosis was found in the nymphal guts and CLas titer increases at a faster rate when the bacterium is acquired by nymphs compared to adults (Ghanim et al., 2016; Mann et al., 2018). Genes involved in ubiquitin mediated proteolysis and autophagy pathways were up-regulated in response to LsoB after an AAP of 7 days. For example, a large number of ubiquitin-protein ligases, and genes encoding autophagy-related proteins (ATGs) were up-regulated in response to LsoB (Table 3.1 and 3.2). In addition, eight serine/threonine-protein kinase genes involved in signal transduction for numerous physiological events

were induced specifically by LsoB after an AAP of 7 days. The genes encoding protein kinase C, nitrogen permease regulator 2-like protein and ras-related GTP-binding proteins, which are involved in mammalian target of rapamycin (mTOR) signaling pathway, and ETS-like proteins and mitogen-activated protein kinase (MAPK), which are involved in MAPK signaling pathway, were up-regulated by LsoB after an AAP of 7 days as well (Table 3.1). Both of these two pathways also play important roles in energy homeostasis and innate immunity, regulating cell proliferation and survival (Haissaguerre et al., 2014; Hung et al., 2012; Lasithiotakis et al., 2008).

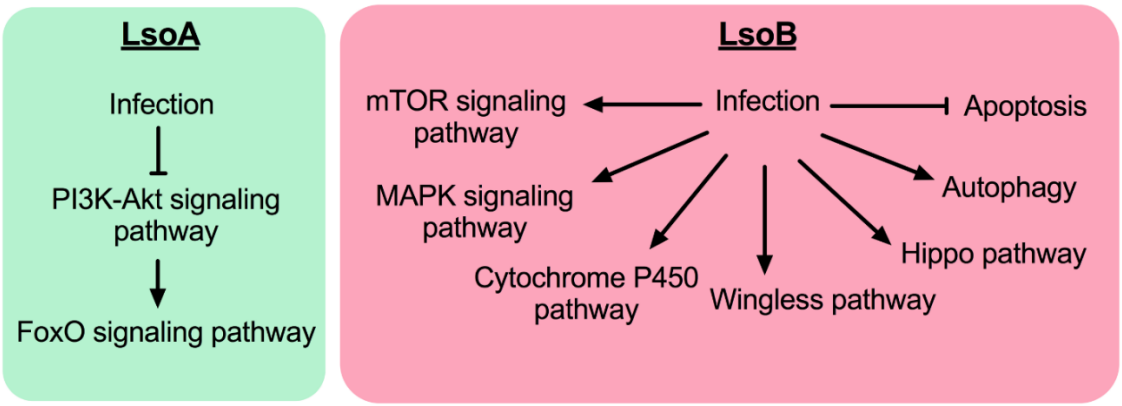

Figure 3.3 Distinct immune pathways were triggered by LsoA and LsoB in the gut of potato psyllid.

It is noteworthy that we did not detect a role for the Toll pathway, which is mainly activated by Gram-positive bacteria (Michel et al., 2001). In addition, genes of the immune deficiency (Imd) pathway were absemt in the transcriptome dataset (Nachappa et al., 2012a) used to map the RNA-seq fragments. Indeed, the absence of the components in IMD pathway appears to be common in the hemipteran insects. For example, the genome

of pea aphid (*Acyrthosiphon pisum*) was shown to lack genes in the IMD pathway (Gerardo et al., 2010); the IMD pathway genes are also notably absent from the transcriptome of the Asian citrus psyllid and potato psyllid (Kruse et al., 2017; Nachappa et al., 2012a). We hypothesize that hemipterans may rely on alternative measures or complementary immune mechanisms for defending against Gram-negative bacteria.

Finally, LsoB also triggered cytochrome P450 pathway, one of the detoxification pathways, by up-regulating GSTs and UDP-glucuronosyltransferase genes. GSTs comprise a diverse class of enzymes that detoxify stress-causing agents, including toxic oxygen free radical species. These genes are up-regulated in some arthropods upon oxidative stress and microbial challenges (Aguilar et al., 2005; Girardot et al., 2004). In Asian citrus psyllid gut, cytochrome p450s, glutathione S-transferases and UDP-glucuronosyltransferase were also induced by CLas but showed decreased expression (Kruse et al., 2017). Obviously, these two *Liberibacter* species have distinct toxic effects on their psyllid vectors. Indeed, it has been demonstrated that CLas increases fecundity of Asian citrus psyllid, while Lso decreases fecundity of potato psyllids (Albuquerque Tomilhero Frias et al., 2020; Nachappa et al., 2014; Pelz-Stelinski & Killiny, 2016; Ren et al., 2016). Besides, as indicated above, ABC transporters that are also involved in detoxification in insects such as whitefly (Tian et al., 2017) were up-regulated by LsoA and LsoB as well.

Table 3.1 DEGs associated with stress response, immunity, and detoxification of potato psyllid.

	GI number	Annotation	Fold change
Objective1: Haplotype	**Lso-free(7d) vs LsoA (7d)**		
	gi|646706993	Laminin subunit alpha, partial	-5.77
	gi|662224198	phosphoenolpyruvate carboxykinase, cytosolic [GTP]-like	4.74
	Lso-free (7d) vs LsoB (7d)		
	gi|1041541888	baculoviral IAP repeat-containing protein 6-like	4.5
	gi|1041533742	heat shock 70 kDa protein cognate 2-like	4.06
	gi|1062672951	serine/threonine-protein kinase N isoform X7	5.58
	gi|1314957697	serine/threonine-protein kinase PLK4	8.25
	gi|1037109585	ETS-like protein pointed isoform X1	3.5
	gi|1036052162	protein kinase C, brain isozyme isoform X3	4.38
	gi|1062685985	nitrogen permease regulator 2-like protein	4.81
	gi|31542100	tribbles homolog 2	4.96
	gi|662218685	ras-related protein M-Ras-like	7.73
	gi|662219677	short neuropeptide F-like, partial	4.72
Objective2: Time	**LsoA (2d) vs LsoA (7d)**		
	gi|662196271	ras-related protein Rab-40C	2.66
	gi|662191295	probable phospholipid hydroperoxide glutathione peroxidase isoform X1	9.62
	gi|1060228182	laminin subunit alpha	-4.55
	gi|662224198	phosphoenolpyruvate carboxykinase, cytosolic [GTP]-like	5.89
	LsoB (2d) vs LsoB (7d)		
	gi|1101339243	autophagy-related protein 2 homolog B isoform X1	6.44
	gi|662185953	baculoviral IAP repeat-containing protein 5	7.41
	gi|1041541888	baculoviral IAP repeat-containing protein 6-like	8.81
	gi|1041533742	heat shock 70 kDa protein cognate 2-like	4.51

Table 3.1 Continued.

	GI number	Annotation	Fold change
Objective2: Time	gi|1041543694	glutathione S-transferase 1-like isoform X1	2.83
	gi|110456486	glutathione S-transferase-like protein, partial	4.7
	gi|1036955918	glutathione S-transferase D2-like	5.3
	gi|662189599	UDP-glucuronosyltransferase 2C1-like	7.19
	gi|1314957697	serine/threonine-protein kinase PLK4	5.87
	gi|1041531693	probable serine/threonine-protein kinase MARK-A	5.03
	gi|1062672951	serine/threonine-protein kinase N isoform X7	6.54
	gi|1041542874	serine/threonine-protein kinase SMG1-like	3.78
	gi|662225644	probable serine/threonine-protein kinase fhkE, partial	4.66
	gi|662194098	serine/threonine-protein kinase MARK2	4.38
	gi|662205647	microtubule-associated serine/threonine-protein kinase 3	5.16
	gi|1041543301	serine/threonine-protein kinase Genghis Khan	4.07
	gi|1037109585	ETS-like protein pointed isoform X1	3.86
	gi|1062685985	nitrogen permease regulator 2-like protein	4.68
	gi|662214654	ras-related GTP-binding protein A	5.3
	gi|58332432	tribbles homolog 2	7.34
	gi|662218685	ras-related protein M-Ras-like	11.61
	gi|662219677	short neuropeptide F-like, partial	6.48
	gi|1041532994	GTP-binding protein Rheb homolog	4.62
	gi|1041549075	atrial natriuretic peptide receptor 2-like	3.14
	gi|1041529912	low-density lipoprotein receptor-related protein 6	3.06
	gi|1041546276	mitogen-activated protein kinase kinase kinase kinase 5-like	5

Negative fold changes indicate down-regulation in the second condition (on the right side of "vs").

Table 3.2 DEGs involved in ubiquitin mediated proteolysis pathway.

	GI number	Annotation	Fold change
Objective1: Haplotype	**Lso-free (7d) vs LsoB (7d)**		
	gi|1101399989	ubiquitin conjugation factor E4 A	6.18
	gi|662221799	ubiquitin carboxyl-terminal hydrolase 15-like	3.67
	gi|662213445	ubiquitin-fold modifier 1 isoform X1	3.51
	gi|1062650979	(E3-independent) E2 ubiquitin-conjugating enzyme UBE2O	4.14
	Lso-free (7d) vs LsoA&LsoB (7d)		
	gi|1041552333	E3 ubiquitin-protein ligase TRIP12	4.48/3.16
Objective2: Time	**LsoA (2d) vs LsoA (7d)**		
	gi|1036784377	ubiquitin-conjugating enzyme E2 variant 2	3.68
	LsoB (2d) vs LsoB (7d)		
	gi|1041538933	mitochondrial ubiquitin ligase activator of nfkb 1-A-like	3.11
	gi|1101399989	ubiquitin conjugation factor E4 A	10.63
	gi|662221799	ubiquitin carboxyl-terminal hydrolase 15-like	9.57
	gi|662213445	ubiquitin-fold modifier 1 isoform X1	4.47
	gi|662185713	E3 ubiquitin-protein ligase RNF103-like	2.95
	gi|1060217161	ubiquitin-conjugating enzyme E2 W isoform X2	2.87
	gi|1062650979	(E3-independent) E2 ubiquitin-conjugating enzyme UBE2O	5
	gi|662212044	E3 ubiquitin-protein ligase HECTD1-like	4.81
	gi|662198106	E3 ubiquitin-protein ligase RNF180-like isoform X1	4.4
	gi|662197593	E3 ubiquitin-protein ligase UBR3	4.13
	gi|1314983068	E3 ubiquitin-protein ligase Nedd-4 isoform X9	7.64
	LsoA&LsoB (2d) vs LsoA&LsoB (7d)		
	gi|1041552333	E3 ubiquitin-protein ligase TRIP12	7.63/7.8

For LsoA&LsoB, the value beside "/" indicates Lso-free vs. LsoA, and Lso-free vs. LsoB, respectively. Negative fold changes indicate down-regulation in the second condition (on the right side of "vs").

3.3.5 DEGs associated with gut epithelium renewal, cell cycle and DNA repair

The ability of host to survive an infection relies not only on resistance mechanisms that eliminate the pathogen but also on tolerance mechanisms that increase the capacity of the host to endure the infection (Schneider & Ayres, 2008). The function of gut epithelial renewal in host-pathogen interactions has been well demonstrated. For example, In *Drosophila*, Buchon et al. (2009) observed that ingestion of bacterium *Erwinia carotovora* carotovora 15 (Ecc15) provokes a massive increase in epithelial renewal, as evidenced by an increased number of dividing cells. In our study, we found that the genes or pathways involved in gut epithelium renewal, cell cycle and DNA repair were exclusively induced by LsoB after an AAP of 7 days. First, the genes encoding armadillo segment polarity protein, protein kinase C, and protein wingless-like, which are involved in Wnt signaling pathway, as well as patj homolog and ras association domain-containing protein, which are involved in Hippo signaling pathway, showed up-regulated profiles after an AAP of 7 days (Table 3.3). Probably, the genes encoding proteins such as wingless-like and patj homolog in Wnt and Hippo signaling pathway may help attenuate the gut cell damage inflicted by LsoB infection. We also noted that LsoB repressed wingless-like gene, showing a down-regulation profile after an AAP of 2 days, just the time LsoB is entering the gut cells. In addition, genes from the ubiquitin-proteasome system play roles in regulating the Hippo pathway. For example, E3 ubiquitin-protein ligase Nedd4 works as a key regulator of the Hippo signaling pathway and overexpression of this gene in *D. melanogaster* induces proliferation of the midgut epithelium (Bae et al., 2015). In our study, the Nedd4 gene was also up-regulated by LsoB after an AAP of 7 days.

Second, it has been demonstrated that pathogens are able to alter the host cell cycle to achieve the replication and expression of their genomes (Geng et al., 2018). The genes involvedin to the cell proliferation process such as cell cycle and repair were also up-regulated in response to LsoB after an AAP of 7 days. For example, LsoB significantly induced the genes encoding ubiquitin-protein ligases, serine/threonine-protein kinase, sister chromatid cohesion protein, protein lin-52 homolog, general transcription factor IIH subunit as well as TATA element modulatory factor (Table 3.3). The up-regulation of these genes suggested that LsoB probably disturbs the normal cell cycle and DNA repair in potato psyllid gut (Diallo & Prigent, 2011; Rankin, 2005).

3.3.6 DEGs associated with mitochondrial dysfunction and other functions

A total of 21 genes encoding mitochondrial proteins were differentially expressed in Lso-infected psyllid gut. Almost all of those genes were specifically up-regulated upon exposure to LsoB (Table 3.4). Two of those proteins encoding pyruvate dehydrogenase and succinyl-CoA ligase, which are involved in the citric acid (TCA) cycle, displayed up-regulated profiles after an AAP of 7 days. In addition to mitochondria-related genes, a large number of zinc finger genes involved in multiple functions (e.g., DNA binding) were significantly induced in response to LsoA and LsoB after an AAP of 7 days (Table A.4). We also listed all the well-annotated down-regulated DEGs in Table A.5. For example, whether from haplotype or temporal perspective, after an AAP of 7 days, LsoB repressed shootin-1 gene, which is involved in neuronal polarization and axon outgrowth. Many of

the DEGs were uncharacterized proteins with unknown functions, which might also play key roles in Lso and potato psyllid interactions (Table A.5).

Table 3.3 DEGs associated with cell renewal, cell cycle and DNA repair.

	GI number	Annotation	Fold change
Objective1: Haplotype	**Lso-free (2d) vs LsoB (2d)**		
	gi|662221226	protein wingless-like	-17.56
	Lso-free (7d) vs LsoB (7d)		
	gi|1060270998	armadillo segment polarity protein isoform X2	3.91
	gi|1036052162	protein kinase C, brain isozyme isoform X3	4.38
	gi|662221226	protein wingless-like	7.51
	gi|662219483	cyclin-K isoform X1	10.6
Objective2: Time	**LsoB (2d) vs LsoB (7d)**		
	gi|1101350861	ras association domain-containing protein 2 isoform X2	4.3
	gi|1189064107	patj homolog	6
	gi|662221226	protein wingless-like	12.96
	gi|1060270998	armadillo segment polarity protein isoform X2	5.02
	gi|1036950774	sister chromatid cohesion protein DCC1	4.42
	gi|662203336	protein lin-52 homolog	7.17
	gi|662209774	general transcription factor IIH subunit 4-like	5.16
	gi|1036716397	TATA element modulatory factor	3.85
	gi|1041548215	centrosomal protein of 97 kDa, partial	6
	gi|1698453	transposase	6.36
	gi|1101363356	GAS2-like protein pickled eggs	4.09
	gi|1041532257	transformation/transcription domain-associated protein-like	10.22
	gi|662219483	cyclin-K isoform X1	25.7

Negative fold changes indicate down-regulation in the second condition (on the right side of "vs").

Table 3.4 DEGs associated with mitochondrial function.

	GI number	Annotation	Fold change
Objective1: Haplotype	**Lso-free (2d) vs LsoA (2d)**		
	gi|662191692	HIG1 domain family member 2A, mitochondrial	30.98
	Lso-free (7d) vs LsoB (7d)		
	gi|662212934	NADH dehydrogenase [ubiquinone] 1 alpha subcomplex subunit 10, mitochondrial	5.23
	gi|164450052	mitochondrial ribosomal protein L12	3.4
	gi|1041551426	pyruvate dehydrogenase [acetyl-transferring]-phosphatase 1, mitochondrial-like	4.01
	gi|1036790856	ATP synthase subunit beta, mitochondrial	5.74
	gi|662194219	succinyl-CoA ligase [ADP-forming] subunit beta, mitochondrial	4.08
	Lso-free (7d) vs LsoA&LsoB (7d)		
	gi|662191692	HIG1 domain family member 2A, mitochondrial	15.19/23.26
Objective2: Time	**LsoB (2d) vs LsoB (7d)**		
	gi|1041538933	mitochondrial ubiquitin ligase activator of nfkb 1-A-like	3.11
	gi|1041536900	mitochondrial import inner membrane translocase subunit Tim17-B-like isoform X1	5.32
	gi|662212934	NADH dehydrogenase [ubiquinone] 1 alpha subcomplex subunit 10, mitochondrial	7.17
	gi|662191692	HIG1 domain family member 2A, mitochondrial	36.96
	gi|662207693	glutamyl-tRNA(Gln) amidotransferase subunit C, mitochondrial	5.05
	gi|662185185	28S ribosomal protein S11, mitochondrial isoform X4	5.06
	gi|662214960	probable 39S ribosomal protein L45, mitochondrial	4.03

Table 3.4 Continued.

	GI number	Annotation	Fold change
Objective2: Time	gi|1041551426	pyruvate dehydrogenase [acetyl-transferring]-phosphatase 1, mitochondrial-like	4.84
	gi|662203079	28S ribosomal protein S15, mitochondrial	3.64
	gi|662187983	D-beta-hydroxybutyrate dehydrogenase, mitochondrial	4.63
	gi|662206948	28S ribosomal protein S33, mitochondrial	4.2
	gi|1041544248	aldehyde dehydrogenase, mitochondrial	4.69
	gi|1006107229	Lipoamide acyltransferase component of branched-chain alpha-keto acid dehydrogenase complex, mitochondrial	3.61
	gi|1060142930	mitochondrial chaperone BCS1	5.92
	gi|1036790856	ATP synthase subunit beta, mitochondrial	5.12
	gi|662189998	mitochondrial fission process protein 1	4.79
	gi|662194219	succinyl-CoA ligase [ADP-forming] subunit beta, mitochondrial	3.49
	gi|1041543152	rRNA methyltransferase 2, mitochondrial isoform X2	4.02
	gi|1036769629	mitochondrial cardiolipin hydrolase-like	6.57
	gi|662190957	39S ribosomal protein L30, mitochondrial	-3.57

For LsoA&LsoB, the value beside "/" indicates Lso-free vs. LsoA, and Lso-free vs. LsoB, respectively. Negative fold changes indicate down-regulation in the second condition (on the right side of "vs").

3.3.7 GO annotation and KEGG pathway

To have a better idea of the biological roles of the identified DEGs, we further utilized GO enrichment analysis to determine the functions of the DEGs. From the perspective of haplotype effect after a 2 day-infection, the DEGs were categorized into 15

secondary GO categories under the cellular component, molecular function, and biological process divisions. DEGs with a "protein-containing complex" term was only regulated in response to LsoA; while only LsoB changed the expression of genes associated with the terms "signaling" and "response to stimulus" in the categories of biological process (Fig. 3.4A). After 7 days of infection, the DEGs were categorized into 28 secondary GO categories. Specifically, both LsoA and LsoB induced genes associated with GO-terms "catalytic activity", "binding", "metabolic process", and "cellular process". However, the DEGs in "biological adhesion" and "locomotion" were exclusive to the response to LsoA; while LsoB changed the expression of genes associated with "membrane-enclosed lumen", "response to stimulus", and "signaling" terms (Fig. 3.4B). From the temporal perspective, the enrichments of DEGs were largely similar to the assignments from the haplotype perspective with "catalytic activity", "binding", "metabolic process", and "cellular process" as the most represented terms. However, only LsoA infection changed the expression of genes with "antioxidant activity"; while genes associated with the terms "cellular component organization or biogenesis" and "molecular function regulator" were regulated in response to LsoB specifically (Fig. 3.5).

To identify signaling pathways involved in Lso and potato psyllid interactions at the gut interface, we mapped the DEGs to the KEGG database. The top 20 enriched pathways in response to LsoB are shown in Fig. 3.6. From the haplotype effect perspective (for both 2 and 7 days' infection), DEGs were highly clustered in the signaling pathways of "Metabolic", "Ubiquitin mediated proteolysis", "Wnt signaling pathway" and "mTOR signaling" (Fig. 3.6A). From the temporally perspective, the pathways such as

"Metabolic", "Ubiquitin mediated proteolysis", "Hippo signaling pathway", and "Ribosome" were the main regulated pathways (Fig. 3.6B). However, few enriched pathways such as metabolic and ubiquitin-mediated pathways were identified for the DEGs in response to LsoA, possibly due to the lower number of genes significantly induced/repressed.

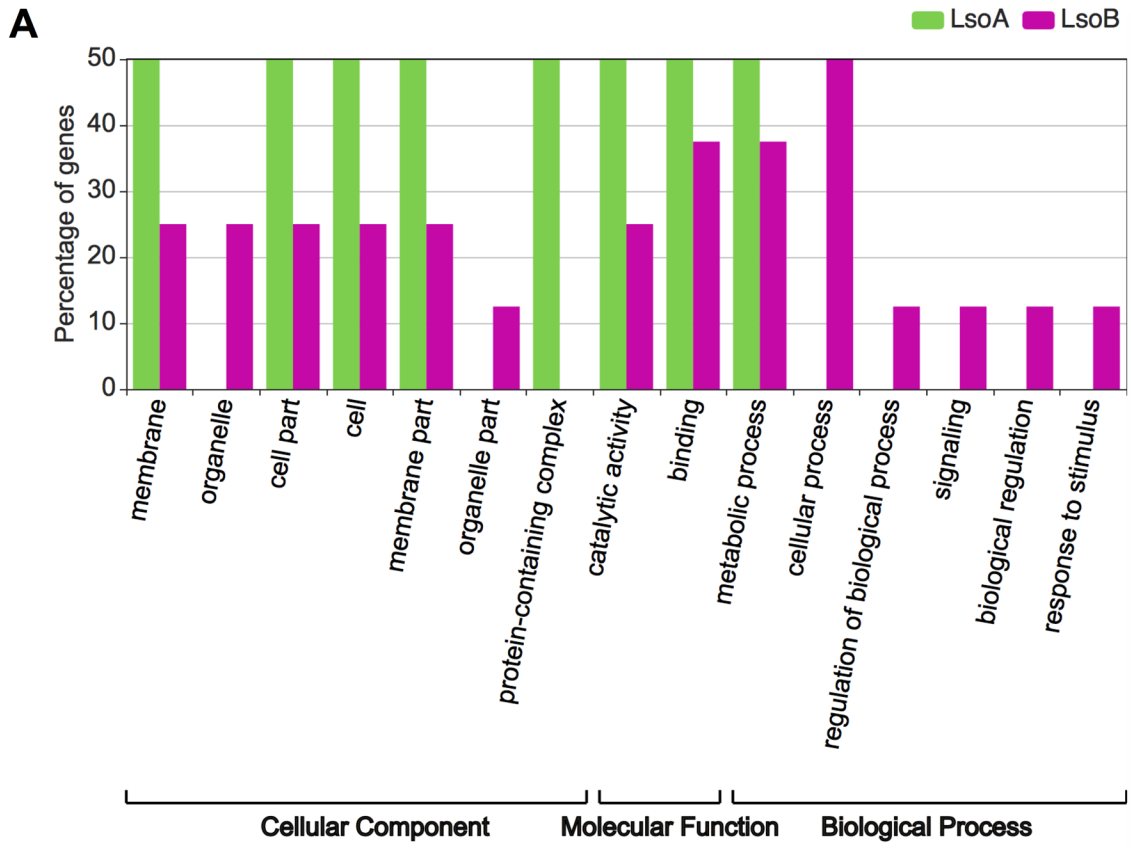

Figure 3.4 Histogram presentations of GO classification of DEGs (haplotype). (A) GO classification of DEGs based on analysis of the haplotype effect (2 days' infection); (B) GO classification of DEGs based on analysis of the haplotype effect (7 days' infection) The functions of genes identified cover three main categories: biological process, cellular component and molecular function. GO analysis showed that the distributions of gene functions for the DEGs.

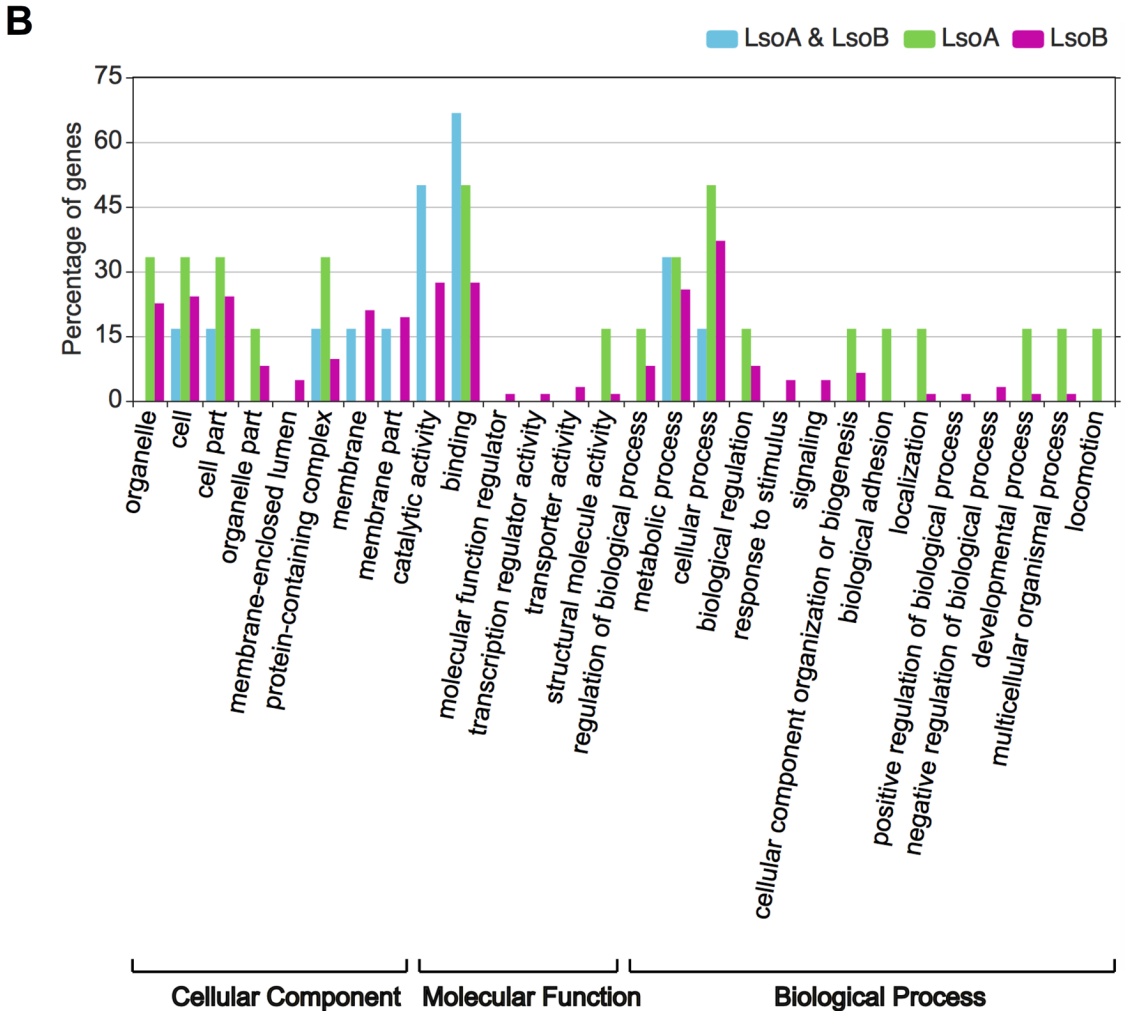

Figure 3.4 Continued.

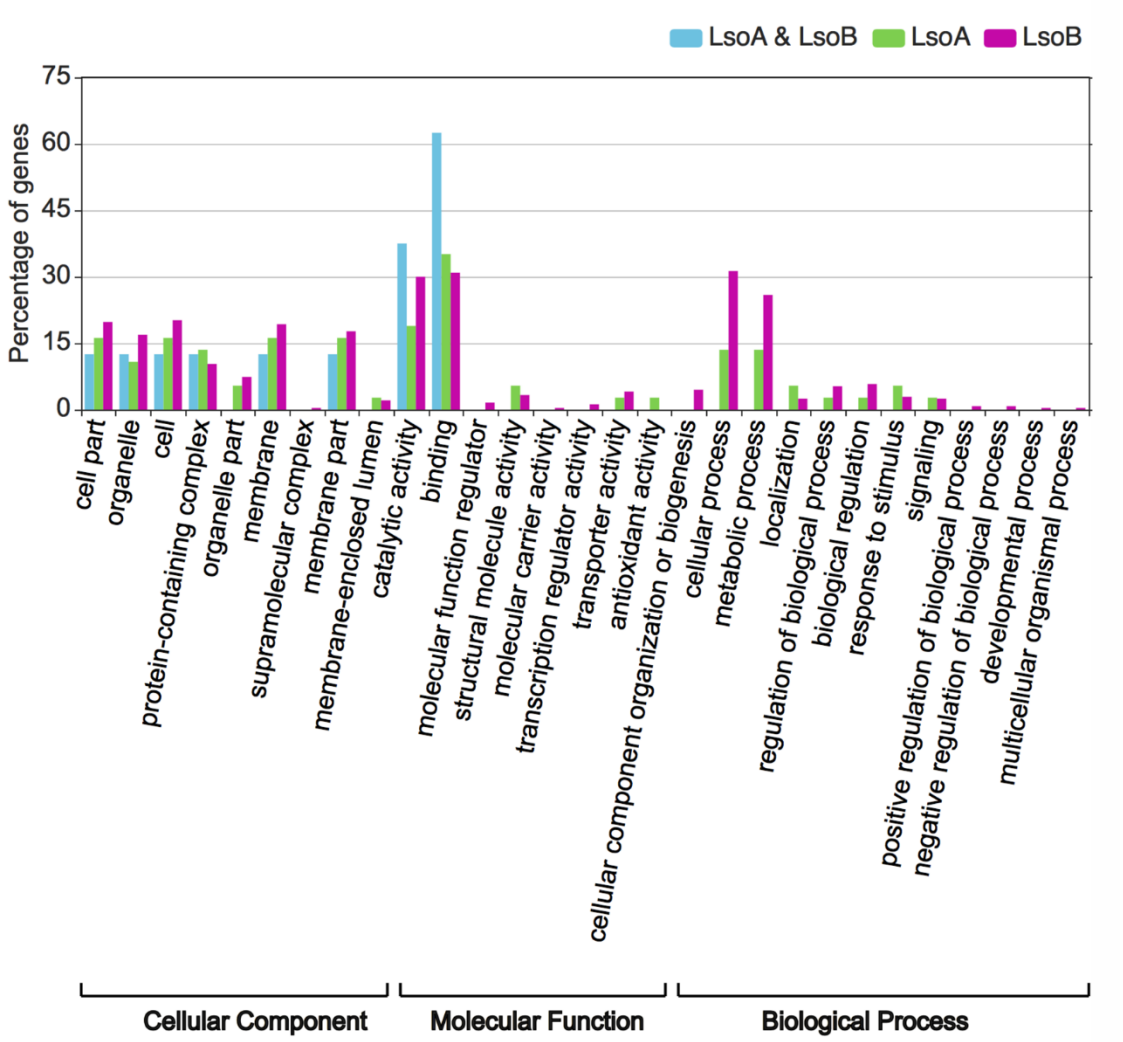

Figure 3.5 Histogram presentations of GO classification of DEGs (time). GO classification of DEGs based on analysis of temporal profile (from 2 days to 7 days), which indicates the regulation at day 7 differentially with day 2. The functions of genes identified cover three main categories: biological process, cellular component and molecular function. GO analysis showed that the distributions of gene functions for the DEGs.

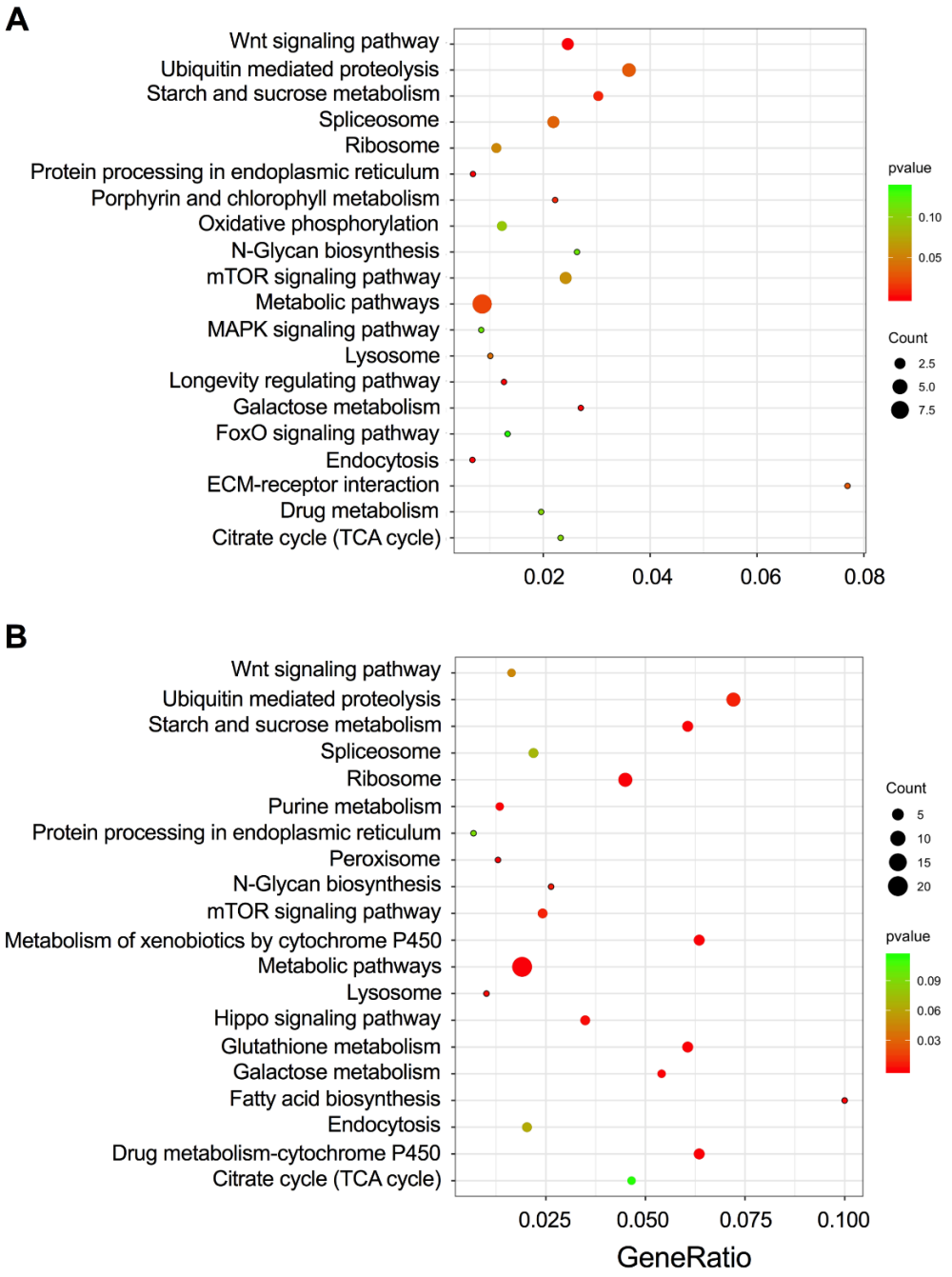

Figure 3.6 KEGG pathway analyses of DEGs in response to LsoB. (A) The top 20 significant enriched pathways based on analysis of the first objective of haplotype effects (for both 2 days and 7 days' infection); (B) The top 20 significant enriched pathways based on analysis of the second objective of temporal profile (from 2 days to 7 days), which indicates a global effect during day 2 and day 7. Y-axis label represents pathway and X-axis label represents enrichment factor.

3.3.8 Validation and expression profiles of DEGs

To validate the accuracy and reproducibility of the transcriptome bioinformatic analyses, ten DEGs related to transport, ubiquitin, immunity, mitochondrial proteins, cell repair or zinc finger proteins were selected for qPCR verification. The ten genes included E3 ubiquitin-protein ligase Nedd-4 isoform X9 (Nedd4), heat shock 70 kDa protein cognate 2-like (Hsp70), patj homolog (Patj), ras association domain-containing protein 2 isoform X2 (RASSF2), zinc finger protein 728-like (ZN728), facilitated trehalose transporter Tret1 (Tret1), zinc finger protein 91 (ZN91), HIG1 domain family member 2A, mitochondrial (HIGD2A), ubiquitin conjugation factor E4 A (UBE4A), and E3 ubiquitin-protein ligase TRIP12 (TRIP12). Overall, the results indicated that most of the genes showed concordant direction of change between the bioinformatic and the qPCR results except two genes, ZN728 and Tret1 (Figs. 3.7 and 3.8), indicating the accuracy and reliability of our DGEs libraries.

In general, we found that each Lso haplotype triggered a unique transcriptional response, with most of the distinct genes elicited by LsoB. Indeed, results from our previous studies indicated that LsoB was found to be more pathogenic in association with their host plants and insect vector (Harrison et al., 2019; Mendoza Herrera et al., 2018; Yao et al., 2016). It is also worthy to note that most DEGs were up-regulated by Lso infection, while only few were down-regulated. This observation is in contrast to DEGs regulations in the gut transcriptome of Asian citrus psyllid and *Ca*. L. asiaticus (CLas) system (Kruse et al., 2017), which indicated most of the DEGs showed down-regulation profiles. This discrepancy between the two systems is not unexpected because Ghanim et

al. (2016) determined that there is a strong apoptotic response in the gut of the adults in response to CLas, while apoptosis was undetectable in the gut of potato psyllids in response to either LsoA or LsoB (Tang & Tamborindeguy, 2019).

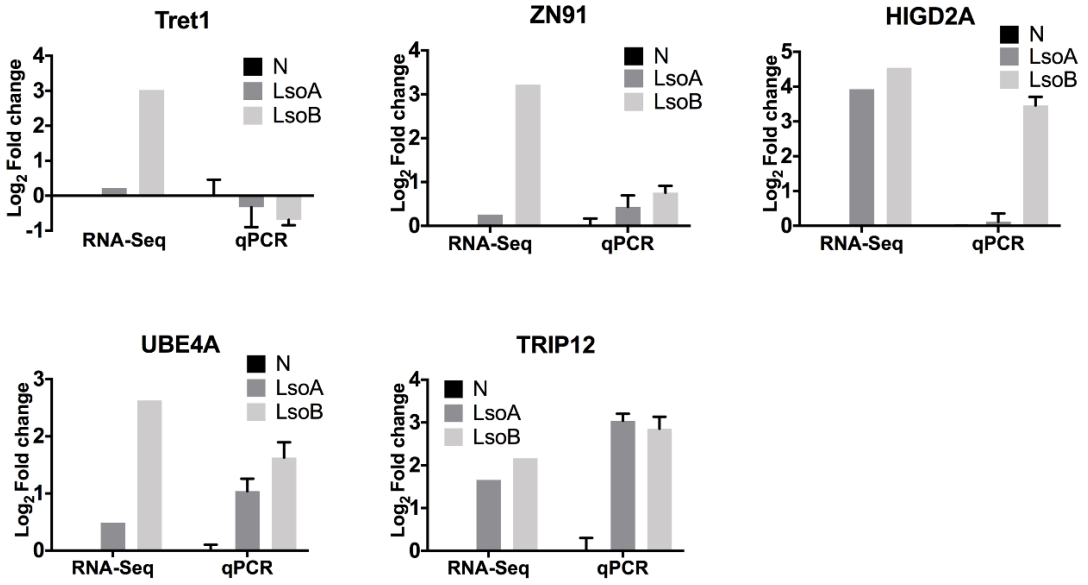

Figure 3.7 Comparison of gene expression patterns obtained by RNA-Seq and RT-qPCR regarding of haplotype effect. The mean ± SE was calculated to determine the relative transcript levels using the delta delta CT method.

In addition, compared to our previous transcriptome dataset of whole body, the gut of potato psyllid mounts distinct responses to Lso. Specifically, the whole body transcriptome had an abundance of genes differentially expressed such as reproduction (e.g., vitellogenin), stress (e.g., heat shock protein) and a large extent on genes involved in metabolic processes and to a small extent on immune and stress response genes (Nachappa et al., 2012a). Furthermore, other researchers found that many key genes involved in the ERAD and UPR pathways in carrot psyllid *B. trigonica* gut were induced

by Lso haplotype D (Ghosh et al., 2019). In contrast, in the present study, large numbers of the DEGs were involved in digestion and metabolism, stress response, immunity, detoxification, as well as cell regeneration.

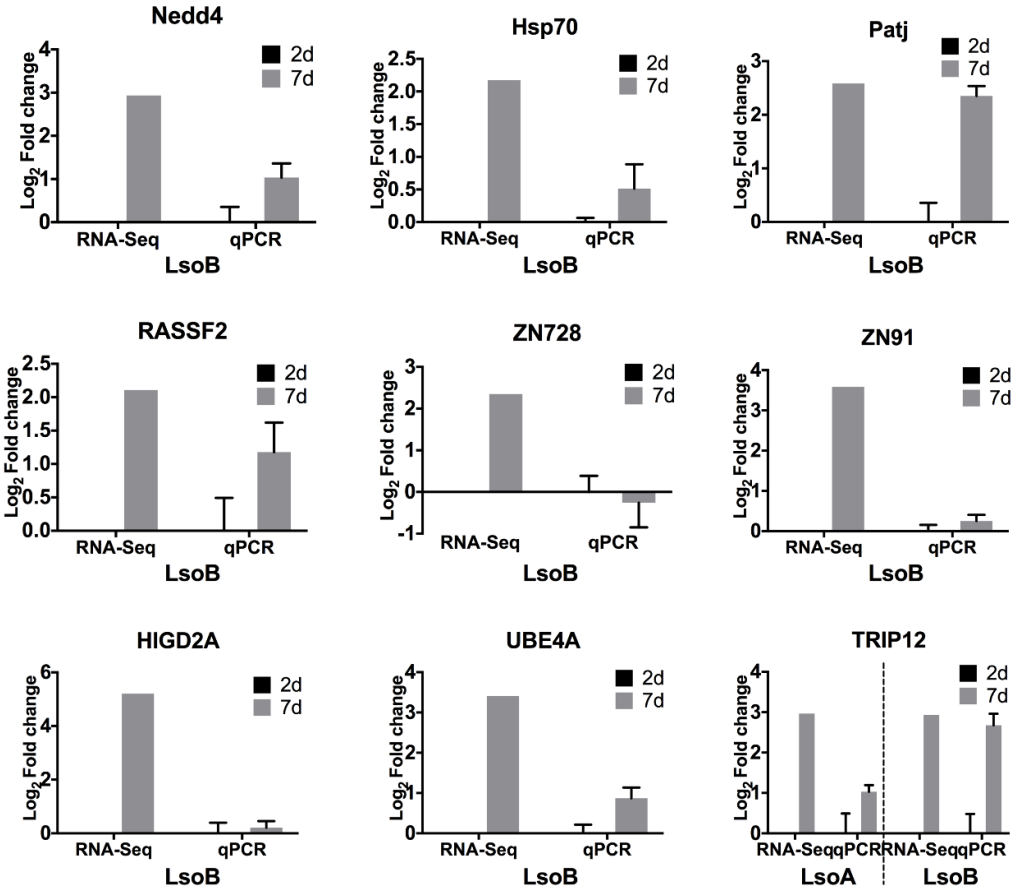

Figure 3.8 Comparison of gene expression patterns obtained by RNA-Seq and RT-qPCR regarding of temporal effect. The mean ± SE was calculated to determine the relative transcript levels using the delta delta CT method.

In summary, our data showed that potato psyllid mounts distinct intestinal responses (whether on numbers or categories of genes) upon infection of two Lso

haplotypes from both haplotype and temporal perspectives. Importantly, LsoA and LsoB triggered different immune pathways in the gut of potato psyllid. The information in our study may offer hints for discovery of novel and specific molecular targets for disrupting Lso transmission within psyllid vector.

CHAPTER IV

LACK OF EVIDENCE OF APOPTOTIC RESPONSE OF THE POTATO PSYLLID, *BACTERICERA COCKERELLI*, TO '*CANDIDATUS* LIBERIBACTER SOLANACEARUM' AT THE GUT INTERFACE[*]

4.1 INTRODUCTION

In the last two decades, several diseases associated with psyllid-borne bacterial pathogens have emerged worldwide resulting in great economic losses. Some of these devastating diseases are caused by bacterial pathogens in the genus *Liberibacter*, including "*Candidatus* (*Ca*.) Liberibacter (L.) solanacearum" (Lso), "*Ca*. L. americanus", "*Ca*. L. Africanus", and "*Ca*. L. Asiaticus" (CLas) (Tamborindeguy et al., 2017).

Lso is a phloem-limited, Gram-negative fastidious bacterium. It is the causative agent of potato zebra chip and other diseases in solanaceous crops in the United States, Mexico, Central America, and New Zealand (Munyaneza, 2012). Presently, seven Lso haplotypes (LsoA, LsoB, LsoC, LsoD, LsoE, LsoF, and LsoU) have been identified in the world (Glynn et al., 2012; Haapalainen et al., 2018; Lin et al., 2012; Nelson et al., 2013; Swisher Grimm & Garczynski, 2019). In North America, the haplotypes LsoA and LsoB are transmitted by the potato psyllid (or tomato psyllid), *Bactericera cockerelli* (Šulc) (Hemiptera: Triozidae) (Hansen et al., 2008). Similarly, CLas, another phloem-limited

[*]Reprinted with permission from Tang XT and Tamborindeguy C (2019) No Evidence of Apoptotic Response of the Potato Psyllid *Bactericera cockerelli* to "*Candidatus* Liberibacter solanacearum" at the Gut Interface. *Infection and Immunity*. **88**: e00242-19. Copyright 2019 by American Society for Microbiology.

bacterium, causes the most devastating disease of citrus, huanglongbing. This bacterium is mainly transmitted by the Asian citrus psyllid, *Diaphorina citri* Kuwayama (Hemiptera: Liviidae).

Both, Lso and CLas, are transmitted in a circulative and persistent manner (Ammar et al., 2011a; Ammar et al., 2011b; Cicero et al., 2016; Cicero et al., 2017). After being acquired from infected plants, these pathogens first colonize the psyllid gut. After replicating in the gut, these bacteria proceed to the hemolymph and infect other insect tissues, including the salivary glands, prior to their inoculation to the host plants during a subsequent feeding. Despite our understanding of their invasion route within the psyllid body, the mechanisms underlying the transmission of these two pathogens by the vectors remain largely unknown.

The gut, as the first organ that Lso and CLas encounter, provides an essential link for understanding *Liberibacter* transmission by psyllid vectors. Recent reports indicate that CLas induces apoptosis in the gut of *D. citri* adults, while no evidence of apoptosis was found in the nymphal guts (Ghanim et al., 2016; Mann et al., 2018). Furthermore, CLas titer increases at a faster rate when the bacterium is acquired by nymphs compared to adults (Ammar et al., 2016). Therefore, the induction of apoptosis in the gut of adults may be a factor explaining the developmental differences of CLas acquisition by the vector. Interestingly, no evidence of apoptosis was found in the gut of adult carrot psyllids infected with LsoD (Ghanim et al., 2017). In contrast to CLas, Lso can be efficiently acquired during the nymphal and adult phases. Importantly, although the parameters for acquisition, transmission and retention of Lso by potato psyllids have been preliminarily

investigated, the interactions between the potato psyllid and Lso are not as well understood when compared to the CLas - *D. citri* system.

Therefore, in this study, we investigated the molecular interaction between the potato psyllid and Lso haplotypes A and B. Specifically, we explored whether either of these two Lso haplotypes triggered an apoptotic response in the gut of the adult potato psyllid. Toward this aim, we employed a four-step approach. First, we investigated whether differences of accumulation or localization of LsoA and LsoB in the gut of the potato psyllid were observed. Second, we evaluated the occurrence of markers of apoptosis using microscopy, annexin V cell death assays, and DNA fragmentation assays. Third, we annotated a set of apoptosis-related genes using the potato psyllid transcriptome. Fourth, we evaluated the expression of the identified apoptosis-related genes in the psyllid gut in response to the infection with each Lso haplotype. This study advances our understanding of the interactions between Lso and the potato psyllid. Our study may also contribute to developing new strategies to control diseases caused by different *Liberibacter* bacteria.

4.2 MATERIALS AND METHODS

4.2.1 Insect colonies and gut tissue collection

Lso-free, and LsoA- and LsoB-infected psyllid colonies were maintained separately on tomato plants (Moneymaker variety; Victory Seed Company, Molalla, OR) in insect-proof cages (24 × 13.5 × 13.5 cm, BioQuip®, Compton, CA) at room temperature 24 ± 2°C and under a photoperiod of 16: 8 h (L: D), as described in Yao et al. (2016). Guts

of Lso-free, LsoA- and LsoB-infected adult female psyllids (approximately seven-day-old) were dissected under the dissecting microscope as described in Ibanez et al. (2014a).

4.2.2 Quantification of Lso

To quantify Lso in the gut of LsoA- or LsoB-infected psyllids, DNA from pools of 50 guts was purified following the protocol of DNeasy Blood & Tissue kit (Qiagen, Hilden, Germany). Each pool represented one replicate and was used as an individual template for quantitative real-time PCR (qPCR) analyses. A total of three replicates were analyzed for each Lso haplotype. qPCR was performed using the SYBR Green Supermix kit (Bioline, Taunton, MA) according to the manufacturer's instructions. Each reaction included 25 ng of DNA, 250 nM of each primer, and 1X of SYBR Green Master Mix. The volume was adjusted with nuclease-free water to 10 µL. The qPCR program was 95 °C for 2 min followed by 40 cycles at 95 °C for 5 sec and 60 °C for 30 sec. qPCR assays were performed using a QuantStudio™ 6 Flex Real-Time PCR System (Applied Biosystems, Foster City, CA). Reactions for all samples were performed in triplicates with a negative control in each run. The Lso specific primers for the gene encoding a hypothetical protein (WP_013462289.1) (HP1Lso F: 5'- GGAAAAGCACAGTCAGTTTATG-3' and HP1Lso R: 5'- GGCAATTCGCAACTTAGACA -3') were used for Lso quantification in psyllids. This gene is only found in Lso and the specificity of the primers was verified using the Primer-Blast tool from NCBI searching against the nr database. Psyllid 28S rDNAF and 28S rDNAR primers (Nachappa et al., 2014) were used to amplify 28S rDNA which was used as an internal control. The average Ct value from the three replicates was

used to quantify the Lso levels. Data are reported as delta Ct = (Ct of HP1Lso gene) - (Ct of psyllid 28S gene). The Lso relative abundance in each sample was estimated by comparing the delta Ct value of the sample to a standard curve prepared following the methods described in (Levy et al., 2011) .

4.2.3 Immunolocalization of Lso

To visualize Lso in the Lso-infected psyllid alimentary canal tissues, psyllid guts were first dissected in 1X phosphate buffered saline (PBS) (Sigma-Aldrich, St. Louis, MO) from Lso-free, LsoA- and LsoB-infected adult psyllids and fixed in 4% paraformaldehyde for 30 min at room temperature. After fixation, the guts were incubated with Sudan Black B (SBB) (Sigma-Aldrich) for 20 min to quench autofluorescence, as described in Tang et al. (2019). Next, the guts were permeabilized by incubating in 0.1% Triton X-100 (Calbiochem/EMD Chemicals, Gibbstown, NJ) for 30 min at room temperature. After washing three times with PBS containing 0.05% Tween 20 (PBST), blocking was performed for 1 h at room temperature with blocking buffer (PBST with 1% [w/v] bovine serum albumin). Lso immunolocalization was performed as described in Tang et al. (2019) using a rabbit-derived polyclonal antibody (GenScript Corp, Piscataway, NJ) raised against the synthesized peptide Lso OMP-B “VIRRELGFSEGDPIC”. The guts were incubated with the antibody (diluted 1: 500) overnight at 4 °C. Then, the guts were washed three times with PBST and incubated with an Alexa Fluor 594-labeled goat anti-rabbit IgG secondary antibody (diluted 1: 2000; Invitrogen, Carlsbad, CA) for 1 h at room temperature. Guts were washed again three times with PBST, and mounted with one drop

of Vectashield mounting medium with 4′,6-diamidino-2-phenylindole (DAPI) (Vector Laboratories Inc., Burlingame, CA) on a microscope slide. The slide was covered with a coverslip and sealed with nail polish. At least 20 guts per colony were examined using an Axioimager A1 microscope (Carl Zeiss microimaging, Thornwood, NY, USA) using the rhodamine filter (594 nm, red) and the images were collected and analyzed with the Axiovision Release 4.8 software (Carl Zeiss).

4.2.4 Nuclear morphology, actin cytoskeleton architecture and annexin V cell death assays

To test whether Lso infection resulted in apoptosis in the potato psyllid gut, the nuclear morphology and the actin cytoskeleton architecture of the gut cells of adult potato psyllids from the Lso-free, LsoA-, and LsoB-infected colonies were observed. For that, the guts of adult insects from each colony were dissected, fixed, and incubated with SBB, as previously described. Next, the guts were incubated with Alexa Fluor 488-labeled phalloidin (dilution 1:200; Invitrogen) for 30 min. The guts were washed three times with PBST, and mounted with one drop of Vectashield mounting medium with DAPI (Vector Laboratories Inc.).

Similarly, annexin staining was performed using the Annexin V-FITC apoptosis detection kit (Abcam, Mountain View, CA) following the manufacturer's instructions. For that, after the guts were dissected in 1× PBS as described above, they were re-suspended with 1X Binding Buffer and incubated with Annexin V-FITC for 30 mins in the dark. Then the guts were fixed with 4% paraformaldehyde in 1× PBS for 15 mins, washed with

Binding Buffer three more times, mounted on microscope slides, covered with a coverslip, and sealed with nail polish.

At least 20 guts per colony and treatment were examined. All the guts were examined using an Axioimager A1 microscope (Carl Zeiss microimaging) using the FITC (488 nm, green) and rhodamine (594 nm, red) filters. The images were collected and analyzed with Axiovision Release 4.8 software (Carl Zeiss).

4.2.5 DNA fragmentation assay

Apoptosis is characterized by DNA fragmentation producing a characteristic DNA ladder. To test the integrity of the genomic DNA in the gut cells, the guts of Lso-free, LsoA-, and LsoB-infected insects were dissected as previously described. A total of three replicates were analyzed for each colony. Genomic DNA was purified using the DNeasy Blood & Tissue kit (Qiagen), and subsequently, the DNA samples were treated with RNase A (Invitrogen). Approximately 1 μg of DNA per sample were separately subjected to electrophoretic analysis. The DNA samples were run on 2% agarose gels containing ethidium bromide and visualized using UV light.

4.2.6 Identification of apoptosis related genes

Genes potentially involved in apoptosis were identified through blast searches of the psyllid transcriptome (Nachappa et al., 2012a) using *Drosophila melanogaster*, *Acyrthosiphon pisum*, *Bemisia tabaci,* and *D. citri* predicted genes as query. The gene

structure or domains of all apoptosis-related genes were identified with the Conserved Domain tool in NCBI.

To validate the bioinformatic predictions, primers for each candidate gene (except for IAP6, the homolog of Dbruce) were designed (Table A.6). RNA from a pool of 50 psyllid adults was purified using the RNeasy Mini Kit (Qiagen). Then the total RNA was reverse transcribed using the Verso cDNA Synthesis kit (Thermo, Waltham, MA) and anchored-Oligo (dT) primers following the manufacturer's instructions. Candidate genes were amplified by PCR. The PCR conditions were 95 °C for 2 min; followed by 35 cycles of 95 °C for 30 secs, 60 °C for 30 secs, and 72 °C for 30-90 secs (depending of amplicon size); and a final extension at 72 °C for 5 min. Amplicons were visualized in a 1 % agarose gel, and amplicons of the expected size were excised from the gel and purified using the PureLink Quick Gel Extraction kit (Invitrogen). Each PCR fragment (150 ng) was cloned into the pGEM-T easy vector using the pGEM-T easy cloning kit (Promega, Madison, WI) and transformed into NovaBlue Singles Competent cells (Novagen, Temecula, CA). For each construct, plasmid DNA from at least three colonies was purified using the PureLink Quick Plasmid Miniprep kit (Invitrogen) and sequenced by Eton Bioscience Inc. (San Diego, CA, USA). The obtained sequences were compared to the bioinformatics predictions.

For the phylogenetic analysis, potato psyllid caspase sequences were aligned with caspases from *D. melanogaster*, *D. citri, A. pisum* and *B. tabaci* using ClustalW with the MEGA 5.2 software (Tamura et al., 2013). The phylogenetic reconstruction was done by Bayesian inference using MrBayes 3.2 (Ronquist et al., 2012) with the *Caenorhabditis*

elegans caspase CED-3 as an outgroup. Markov chain Monte Carlo runs were carried out for 2,000,000 generations, and the first 25% of sampled trees were discarded as burn-in. Tree information was visualized and edited using FigTree v1.4.3 (http://tree.bio.ed.ac.uk/software/figtree).

4.2.7 Expression of apoptosis-related genes

The guts of Lso-free, LsoA-, or LsoB-infected psyllids were dissected in 1× PBS with RNAlater (Ambion, Invitrogen) under the stereomicroscope. Guts from 200 adult psyllids of mixed sex and age were pooled. RNA purification from each pool was performed as described above, and genomic DNA was eliminated by DNase I treatment with Turbo DNase (Ambion, Invitrogen). cDNA synthesis from each pool was performed as described above. Each pool represented one replicate. A total of three replicates were analyzed for each colony. The expression of apoptosis-related genes in the Lso-free and Lso-infected guts was evaluated by qPCR using the SensiFAST SYBR Hi-ROX kit (Bioline) according to manufacturer's instructions as described above. The primers for qPCR are listed in Table A.6. The relative expression of the candidate genes was estimated with the delta delta CT method (Schmittgen & Livak, 2008), using the two reference genes, elongation factor-1a (GenBank KT185020) and ribosomal protein subunit 18 (GenBank KT279693) since they are the most stable genes to analyze gene expression in the presence of Lso (Ibanez & Tamborindeguy, 2016).

4.2.8 Data analysis

All data were analyzed with JMP Version 12 (SAS Institute Inc., Cary, NC, USA). Quantification of LsoA and LsoB was compared with Student's *t* tests. Percentage of normal nuclei and regulation of apoptosis-related genes was determined using one-way ANOVA with Tukey's *post hoc* test.

4.3 RESULTS

4.3.1 Quantification and immunolocalization of Lso in the gut of potato psyllids

To characterize Lso accumulation in the gut, we first quantified Lso in pools of 50 guts of adult potato psyllids by qPCR. The quantification results showed that there were approximately $1.0x10^7$ to $3.0x10^7$ genomes of LsoA or LsoB per pool and there was no significant difference between them ($P > 0.05$) (Fig. 4.1A). Then, Lso was immunolocalized in the gut of LsoA- and LsoB-infected adults (Fig. 4.1B and C). In both cases, Lso distribution was widespread in the gut, and high signal level was observed in the filter chamber or along the actin cytoskeleton of the gut cells (Fig. 4.1B and C). In contrast, no signal was detected in the guts of Lso-free psyllids under the same conditions (Fig. 4.1B).

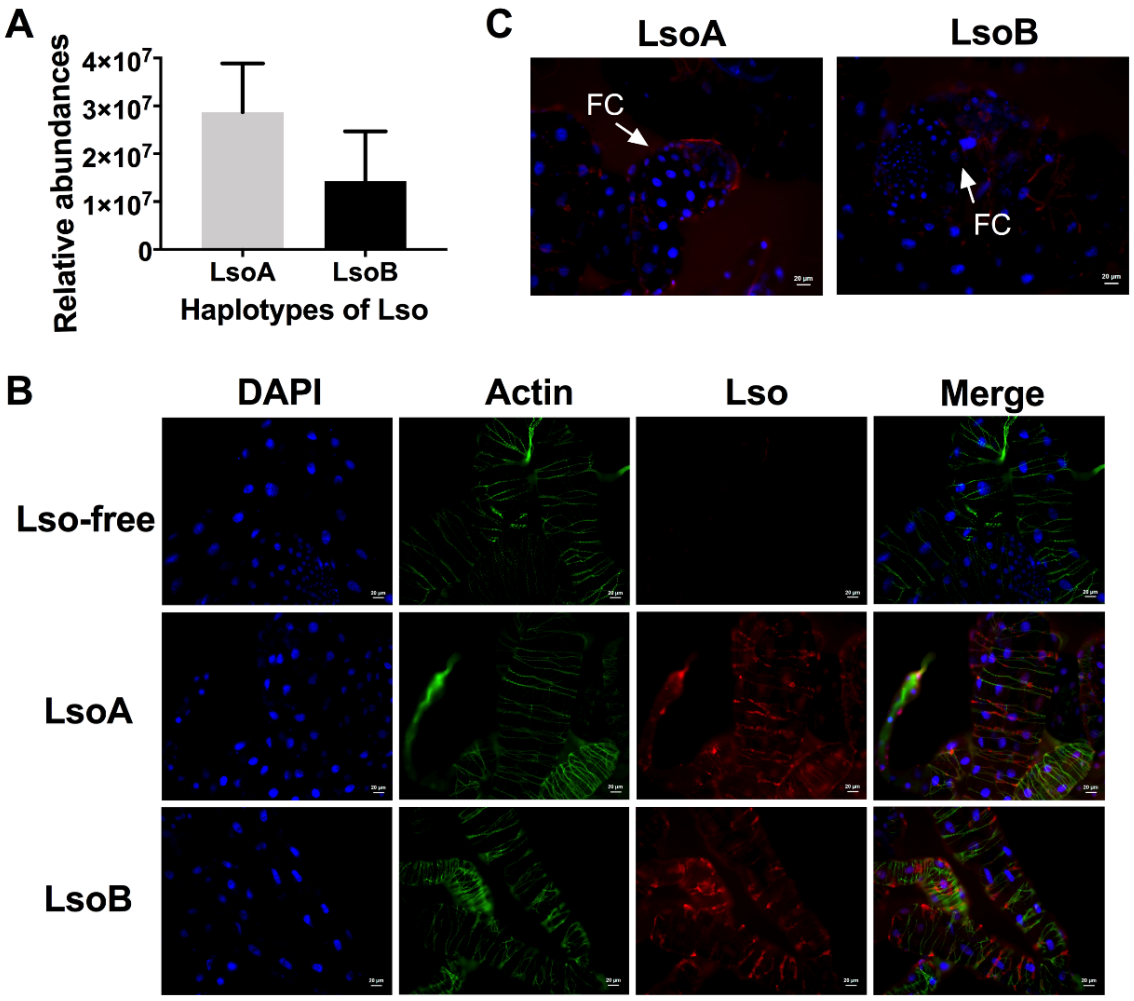

Figure 4.1 Quantification and immunolocalization of Lso in the alimentary canal of potato psyllids. (A) Relative abundances of LsoA (grey) and LsoB (black) in pools of 50 guts from LsoA- and LsoB-infected adult psyllids, respectively (n=3). (B) Immunolocalization of Lso in the midgut of potato psyllids from the Lso-free, LsoA- and LsoB-infected colonies. DAPI-counterstained nuclei are blue, actin is stained in green with phalloidin, and Lso signal is in red; Lso is frequently observed along the actin cytoskeleton. Bar: 20 µm. (C) Immunolocalization of LsoA and LsoB in the filter chamber of potato psyllid. FC: filter chamber. Bar: 20 µm.

4.3.2 Nuclear morphology and actin cytoskeleton architecture

The nuclear architecture and actin cytoskeleton of cells from LsoA- and LsoB-infected adult psyllids were observed and compared to those from Lso-free individuals.

Nuclei from both LsoA- and LsoB-infected gut cells appeared regularly dispersed in the cells and were of uniform round shape and size based on DAPI staining (blue, Fig 4.2A). No differences were observed when comparing the nuclear morphology of the gut cells between the Lso-infected and Lso-free psyllids (Fig. 4.2A). In addition, the number of regular and irregular nuclei were counted and compared among the Lso-infected and Lso-free guts. There were no differences in percentage of cells with irregular nuclei among the guts of Lso-free, LsoA-, and LsoB-infected adult psyllids ($P > 0.05$) (Fig. 4.2B).

The actin cytoskeleton in the gut of Lso-free and Lso-infected adults was stained using phalloidin (green, Fig. 4.2A). In general, the actin filaments appeared organized without disruption and no differences were observed among the Lso-free and Lso-infected insects.

4.3.3 Annexin V cell death assay

An annexin V cell death assay was performed to further determine whether Lso induced apoptosis in the cells of the gut of potato psyllids. The assay showed a similar staining pattern in insects from the different colonies: non-specific signal was observed in the membrane of the gut cells from Lso-free, LsoA-, or LsoB-infected adult psyllids, indicating that these cells were not undergoing apoptosis (Fig. 4.2A).

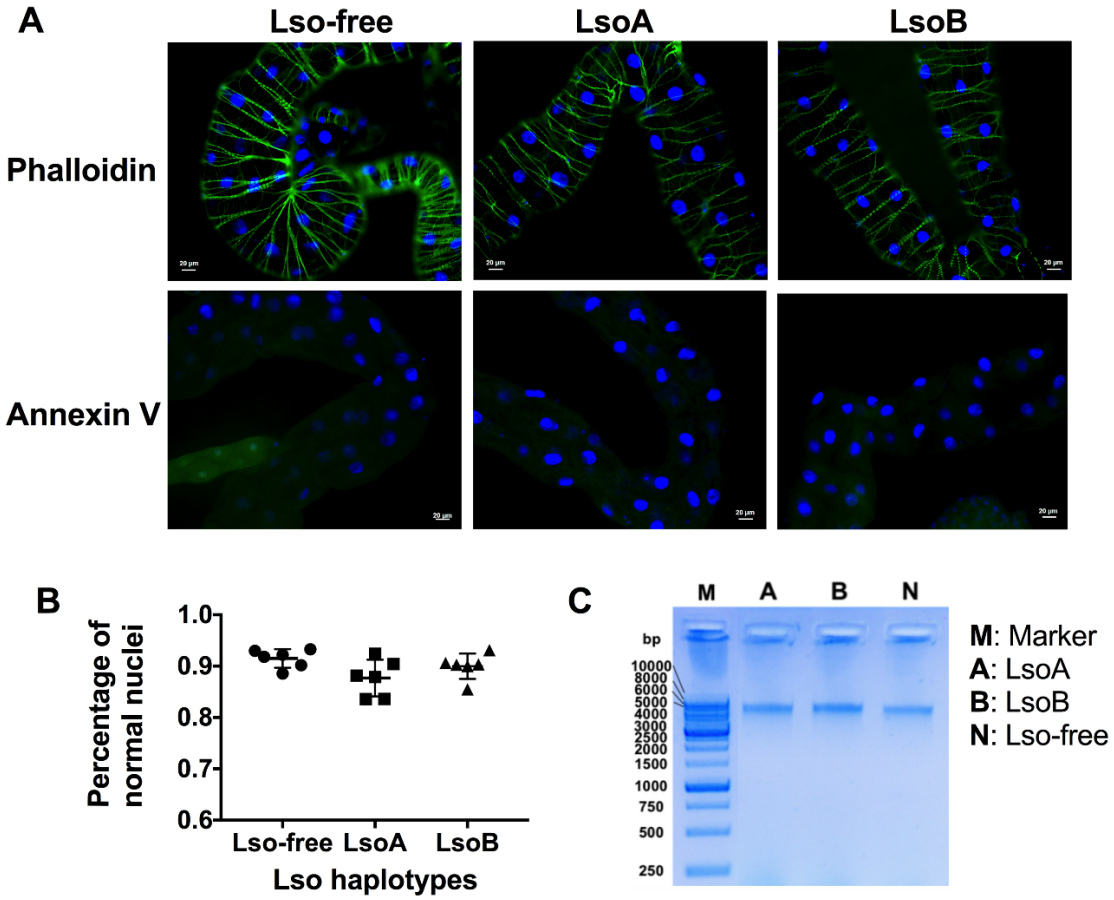

Figure 4.2 Evaluation of the occurrence of apoptosis by microscopy, annexin V cell death assay, and DNA degradation assay. (A) Phalloidin and annexin V staining of Lso-free, LsoA- and LsoB-infected psyllid guts. In the top panel, DAPI-counterstained nuclei are blue and actin is stained in green with phalloidin. In the bottom panel, for annexin V staining, DAPI-counterstained nuclei are blue. Bar: 20 µm. (B) Percentage of normal nuclei in gut epithelial cells of Lso-free, LsoA- and LsoB-infected psyllids. Nuclei from six representative guts from each colony were assessed and counted. (C) Assessment of DNA integrity by agarose gel electrophoresis following extraction from guts of Lso-free (N), LsoA- (A) and LsoB-infected (B) psyllids. M represents molecular weight markers in base pairs.

4.3.4 DNA fragmentation assay

The integrity of the gut DNA from the Lso-free, LsoA- and LsoB-infected psyllids was evaluated by agarose gel electrophoresis. No differences among the samples were

observed (Fig. 4.2C). In particular, there was no detection of a DNA ladder which is a distinctive biochemical feature of apoptosis.

4.3.5 Apoptosis-related genes in potato psyllid

Putative apoptosis-inducing factors (AIF), inhibitors of apoptosis (IAP), and caspases were identified from the psyllid transcriptome datasets (Nachappa et al., 2012a). In total, twelve apoptosis related genes were identified and their sequences were verified, except for IAP6, the Dbruce homolog. The gene names and abbreviations used hereafter are listed in Table 4.1.

Table 4.1 Name of *B. cockerelli* apoptosis-related genes and their codes used in this study.

Gene name	Code
TP53-regulated inhibitor of apoptosis protein 1	TRIAP1
Inhibitor of apoptosis protein 1	IAP1
Inhibitor of apoptosis protein 2	IAPP2
Inhibitor of apoptosis protein 5	IAP5
Baculoviral IAP repeat-containing protein 5	IAPP5
Baculoviral IAP repeat-containing protein 5.2-like	IAPP5.2
Baculoviral IAP repeat-containing protein 6-like[1]	IAP6
Apoptosis-inducing factor 1	AIF1
Apoptosis-inducing factor 3	AIF3
Caspase 1	Caspase 1
Caspase 2	Caspase 2
Caspase 3	Caspase 3

Three caspases were identified: two putative initiator caspases with a long pro-domain (caspase 2 and caspase 3) and one putative effector caspase (caspase 1). A Bayesian inferred phylogenetic analysis of *B. cockerelli*, *A. pisum*, *B. tabaci*, *D. citri,* and *D. melanogaster* caspases clustered these sequences into three distinct clades (Fig. 4.3). Caspase 2 is predicted to contain one CARD (Caspase activation and recruitment domain). This protein clustered with phloem-feeding insect caspases containing CARD, with the exception of *B. tabaci* Caspase 2 (LOC109030899). *A. pisum* was the only species encoding two CARD-containing caspases (LOC100569019 and LOC100571705). These proteins clustered with *D. melanogaster* initiator caspases Dronc, which contains CARD, and Dredd.

Caspase 3 is another predicted caspase with a long pro-domain. It clustered with other long pro-domains-containing caspases (Fig. 4.3). The pro-domains of these caspases were serine- and threonine- (ST-) rich. Two *D. citri* proteins encoded by the loci LOC10350169 and LOC103522950 clustered in this group. Both of these loci are probably incomplete because they appear to lack the C-terminal region. Further, while the protein encoded by LOC103522950 does not have a long pro-domain, it only encodes an 81 amino acid-long protein with 100% identity to the protein encoded by LOC10350169.

One putative effector caspase was identified in *B. cockerelli*, Caspase 1. This caspase clustered with short caspases (Fig. 4.3). *A. pisum* and *D. citri* each encode two putative effector caspases, however, both *D. citri* predicted loci appear to be incomplete. This group of caspases clustered with *D. melanogaster* effector caspases Dcp-1 and DrICE.

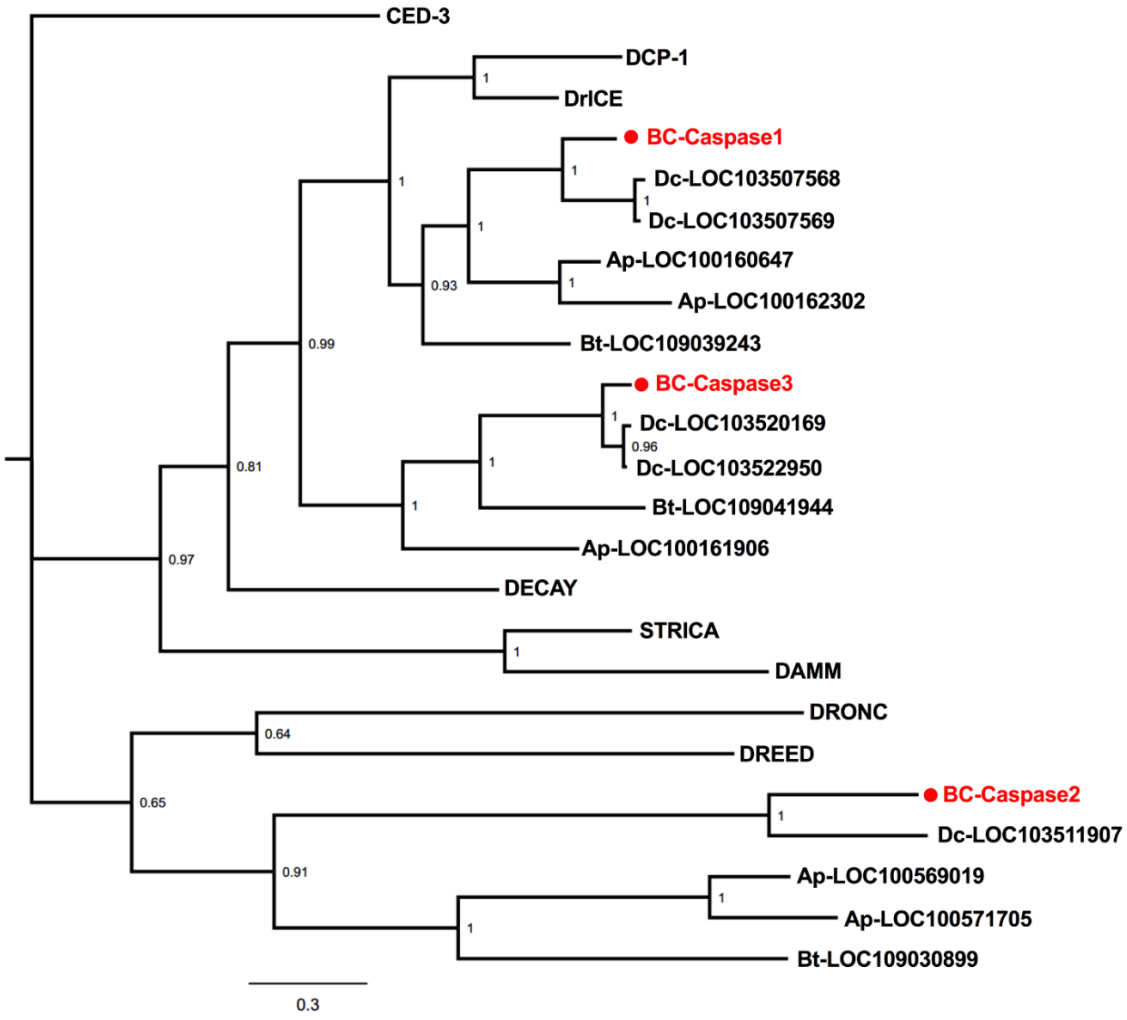

Figure 4.3 Phylogenetic relationships between caspase sequences of *B. cockerelli*, *D. melanogaster*, *A. pisum* and *B. tabaci*. Amino acid alignments of caspase sequences were used to build a phylogenetic tree using a Bayesian inferred method with the *C. elegans* caspase CED-3 as an outgroup. The numbers at the nodes denote posterior probabilities. The red sequences with dots (●) indicate the sequences from *B. cockerelli.* The prefix Bc, Ap, and Bt indicate *B. cockerelli*, *A. pisum and B. tabaci*, respectively.

Seven IAPs were identified in the potato psyllid transcriptome dataset. We identified two deterin-like (IAPP5 and IAPP5.2), one DIAP1-like (IAP1), one DIAP2-like (IAPP2), one Dbruce-like (IAP6), one AAC11-like (IAP5), and one TP53-regulated inhibitor of apoptosis 1-like (TRIAP1) genes. A variable number of IAPs were identified

among the different phloem-feeding species (Table A.7). Of note, one homolog to AAC11 with an API5 domain was identified in each species, except in *D. citri* in which three partial loci are predicted. No Dbruce homolog was identified in *A. pisum,* and several loci with partial similarity to these proteins are predicted in the *D. citri* genome which probably represent different portions of the same gene.

Two putative AIFs were identified in the potato psyllid transcriptome. One showed similarity to AIF3 from several insects including *D. citri* and *D. melanogaster* uncharacterized protein Dmel_CG4199 (e-value 2e-164). The other AIF candidate was similar to AIF1 from several insects, including *D. citri* AIF1-like and *D. melanogaster* apoptosis inducing factor. All phloem-feeding hemipterans encoded two putative AIFs, one with a Pyr-redox_2 and a AIF_c domain (AIF1-type) and one with a Rieske AIFL_N and a Pyr_redox_2 domain (AIF3). The only exception was *D. citri* in which four loci are annotated as potential AIF1 (LOC103523312, LOC103516341, LOC108254404, and LOC103519937), three loci are annotated as AIF3 (LOC103523149, LOC113468611, and LOC103506257), and two loci are annotated as AIF3 pseudogenes (LOC103523148 and LOC103523147).

4.3.6 Expression of apoptosis-related genes

The expression pattern of the identified apoptosis-related genes was evaluated in Lso-free, LsoA-, and LsoB-infected gut samples. Of the twelve tested genes, only three were significantly regulated in response to Lso infection. Specifically, the inhibitor IAPP5 was significantly down-regulated and IAP6 was up-regulated in response to LsoB, while

the inducer AIF3 was significantly down-regulated in response to LsoA (Fig. 4.4). The other nine genes, in particular the three caspase genes, were not regulated in response to either LsoA or LsoB.

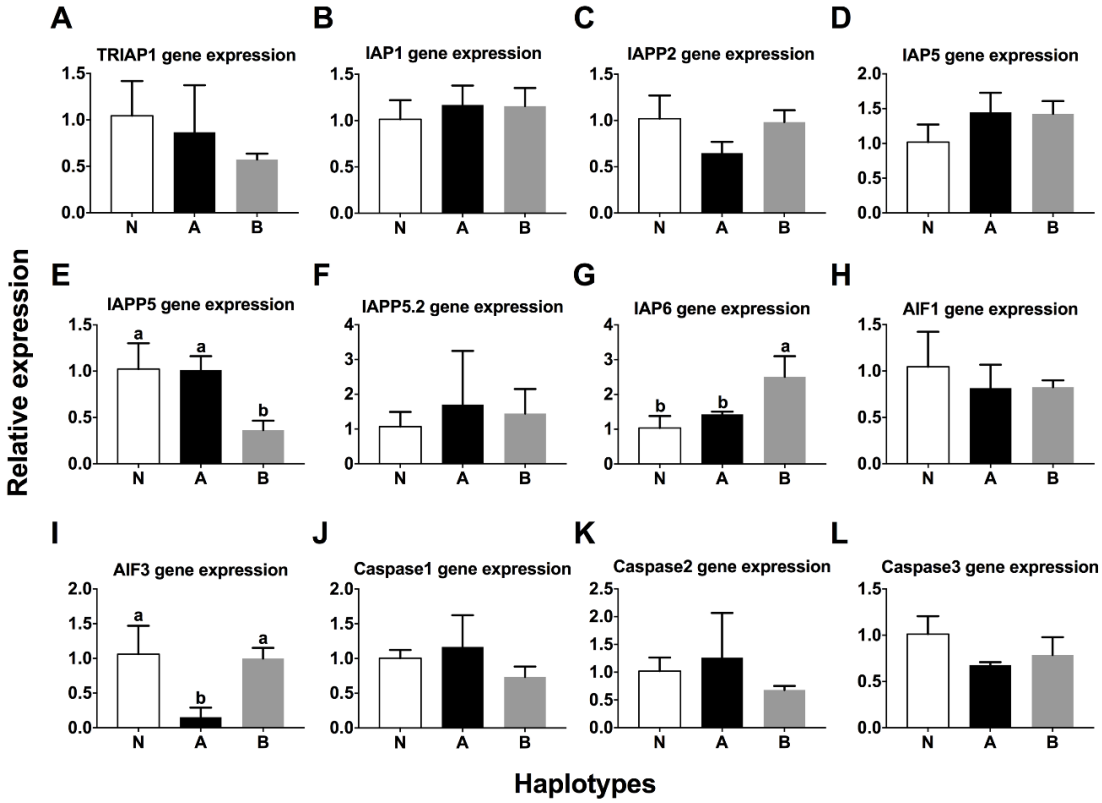

Figure 4.4 Regulation of apoptosis-related genes in the guts of Lso-free, LsoA- and LsoB-infected psyllids. (A) TRIAP1; (B) IAP1; (C) IAPP2; (D) IAP5; (E) IAPP5; (F) IAPP5.2; (G) IAP6; (H) AIF1; (I) AIF3; (J) caspase 1; (K) caspase 2; (L) caspase 3. N: Lso-free; A: LsoA-infected; B: LsoB-infected. Data represent means ± SD of three independent experiments. Different letters indicate statistical differences at $P < 0.05$ using one-way ANOVA with Tukey's *post hoc* test.

4.4 DISCUSSION

Understanding the mechanisms underlying pathogen acquisition by insect vectors is critical for the development of effective strategies to control the diseases they cause.

Recently, it was reported that apoptosis is induced in the gut of adult Asian citrus psyllids from CLas-infected colonies (Ghanim et al., 2016), but no evidence of apoptosis was found in the gut of the nymphs (Ghanim et al., 2016; Mann et al., 2018) or in the gut of adult LsoD-infected carrot psyllids (Ghanim et al., 2017). Further, CLas titer increases at a faster rate when the bacterium is acquired by nymphs compared to adults (Ammar et al., 2016). Therefore, the reduced apoptotic response of nymphs to CLas could be linked to the differences in acquisition between Asian citrus psyllid adults and nymphs. In this study, we examined the molecular interactions between Lso and the potato psyllid gut. Specifically, we first examined the accumulation of two Lso haplotypes, LsoA and LsoB, in the gut of adults, and second, we evaluated whether an apoptotic response was mounted in the gut.

Lso accumulation and colonization sites in the gut were examined by qPCR and immunolocalization, respectively. The results showed that both Lso haplotypes were abundant in the cytoplasm of gut cells. Strong Lso-derived signal was observed in the filter chamber and along the actin cytoskeleton of the gut cells. A similar pattern of accumulation was described for CLas which was also located along the actin cytoskeleton of gut cells in the Asian citrus psyllid (Kruse et al., 2017). In eukaryotic cells, actin cytoskeleton regulates a variety of functions. For example, it provides structure at cell-cell junctions to maintain tissue integrity; it can also dynamically reorganize to promote the formation of membrane extensions or invaginations during cell migration and intracellular trafficking (Lamason & Welch, 2017). Modulation of the host cell actin cytoskeleton by invasive bacteria allows them to control the steps of attachment and entry into cells,

survival in the phagosome, and movement in the cytoplasm (Yam & Theriot, 2004). Some bacterial pathogens such as *Salmonella* use secretion systems to inject protein effectors that interact with the actin cytoskeleton of intestinal epithelium, and then stimulate actin cytoskeleton rearrangements, which promote actin-based motility and coordinate motility with cell-to-cell spread, facilitating further bacterial internalization and colonization in intestinal epithelium (Barreau & Hugot, 2014; Galán, 1999; Ribet & Cossart, 2015; Zhou et al., 2001). We therefore hypothesize that actin cytoskeleton could be involved in the colonization and translocation of *Liberibacter* bacteria in the psyllid gut.

Next, we evaluated whether apoptosis was induced in the potato psyllid gut. No evidence of apoptosis was obtained in the guts of Lso-infected adult psyllids based on nuclei morphology, actin cytoskeleton architecture, analysis of DNA fragmentation, or annexin V cell death assays. Two hypotheses for the reduced apoptotic response of potato psyllid adults in response to Lso infection can be proposed. First, the Lso-induced intracellular immune response did not reach or exceed the threshold to trigger an intracellular apoptotic immune reaction (Maiuri et al., 2007). Although CLas and Lso have similar genomes (Lin et al., 2011; Thompson et al., 2015; Wang et al., 2017; Wulff et al., 2014), their effects on the respective vectors are distinct (Nachappa et al., 2012b; Pelz-Stelinski & Killiny, 2016). Also, we speculate that other factors may be involved in the interactions between psyllids and *Liberibacter* bacteria. For example, CLas and Lso infect different host plants, and the insects mount responses not just to the pathogen, but also to the defense compounds from the infected plant (Ghanim et al., 2016). The second hypothesis is that Lso may inhibit the insect immune response, which could lead to a high

acquisition efficiency by potato psyllids. Indeed, potato psyllid adults efficiently transmit Lso even when the pathogen is acquired by adults (Sengoda et al., 2014).

Because apoptosis has emerged as a potential mechanism involved in pathogen transmission, we identified putative apoptosis-related genes in the potato psyllid transcriptome and performed a comparative analysis with other phloem-feeding hemipterans that are also vectors of plant pathogens. We found that phloem-feeding hemipterans had a reduced set of caspase genes in comparison with *D. melanogaster.* We identified three putative caspases in *B. cockerelli*. Caspases 2 and 3 were characterized by long pro-domain. Caspase 2 is predicted to encode a CARD which is found in initiator caspases, and it clustered with other CARD-containing caspases including *D. melanogaster* Dronc which is essential for apoptosis during multiple biological processes including development (Kumar & Doumanis, 2000). The Caspase 3 pro-domain was ST-rich, which is a feature only found in insects, for example in *D. melanogaster* Strica. No homolog to *D. melanogaster* Dredd was identified in the potato psyllid transcriptome or any of the other phloem-feeding insect analyzed. Dredd is under the control of the IMD pathway activating the innate immunity in response to Gram-negative bacteria (Leulier et al., 2000). The absence of a Dredd homolog in the phloem-feeding insects evaluated fits the hypothesis that these insects lack a complete IMD pathway; for example, the genome of pea aphid has been sequenced and shown to lack genes or key components in the IMD pathway; the IMD pathway genes are also notably absent from the transcriptome of the Asian citrus psyllid and potato psyllid (Gerardo et al., 2010; Kruse et al., 2017; Nachappa et al., 2012a). Only one putative executioner caspase was identified, Caspase 1, which

clustered with the *D. melanogaster* executioner caspases Dcp-1 and DrICE, which have overlapping functions (Xu et al., 2006).

On the other hand, more potential IAPs were identified in potato psyllids and in the other phloem-feeding hemipterans compared to *D. melanogaster*. We identified a homolog of *D. melanogaster* DIAP1 which regulates cell death by binding and inactivating Dronc (Meier et al., 2000; Wilson et al., 2002), and can interact with DrICE and DCP-1 (Zachariou et al., 2003). We also identified a homolog of *D. melanogaster* DIAP2 in psyllids. DIAP2 exclusively regulates DrICE and does not bind other caspases (Leulier et al., 2006b). This protein is involved in the IMD pathway as signal transducer downstream the activation of Dredd instead of as a modulator of apoptosis (Leulier et al., 2006a). Similarly, we identified a homolog of Dbruce which inhibits apoptosis through ubiquitination of the IAP-antagonist Reaper (Domingues & Ryoo, 2012). We identified two homologs of Deterin which controls cytokinesis (Silke & Vaux, 2001). One AAC11 homolog was identified which prevents apoptosis after growth factor deprivation (Tewari et al., 1997) by directly binding Caspase 2 CARD regulating cell death, autophagy and aging (Imre et al., 2017). Finally, we identified a homolog of TP53-regulated inhibitor of apoptosis 1 is a small conserved protein induced by TP53 under low levels of genotoxic stress, contributing to a reduction in cell death (Park & Nakamura, 2005).

Two AIF proteins were identified in each phloem-feeding species. AIF proteins are mitochondrial oxidoreductase proteins critical for energy metabolism and induction of caspase-independent apoptosis.

Only three of these genes were regulated in response to Lso infection. AIF3 was down-regulated in the gut of the LsoA-infected adult psyllids, while the deterin-like IAPP5 was down-regulated, and IAP6 was up-regulated in the gut of LsoB infected adult psyllids. None of the caspases were regulated in the gut of the potato psyllids in response to Lso. Caspases can be regulated in the gut of vectors in response to pathogens. For example, expression of *Aedronc*, *Aedredd*, and the Strica homolog *caspase 16* increased in the gut of *Aedes aegypti* females from a refractory strain compared to the susceptible strain following a blood meal containing dengue-2 virus (Ocampo et al., 2013). Therefore, the gene expression results obtained here are in line with the previous evidence that Lso does not induce apoptosis in the gut of the adult potato psyllid.

Although the pathogen-vector systems of CLas-Asian citrus psyllid and Lso-potato psyllid are largely similar, the adaptive evolution of the insect vectors with the bacteria might have resulted in different infection strategies. Asian citrus psyllid might exploit the apoptotic response to limit the transmission of CLas, while this does not appear to occur in the potato or carrot psyllid in response to Lso. Therefore, the types of interaction between potato psyllid and Lso need to be evaluated. The information provided in this study in regards to Lso accumulation and the potato psyllid responses elicited by these bacteria may contribute to develop alternative control strategies that could interfere with *Liberibacter* bacteria transmission.

CHAPTER V

'*CANDIDATUS* LIBERIBACTER SOLANACEARUM' INHIBITS APOPTOSIS IN *BACTERICERA COCKERELLI* GUT TO FACILITATE ITS ACQUISITION AND COLONIZATION

5.1 INTRODUCTION

Apoptosis, one of the programmed cell death forms, is an essential physiological process that can occur in response to intracellular or extracellular signals. It plays a critical role in a variety of biological events including development and tissue homeostasis (Liu et al., 2008; Zimmermann et al., 2001). Apoptosis is an evolutionarily conserved mechanism orchestrated by multiple proteins (Kornbluth & White, 2005). Some of the key proteins mediating apoptosis are caspases, a family of conserved intracellular aspartate-specific cysteine proteases (Lamkanfi et al., 2002; Shi, 2004). Once an initiator caspase is activated, it processes downstream effector caspases that are responsible for apoptosis (Earnshaw et al., 1999). Because apoptosis signaling mediated by caspases is an irreversible process (Elmore, 2007), caspase activities must be precisely regulated in order to prevent the undesired death of the organism cells (Goyal, 2001; Liu et al., 2008). Direct inhibition of caspase activity by inhibitor of apoptosis proteins (IAPs) is one of the most important mechanisms for apoptosis inhibition (Bergmann, 2010). To date, eight human IAPs have been identified, including NAIP, c-IAP1, c-IAP2, XIAP, Survivin, Bruce, ILP-2, and Livin (Salvesen & Duckett, 2002). However, the *Drosophila* genome encodes four IAPs: DIAP1, DIAP2, dBruce, and Deterin, the latter protein is a survivin homolog (Hay,

2000; Xu et al., 2009). IAPs are characterized by the presence of one to three baculoviral IAP repeat (BIR) domains, which are required for binding and suppression of specific cell death-inducing caspases (Pedersen et al., 2014).

Apoptosis also plays essential roles in the innate immune system, leading to the rapid destruction of cellular structures or organelles (Danial & Korsmeyer, 2004; Green, 2005). Host cells can employ apoptosis as a defense mechanism to impede replication and spread of intracellular pathogens. However, because intracellular pathogens often rely on the host cell machinery to complete their life cycle and also require intact host cells to shield themselves from the host immune defense system, many intracellular pathogens are able to manipulate the apoptosis pathways of the host cells (Gao & Kwaik, 2000). Indeed, some pathogens such as *Shigella* and *Salmonella* can hijack the immune responses of the host and take control over the fate of the host cells (Gao & Kwaik, 2000). These pathogens are either directly or indirectly engaged in the host cell apoptotic pathways, and many of them target the caspase signaling to impede apoptosis of the infected host cells (Liu et al., 2008).

'*Candidatus* Liberibacter solanacearum' (Lso), are Gram-negative, intracellular and unculturable bacteria infecting crops worldwide. Presently, seven Lso haplotypes (LsoA, LsoB, LsoC, LsoD, LsoE, LsoF, and LsoU) of this pathogen exist in the world (Glynn et al., 2012; Haapalainen et al., 2018; Lin et al., 2012; Nelson et al., 2013; Swisher Grimm & Garczynski, 2019), which are transmitted by several psyllid species and result in large yield loss among different crops. Haplotypes LsoA and LsoB are mainly present in North America where they are transmitted by the potato psyllid (also known as the

tomato psyllid), *Bactericera cockerelli* (Šulc) (Hemiptera: Triozidae). LsoA and LsoB can infect numerous solanaceous crops and cause damaging diseases such as zebra chip in potatoes (Liefting et al., 2009a; Tamborindeguy et al., 2017). Lso is transmitted by psyllids in a circulative and persistent manner (Cicero et al., 2016; Cicero et al., 2017; Cooper et al., 2014). Despite our understanding of its circulation route within the insect body, the molecular mechanisms underlying the transmission process remain largely unknown. The psyllid gut is the first organ Lso encounters and therefore provides an essential link for understanding the biology of Lso acquisition or transmission within the potato psyllid.

Importantly, the psyllid gut could act as a barrier for Lso transmission and determine Lso transmission efficiency. Indeed, the ability of the bacteria to infect the gut depends on the insect immune responses as well as the bacterial strategies deployed to disrupt the host immunity (Vyas et al., 2015). An increasing number of studies have demonstrated that apoptosis in insect vectors can be induced by insect-borne plant pathogens. For instance, apoptosis was observed in the gut of Asian citrus psyllid (*Diaphorina citri*) adults from the '*Ca.* L. asiaticus' (CLas)-infected colonies, but not in the nymphal gut (Ghanim et al., 2016; Mann et al., 2018). It is probable that the apoptotic response serves to limit the acquisition or transmission efficiency of CLas by the Asian citrus psyllid. Indeed, CLas titer increased at a faster rate when the bacterium was acquired by nymphs compared to adults (Ammar et al., 2016). In contrast to CLas, in the last chapter, we showed no evidence of apoptosis was uncovered in the gut of the Lso-infected adult potato psyllids (Tang & Tamborindeguy, 2019). However, all these studies focused on the insects from infected colonies, which most likely acquired the bacteria during the nymphal

stages. It is still possible that apoptosis is induced at the early stages of infection of formerly naïve adults, but as the infection becomes persistent, as in the case of adults from the Lso-infected colonies, there is no evidence of apoptosis. Another possibility is that Lso could manipulate the gut immune response to favor its acquisition or transmission. Interestingly, while adults can efficiently transmit LsoA and LsoB if the pathogens were acquired during the nymphal stages, we have discovered that adults can acquire and transmit LsoA with lower efficiency than LsoB (Chapter II). Therefore, it is still necessary to investigate the apoptotic response in the gut of psyllids upon Lso infection.

In the present study, we investigated the apoptotic response of the adult potato psyllid gut during the early stages of Lso infection. First, the accumulation of the two Lso haplotypes A and B was determined during the early infection period. Second, the occurrence of changes in nuclear morphology, actin cytoskeleton, and the integrity of the gut cell DNA were evaluated because these changes are hallmarks of apoptosis. Third, the expression of apoptosis-related genes (Chapter IV) was evaluated at key time points during the early infection period. Finally, we explored whether Lso could be exploiting the psyllid's cell machinery to avoid the apoptotic immune defenses thereby affecting its acquisition or the colonization of the gut. The present study not only provides insights into the interactions occurring between Lso and its insect vector, the potato psyllid, at the gut interface, but could also represent a stepping stone towards the development of novel control strategies to disrupt the pathogen transmission within insect vector.

5.2 MATERIALS AND METHODS

5.2.1 Insect colonies and tomato plants

Lso-free, LsoA- and LsoB-infected psyllid colonies were maintained separately on tomato plants (Moneymaker; Victory Seed Company, Molalla, OR) in insect cages (24 × 13.5 × 13.5 cm, BioQuip®, Compton, CA) at room temperature 24 ± 1°C and photoperiod of 16: 8 h (L: D) as described in Yao et al. (2016).

To obtain Lso-infected tomato plants, six-week-old tomato plants were infected as described in Nachappa et al. (2014) using three male psyllids harboring LsoA or LsoB, respectively. After one week, the psyllids were removed from the tomato plants. Three weeks after Lso inoculation, the plants were tested for Lso infection using the LsoF/OI2 primers (Li et al., 2009) and the Lso haplotype in the plants was confirmed using the Lso SSR-1 primers (Lin et al., 2012).

5.2.2 Psyllid exposure to Lso and gut dissection

Approximately seven-day-old Lso-free adult psyllids were transferred to LsoA- or LsoB-infected tomato plants. To determine the acquisition profile of LsoA and LsoB in the gut of psyllids, insects were collected after 2-, 3-, 5-, or 7-day acquisition access periods (AAPs) on LsoA- or LsoB-infected plants (Fig. 5.2A). For each specified exposure time, the guts from the LsoA- or LsoB-exposed psyllids were dissected under the dissecting microscope as described in Ibanez et al. (2014a) for Lso quantification and immunolocalization. DNA from pools of 50 guts was purified following the protocol of blood/tissue DNA extraction kit (Qiagen, Hilden, Germany); each pool was used as an

individual template for quantitative real-time PCR (qPCR) analysis. Thus, each pool of 50 guts represented one replicate, there were three replicates for each combination of exposure time point and haplotype. Each replicate was obtained by using independent LsoA- or LsoB-infected plants as Lso inoculum.

5.2.3 Quantification of Lso

The Lso 16S rDNA specific primers (LsoF: 5'-CGAGCGCTTATTTTTAATAGGAGC-3' and HLBR: 5'-GCGTTATCCCGTAGAAAAAGGTAG-3') (Li et al., 2009; Li et al., 2006) were used for Lso quantification in the guts of adult psyllids, and the psyllid 28S rDNA primers (28S rDNAF: 5'-AGTTTCGTGTCGGGTGGAC -3' and 28S rDNAR: 5'-AACATCACGCCCGAAGAC-3') (Nachappa et al., 2014) were used as internal control. Quantitative PCR (qPCR) was performed using SYBR Green Supermix Kit (Bioline, Taunton, MA) according to manufacturer's instructions. Each reaction contained 25 ng of DNA, 250 nM of each primer, and 1X of SYBR Green Master Mix; the volume was adjusted with nuclease-free water to 10 µL. The qPCR program was 95 °C for 2 min followed by 40 cycles at 95 °C for 5 sec and 60 °C for 30 sec. qPCR assays were performed using a QuantStudio™ 6 Flex Real-Time PCR System (Applied Biosystems, Foster City, CA). Reactions for all samples were performed in triplicates with a negative control in each run. In order to standardize the amount of Lso in psyllid guts, data are reported as delta Ct = (Ct of Lso gene) - (Ct of psyllid 28S gene). The biological replicates were analyzed and the average delta Ct value was used to quantify the levels of Lso. A standard

curve was prepared for the quantification of Lso in the psyllid guts using a plasmid containing the Lso 16S rDNA target. For the standard curve, 10-fold serial dilutions of the plasmid were performed. The procedure for the standard curve preparation and the calculations of molecules (relative abundances) followed the methods described in Levy et al. (2011). The Lso relative abundance in each sample was estimated by comparing delta Ct values of each sample to the standard curve.

5.2.4 Immunolocalization of Lso in psyllid guts

Immunolocalization was used to visualize Lso in the Lso-exposed psyllid alimentary canal tissues. The psyllid guts were dissected in 1X phosphate buffered saline (PBS) (Sigma-Aldrich, St. Louis, MO) from adults which were infected for 2, 3, 5, and 7 days (Fig. 5.1A). Then the guts were fixed in 4% paraformaldehyde for 30 min at room temperature. After fixation, the guts were incubated with Sudan Black B (SBB) (Sigma-Aldrich) for 20 min to quench the autofluorescence as described in Tang et al. (2019). Next, the guts were permeabilized by adding 0.1% Triton X-100 (Calbiochem/EMD Chemicals, Gibbstown, NJ) for 30 min at room temperature, and washed three times with PBS containing 0.05% Tween 20 (PBST) prior to a 1 h blocking at room temperature with blocking buffer (PBST with 1% [w/v] bovine serum albumin). Lso immunolocalization was performed using a rabbit-derived polyclonal antibody (GenScript Corp, Piscataway, NJ) directed against Lso outer membrane protein (OMP) raised against the synthesized peptide OMP-B “VIRRELGFSEGDPIC” which reconizes LsoA and LsoB OMP-B protein (Tang & Tamborindeguy, 2019). The guts were incubated with the antibody

(diluted 1: 500) overnight at 4 °C. The guts were then washed three times with PBST and incubated with Alexa Fluor 594 goat anti-rabbit IgG secondary antibody (diluted 1: 2000; Invitrogen, Carlsbad, CA) for 1 h at room temperature. The guts were washed again three times with PBST, and mounted with one drop of Vectashield mounting medium with 4′,6-diamidino-2-phenylindole (DAPI) (Vector Laboratories Inc., Burlingame, CA) on a microscope slide. The slide was covered with a glass coverslip and sealed with nail polish. At least 20 guts per exposure time point and haplotype were examined using an Axioimager A1 microscope (Carl Zeiss microimaging) using the rhodamine filter (594 nm, red) and the images were collected and analyzed with the Axiovision Release 4.8 software (Carl Zeiss).

5.2.5 TUNEL assay

To test the integrity of the genomic DNA in gut cells after Lso exposure, the 2-, 3-, 5-, and 7-day Lso-exposed guts were dissected as previously described. The dissected guts were fixed in 4% paraformaldehyde for 2 h at room temperature. After that, the guts were blocked by 5% bovine serum albumin in 1×PBS with 0.1% Tween 20, then incubated with TUNEL (terminal deoxynucleotidyl transferase dUTP nick end labeling) for 6 h as described in Wang et al. (2018). TUNEL staining was performed using the In Situ Cell Death Detection Kit (Roche, Basel, Switzerland). After washing three times in PBS, the guts were mounted using Vectashield mounting medium with DAPI as described above. At least 20 guts per exposure time point and haplotype were observed using the FITC (488

nm, green) filter. The images were collected and analyzed with Axiovision Release 4.8 software (Carl Zeiss).

We also applied the apoptosis inducer Concanavalin A (ConA) treatment by feeding, as a positive control. Following the protocol of Sprawka et al. (2015) with modifications, the liquid diet used for psyllids feeding bioassays was prepared with a sterilized solution of 15% (w: v) sucrose and 1X PBS (Sigma-Aldrich, St. Louis, MO). ConA (MP Biomedicals, Solon, OH) was incorporated into the diet at a concentration of 2,000 μg/mL (Sprawka et al., 2015). Young adults were placed in plastic feeding chambers (h = 2 cm, Φ = 3 cm), which were covered by two sheets of Parafilm with 100 μL of the liquid diet described above in between the two layers. Next, the guts from the ConA-treated psyllids were dissected after 72 h of feeding. The dissected guts were incubated with TUNEL as described above.

5.2.6 Nuclear morphology and actin cytoskeleton architecture

To investigate whether Lso impact the nuclear morphology and actin cytoskeleton architecture of the psyllid gut cells, the guts from 2-, 3-, 5-, and 7-day Lso-exposed psyllids were dissected and fixed as previously described. After fixation, the guts were first incubated with SBB to remove autofluorescence, then incubated with phalloidin for actin staining (dilution 1:200; Invitrogen). The guts were washed again three times with PBST and mounted with one drop Vectashield mounting medium with DAPI as previously described. At least 20 guts per exposure time point and haplotype were examined using Axioimager A1 microscope (Carl Zeiss microimaging) using the FITC (488 nm, green)

filter. The images were collected and analyzed with Axiovision Release 4.8 software (Carl Zeiss).

5.2.7 Expression of apoptosis-related genes

The apoptosis-related genes were identified through searching the psyllid transcriptome datasets in our previous studies (Chapter IV) (Nachappa et al., 2012a; Tang & Tamborindeguy, 2019). Three caspases and four IAPs with BIR domain(s) were selected to evaluate the gene expression in the psyllid gut upon Lso infection. The gene names and codes are listed in Table 5.1. Of the three caspases, caspase 2 is the initiator caspase, and caspases 1 and 3 are effector caspases. Of the four IAPs, one DIAP1-like gene (IAP1), one DIAP2-like gene (IAP2), and two Deterin/Survivin-like genes (IAPP5 and IAPP5.2) were identified. Seven-day-old Lso-free female adult psyllids were transferred to LsoA- or LsoB-infected plants for 2, 3, 5, and 7 days (Fig. 5.1A). Lso-free colony was used as a control. Three replicates were conducted for each treatment, and each replicate and each time point had 200 psyllid individuals. After exposure, the psyllid guts were dissected under the stereomicroscope (Olympus) as previously described. RNA from pools of guts was purified using the RNeasy Mini Kit (Qiagen). Genomic DNA was eliminated by DNase I treatment with Turbo DNase (Ambion, Invitrogen). Then, the total RNA was reverse transcribed using the Verso cDNA Synthesis kit (Thermo, Waltham, MA) and anchored-Oligo (dT) primers following the manufacturer's instructions. The expression of apoptosis-related genes in the psyllid guts upon Lso infection was evaluated by qPCR using SensiFAST SYBR Hi-ROX Kit (Bioline) according to the manufacturer's

instructions. The primers for qPCR are listed in Table A.8. The qPCR reaction and program were performed as described above. The relative expression of the candidate genes were estimated with the delta delta CT method (Schmittgen & Livak, 2008), using two reference genes elongation factor-1a (GenBank KT185020) and ribosomal protein subunit 18 (GenBank KT279693) (Ibanez & Tamborindeguy, 2016).

Table 5.1 The gene name and code of apoptosis-related genes.

Gene name	Code
Inhibitor of apoptosis isoform X1	IAP1
Baculoviral IAP repeat-containing protein 2	IAP2
Baculoviral IAP repeat-containing protein 5	IAPP5
Baculoviral IAP repeat-containing protein 5.2-like isoform X1	IAPP5.2
Caspase-1 isoform X1	Caspase1
Caspase-2-like	Caspase2
Caspase-3 (CASP3)	Caspase3

5.2.8 RNA interference (RNAi) of IAPP5.2 and its effect on Lso acquisition

The T7 promoter was incorporated into the 5'-end of the forward and reverse IAPP5.2 primers (Table A.8 and Fig. 5.1) to enable *in vitro* transcription. The targeted region was blasted against the transcriptome of potato psyllid (Nachappa et al., 2012a) to ensure its specificity. Double-stranded RNA (dsRNA) were synthesized via the MEGAscript RNAi kit (Invitrogen) using PCR-generated DNA template that contained the T7 promoter sequence at both ends. The dsRNA quality was monitored by agarose gel electrophoresis. dsRNA of the *Aequorea victoria* green fluorescent protein (GFP) was used as a control. RNAi was performed by feeding assay using liquid diet with dsRNA.

Specifically, the liquid diet used for psyllid feeding bioassay was prepared with a sterilized solution of 15% (w: v) sucrose and 1×PBS (Sigma-Aldrich, St. Louis, MO). dsRNA was incorporated into the diet at a concentration of 500 ng/μL. Young female adults from the Lso-free colonies were collected and placed in plastic feeding chambers (h = 2 cm, Φ = 3 cm) for four days. The chambers were covered by two sheets of parafilm with 60 μL of the above liquid diet in between the two layers. The diet was refreshed every two days. There were three replicates with 30 psyllid individuals each. After silencing, the gene expression of apoptosis-related genes and TUNEL assays were performed as described above. The primers for testing silencing can be found in Table A.8 and and Fig. 5.1.

To examine the effects of silencing IAPP5.2 on the accumulation of LsoA or LsoB in the psyllid guts, 30 young psyllids were allowed to feed on LsoA- or LsoB-infected tomato plants for two days before a 4-day feeding on the dsRNA-containing diet. The same number of guts from the control (dsGFP) and IAPP5.2 RNAi treatments were dissected for Lso quantification.

5.2.9 Data analysis

All data were analyzed with JMP Version 12 (SAS Institute Inc., Cary, NC, USA). For gene expression results upon Lso infection, different letters indicate statistical differences at $P < 0.05$ using one-way ANOVA with Tukey's *post hoc* test. For RNAi assays, gene expression and quantification of Lso were determined with Student's t tests.

5′~AGCCGGTGTATTGAAAGTGCCATCGACGCGACGACGCTAGGTCAAAAAGGCGTTAGTTCTTCAGTGATACCTCTAGGA
TGGAAGAGAAAGCAAAATGGCCAGTTCAAGTTCAGGAATATGTTCAGTAGGAGAGTGATGGCAGATTGCTTCACAACGTAA
TCAGTCTCTCCAGTTTCTTGCTTGTTCGGGGGATGGAAAACACGCGTACTCTATCCTCTCTACGAGACCTACTCACGCCGT
ATCTGAGCGGGACTCAGAAGAAAACCCTGCGCATGACTTTCTATCGGAACAGGCTGAAGTCTTTCATCAGCTGGCCGTTCA
CTTCGGCCGGCGACGTGTGTTCGGCCGAGAGCATGGCCGCGGCCGGCTTCTATTCCATTTCCAAGCGGAAGAATGACACCT
CGGTCAAGTGTTTCGTGTGCCTGAAGGAGCTGGATGGGTGGGAGGCGAGGGATGACCCCTGGGAGGAGCATAGGAGACACC
AGGGGGCGTGTCCTTACGTCCAGCTGGGCAAGAGGGAGGACCAGTGGACGCTGGAGGACTGGGTGGCGCTGCAGGAGGGCG
TGGCCGTGAGGCTCTTGGAGGAAAAACAGAACATGGATTTGGAAAATTTGGAAGAACAACTCAAAACTAATGAGAGGAAGC
TGCAGAAAGAAAGAAAGAGGAAGCGAAAATGAGACAACCTGACTTTCAGGATGGGATTAGCTATCCTCATGCTAGATCTTT
ACATCAATAAGTAAATCAGCTAGATGTGCTAGATCTGGTCTGAAAACGTAATGTACCAGTGTTGTTTGAATGTGGGAAGTA
ATAAAAATGTAATAATAA~3′

Figure 5.1 The cDNA sequence of IAPP5.2 gene used for RNAi in this study. The primers for dsRNA amplification are indicated in boxes. The primer for testing silencing are indicated by underlines. The green highlight indicates initiation codon and the red highlight indicates termination codon.

5.3 RESULTS

5.3.1 LsoA and LsoB quantification in the gut of adult potato psyllids

To understand the characteristics of Lso acquisition, each Lso haplotype was quantified in the gut of psyllids following different AAPs. The results showed that both LsoA and LsoB were detectable with ~10,285 genome equivalent copies in pools of 50 guts of adult potato psyllids at the beginning of infection (2-day AAP) (Fig. 5.1B). Similar Lso titers were measured after a 3-day AAP. However, after three days, LsoB titer increased rapidly with on average ~60,031 genome equivalent copies after a 5-day AAP, and reached a high level of ~98,896 genome equivalent copies after a 7-day AAP. In contrast, the titer of LsoA did not increase over time. In addition, LsoB titer was significantly higher than LsoA titer after five days of AAP ($P < 0.05$).

Comparable results were obtained by immunolocalization of Lso in the psyllid guts. No obvious LsoA or LsoB signal could be observed after a 2-day AAP (Fig. 5.2C).

However, weak LsoA- or LsoB-derived signal could first be observed after the 3 days of AAP. In accordance with the quantification analysis by qPCR, LsoA signal remained low after the 5-day and 7-day AAPs; however, increasing LsoB signal was observed after the 5-day AAP. In particular, the LsoB-derived signal was strong and more widespread after seven days of AAP (Fig. 5.2C).

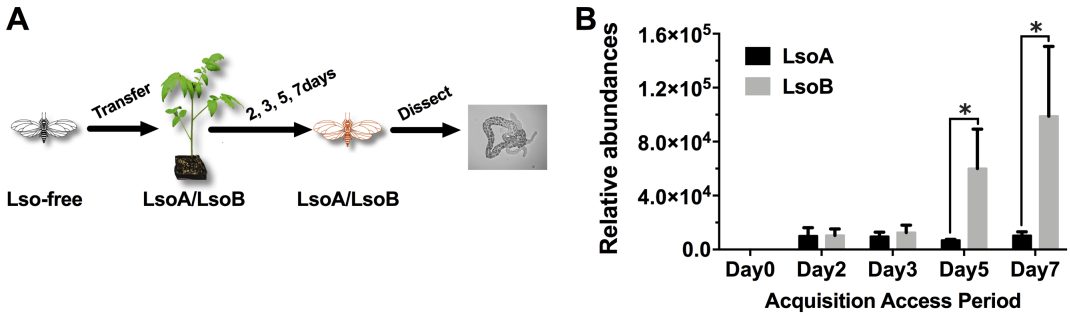

Figure 5.2 Quantification and immunolocalization of Lso in the gut of potato psyllids following continuous acquisition. (A) Adult psyllids were transferred to LsoA- or LsoB-infected tomato plants for 2-, 3-, 5-, and 7-day AAPs, then their guts were dissected for quantification and immunolocalization as shown in the schematic representation. (B) Quantification analysis of Lso relative abundances in the gut of potato psyllids following Lso acquisition. The bars represent the relative abundances of LsoA (black) and LsoB (grey) in pools of 50 guts following a 0-, 2-, 3-, 5-, and 7-day AAP. Data represent means ± SD of three independent experiments. *indicate statistical differences at $P < 0.05$ using the Student's *t* test. (C) Immunolocalization of LsoA and LsoB in the gut of potato psyllids following Lso acquisition. The white dashed rectangle indicates the enlargement region of upper panels. White arrows indicated the Lso signals. The Lso signals can be first observed at infection day 3. The bars of upper and lower panels are 20 μm and 10 μm, respectively.

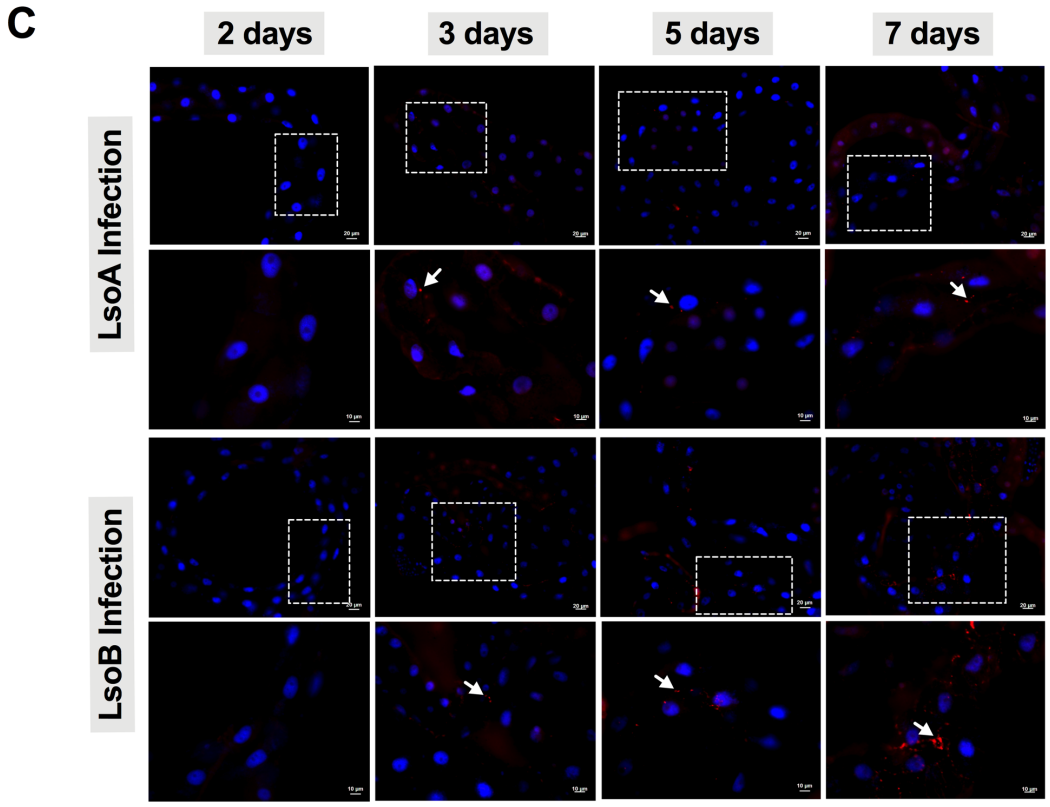

Figure 5.2 Continued

5.3.2 TUNEL assay, nuclear morphology and actin cytoskeleton architecture

The DNA fragmentation of the psyllid gut cells was tested following the 2-, 3-, 5-, and 7-day based on TUNEL assay. No signal of DNA fragmentation was detected in the newly Lso-infected guts (Fig. 5.3 shows the results following the 7-day AAP). In contrast, a number of cell nuclei from the ConA-treated psyllid guts (positive control) showed signals of DNA fragmentation (Fig. 5.3). In addition, the nuclear morphology and actin cytoskeleton architecture of the psyllid gut cells were observed following 2-, 3-, 5-, and 7-day acquisition of LsoA or LsoB based on DAPI and phalloidin staining, respectively. The results showed that both LsoA- or LsoB-exposed gut nuclei appeared regularly

dispersed in the cells and were of uniform round shape and size based on DAPI staining (blue, Fig. 5.4). The actin filaments in those guts appeared organized as well (green, Fig. 5.4).

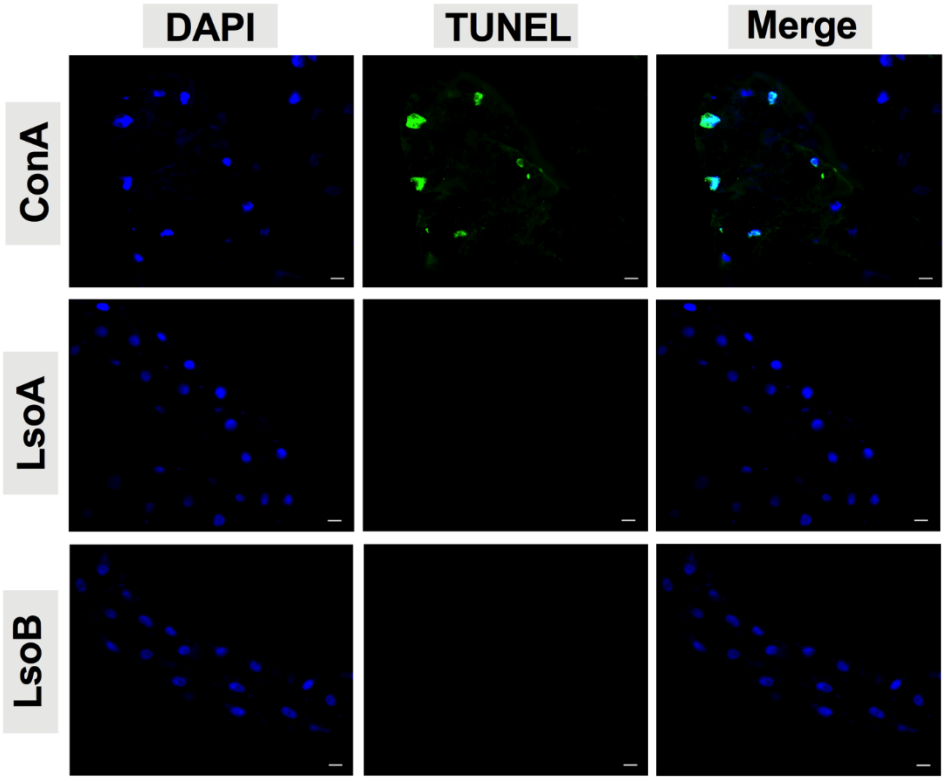

Figure 5.3 Lack of apoptosis in Lso-exposed potato psyllid gut using TUNEL. The newly Lso-exposed guts were stained using TUNEL to detect the apoptotic signals (green) and counterstained with DAPI to show the nuclei (blue) of the gut cells. The ConA treatment was used as a positive control and DNA degradation was detected. Only 7-day LsoA- or LsoB-exposed guts are shown, similar results were found for the other AAPs where the TUNEL assay failed to detect apoptosis. Scale bar is 20 μm.

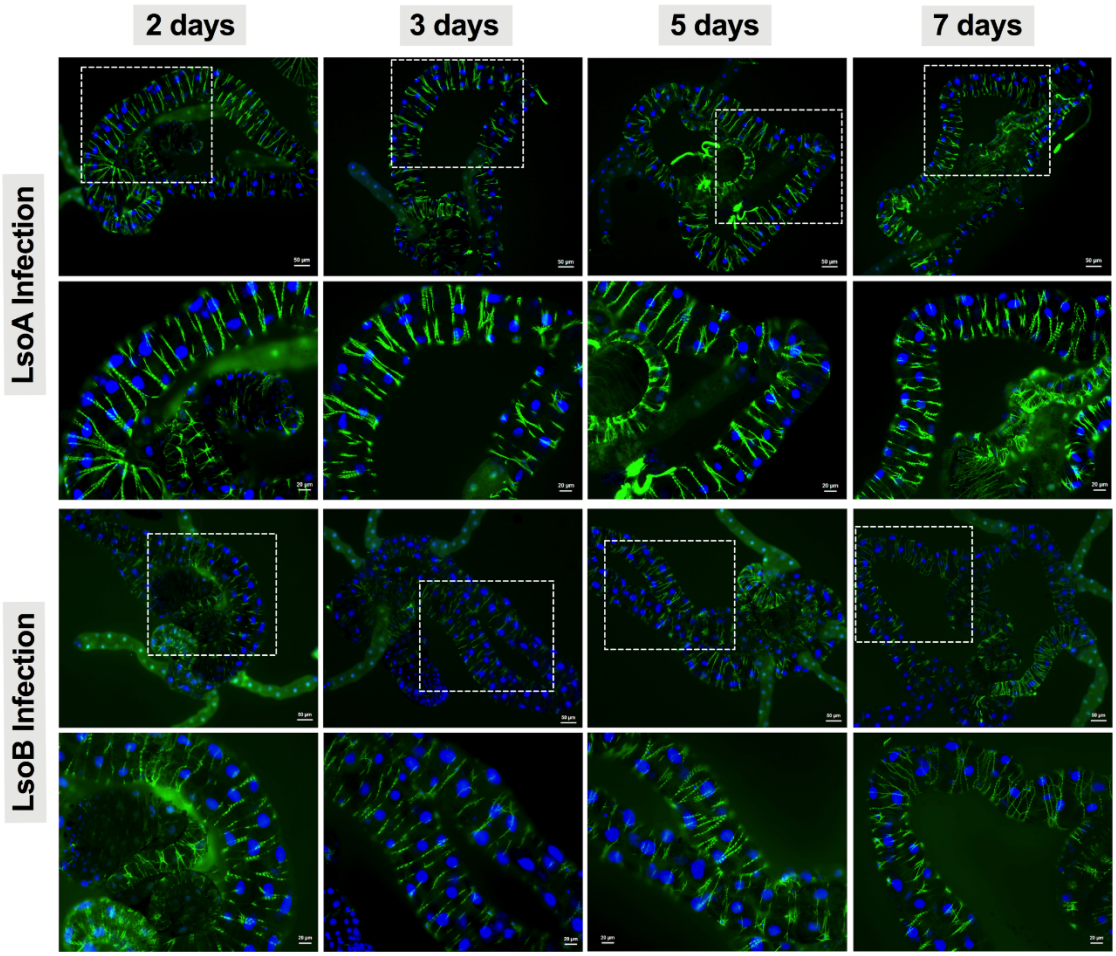

Figure 5.4 Nuclear morphology and actin cytoskeleton organization of gut cells in the potato psyllid following Lso exposure. All the guts showed uniform and round shape of cell nuclei (Blue) and organized structure of the actin filaments (Green). The white dashed rectangle indicates the enlargement region of upper panels. The bars of upper and lower panels are 50 μm and 20 μm, respectively.

5.3.3 Expression of apoptosis-related genes

In response to LsoA acquisition, two inhibitors IAP1 and IAPP5 were up-regulated at day 3 compared to days 2, 5 and 7. IAPP5.2 was significantly up-regulated at day 3 and 5 compared to non-infected guts as well as after a 2- and 7-day AAP. Caspase 3 was significantly up-regulated at day 7 compared to the uninfected guts and guts following the

3- and 5-day AAP. In addition, caspase 3 had the opposite regulation profile than IAPP5.2. No significant regulation of IAP2 and the other two caspases was observed in response to LsoA acquisition (Fig. 5.5).

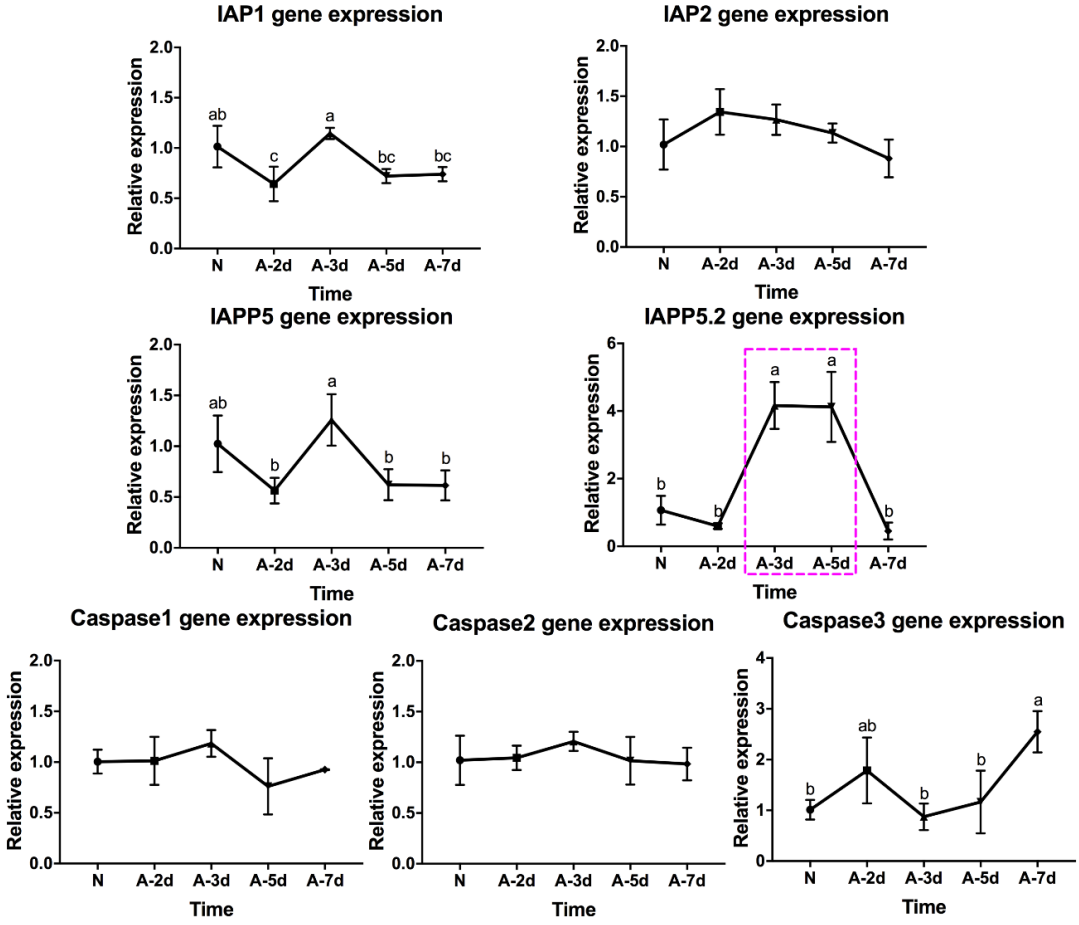

Figure 5.5 Regulation of apoptosis-related genes IAP1, IAP2, IAPP5, IAPP5.2, caspase 1, caspase 2, and caspase 3 in the psyllid gut upon LsoA infection. Data represent means ± SD of three independent experiments. Different letters indicate statistical differences at $P < 0.05$ using one-way ANOVA with Tukey's *post hoc* test. The pink dashed rectangle indicates the significant up-regulation profile of IAPP5.2 gene. The IAPP5.2 gene also had the opposite regulation profile with the effector caspase 3.

In response to LsoB acquisition, one inhibitor IAP1 was up-regulated at day 2 compared to day 3 and 5 infection. IAP2 was significantly up-regulated at day 7 compared to day 2 infection. In addition, IAPP5 was significantly up-regulated at day 2 compared to day 3 infection. Similar to LsoA infection, IAPP5.2 was up-regulated at day 3 compared to day 7, and at day 5 compared to the uninfected gut as well as to the 2- and 7-day infection. Of the three caspase genes, caspase 1 was up-regulated at day 2 compared to day 5 infection. Caspase 2 was up-regulated at day 3 compared to day 7 infection. However, caspase 3, was regulated in response to LsoB acquisition at day 7, and it has the opposite regulation profiles as IAPP5.2 (Fig. 5.6).

5.3.4 Silencing of IAPP5.2 and its effect on Lso acquisition in psyllid gut

IAPP5.2 (survivin-like) gene was significantly up-regulated at day 3 and 5 compared to non-infected psyllid in response to both LsoA and LsoB. Therefore, we silenced IAPP5.2 gene by RNAi to investigate if IAPP5.2 could be involved in the acquisition process of Lso. The oral delivery of dsRNA resulted in 55% decrease of the expression of IAPP5.2 in the gut (Fig 5.7A), and in the up-regulation of the transcriptional expression of the two effector caspases, caspase 1 and caspase 3. However, it had no impact on the initiator caspase, caspase 2 (Fig. 5.7A). Therefore, IAPP5.2 could bind and interact specifically with the two effector caspases with the BIR domain (Fig. 5.7B and Fig. A.3). In addition, silenced guts also showed DNA fragmentation based on TUNEL assay (Fig. 5.7C). Importantly, RNAi of IAPP5.2 significantly decreased both LsoA and LsoB titers in the guts of adult psyllids (Fig. 5.7D).

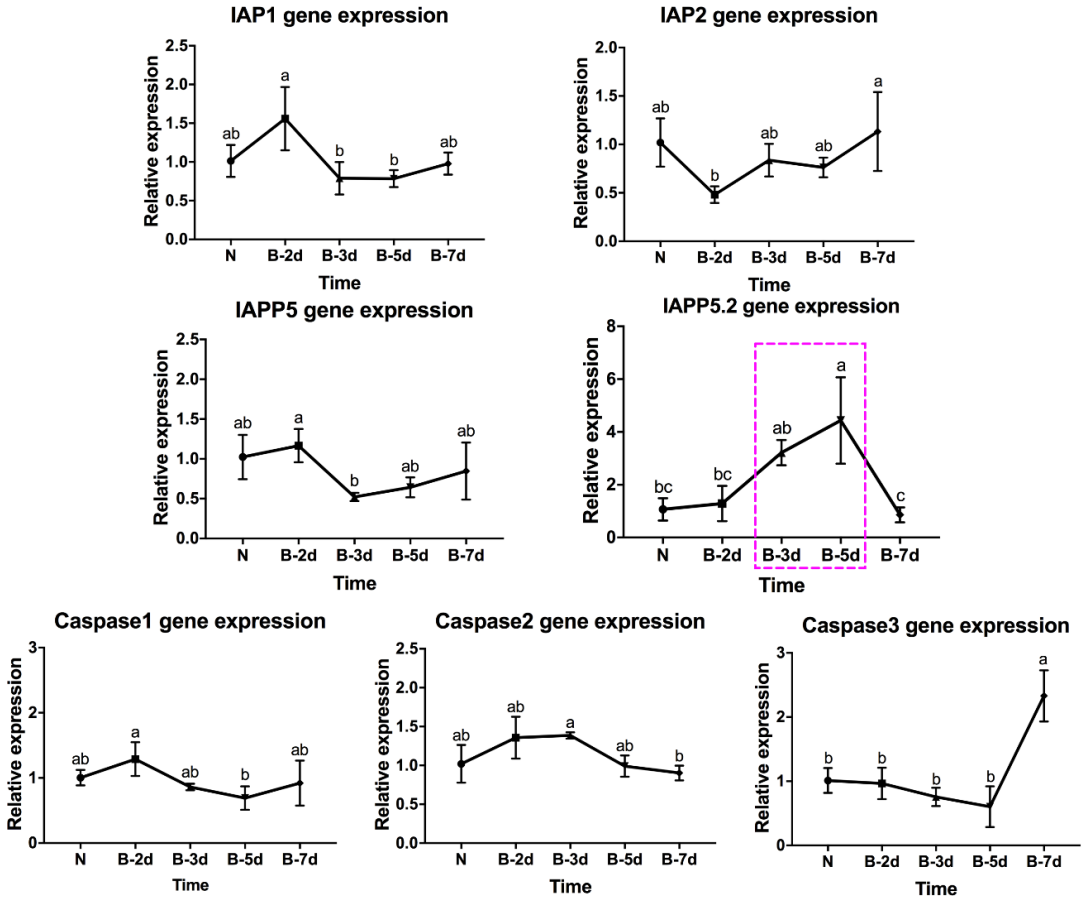

Figure 5.6 Regulation of apoptosis-related genes IAP1, IAP2, IAPP5, IAPP5.2, caspase 1, caspase 2, and caspase 3 in the psyllid gut upon LsoB infection. Data represent means ± SD of three independent experiments. Different letters indicate statistical differences at $P < 0.05$ using one-way ANOVA with Tukey's *post hoc* test. The pink dashed rectangle indicates the significant up-regulation profile of IAPP5.2 gene. The IAPP5.2 gene also had the opposite regulation profiles with the effector caspase 3.

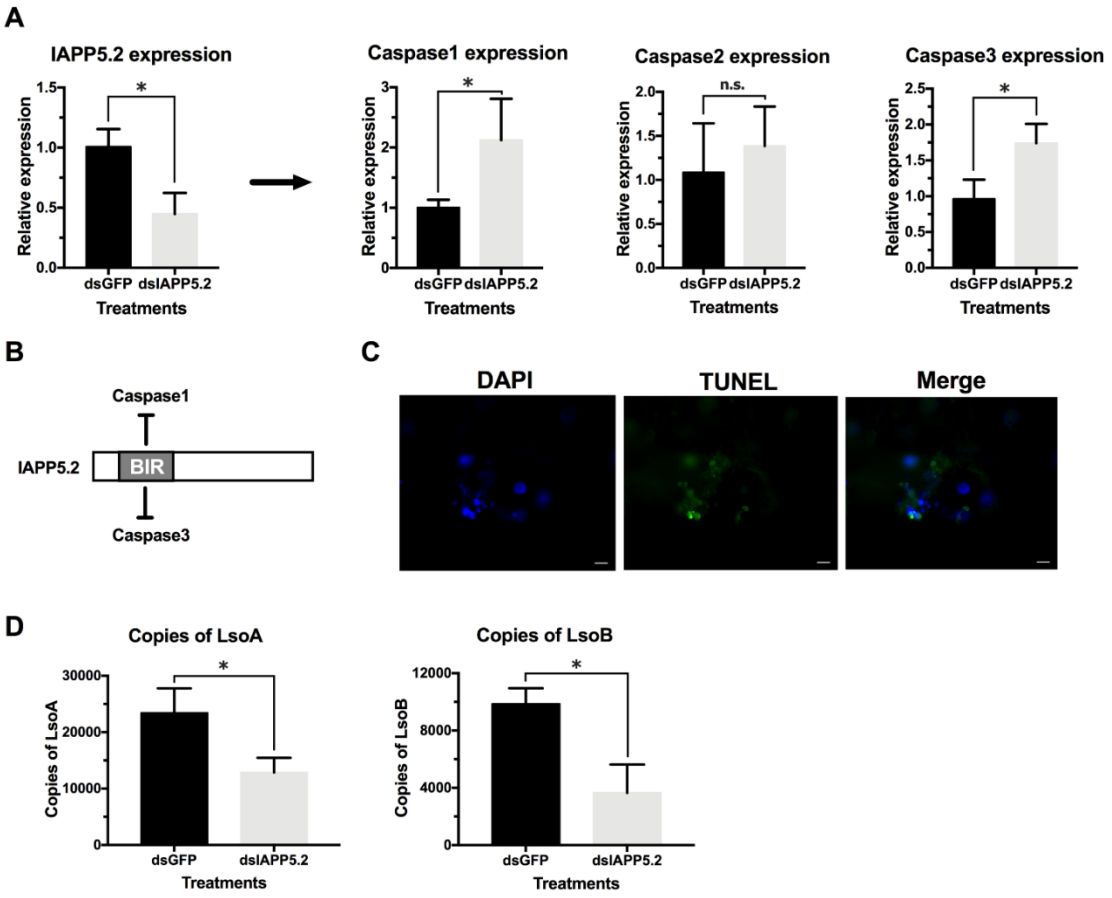

Figure 5.7 Silencing of IAPP5.2 and its effect on Lso acquisition. (A) Relative gene expression of IAPP5.2, caspase 1, caspase 2, and caspase 3 in psyllid gut following RNAi silencing of IAPP5.2. (B) IAPP5.2 probably interacts with caspase 1 and caspase 3 via the BIR domain. (C) DNA fragmentation of guts could be observed based on TUNEL assays after silencing of IAPP5.2. (D) Quantification of LsoA and LsoB in the potato psyllid gut after silencing of IAPP5.2. Silencing of IAPP5.2 in the guts of psyllids resulted in reduced LsoA and LsoB accumulation. * indicates $P < 0.05$.

5.4 DISCUSSION

Understanding the characteristics of pathogens and the transmission mechanisms by insect vectors will greatly contribute to create new approaches for controlling diseases caused by insect-borne plant pathogens. In the present study, we focused on the potential role of apoptosis as a response in the gut of adult potato psyllids upon Lso infection. We

first examined the accumulation of haplotypes LsoA and LsoB in the adult potato psyllid gut over 7 days of AAP. Based on the Lso quantification and immunolocalization, during this period LsoB has probably entered the gut cells and is replicating, however LsoA is not actively replicating yet. Our previous studies determined that this delay in LsoA accumulation in the psyllid gut is accompanied by a significant decrease in Lso transmission (Chapter II). As indicated above, the citrus Huanglongbing pathogen CLas was reported to induce apoptosis in the gut of the adult vector of the Asian citrus psyllid while there was no evidence of apoptosis in the nymphal gut (Ghanim et al., 2016; Mann et al., 2018) and it was suggested that this apoptotic response in adults might contribute to their reduced efficiency to acquire and transmit CLas compared to nymphs (Ghanim et al., 2016; Inoue et al., 2009). No evidence of apoptosis was observed in the gut of adult potato psyllids in response to either Lso haplotype in the case of a persistent infection (Chapter IV), which is also consistent with the efficient transmission of each Lso haplotype by adults that acquired the pathogen during the nymphal stage. Therefore, we hypothesized that apoptosis could be occurring the gut of the adult psyllid upon infection in response to LsoA but not LsoB since adult psyllids were more efficient at acquiring and transmitting LsoB.

A variety of pathogenic organisms can infect insects, including bacteria, viruses, fungi, and other organisms (Dangl & Jones, 2001; Leger & Wang, 2010; Tamborindeguy et al., 2017). The innate immunity plays a critical part in the outcome of pathogens infection of insects (Cao et al., 2015; Hillyer, 2016; Kingsolver et al., 2013). Meanwhile,

pathogens can exploit their host's cell machinery and avoid the host's immune defenses for successful replication and transmission (Vyas et al., 2015).

Apoptosis, as an important part of the innate immunity, plays a crucial role in defending against pathogens and limiting the spread of infections. In turn, many intracellular pathogens target caspase signaling as a means to impede apoptosis of the infected host cells. Different strategies are utilized by pathogens to repress the host apoptotic response via caspase signaling. For instance, the malaria parasite, *Plasmodium falciparum* alters the cell death pathway of the invaded mosquito midgut cells by disrupting c-Jun N-terminal kinase (JNK) signaling, which regulates the activation of the effector caspase-S2 (Ramphul et al., 2015). Another example is the baculovirus caspase inhibitors which block apoptosis downstream of effector caspase DrICE in *Drosophila* cells (Lannan et al., 2007). In fact, IAPs were discovered in baculoviruses and the BIR domain present in the IAP proteins stands for Baculovirus IAP Repeat (Crook et al., 1993). Aside from parasites and viruses, bacteria also have evolved a variety of strategies to block apoptosis at different stages within the apoptotic pathways. For example, *Chlamydia* presumably secretes proteins that result in blocking the release of cytochrome c from the mitochondria and in the inhibition of the activation of effector caspase-3 (Fan et al., 1998).

Numerous studies have focused on the immune responses of host plants to pathogens or the manipulation of plant immunity by pathogens (Asai & Shirasu, 2015; Dodds & Rathjen, 2010; Hacquard et al., 2017; Weiberg et al., 2013). Recently, several studies investigated the immune interactions between insect vectors and plant pathogens, and they found that plant pathogens, in particular plant viruses can induce programmed

cell death in their vectors. The induced cell death may fill different roles: it could be a defensive mechanism to protect the insect against the invasion of the pathogens (Wang et al., 2016), or could help the pathogens be acquired or escape specific tissues (Chen et al., 2017; Huang et al., 2015). In both scenarios, these cell death responses can affect the pathogen acquisition or transmission. However, the understanding of apoptosis induction or inhibition by vector-borne plant pathogenic bacteria remains largely limited.

Therefore, we evaluated if an apoptotic immune response in the psyllid gut occurred between the 2- and 7-day Lso AAP. However, the fluorescent imaging of the TUNEL assay, the nuclear morphology and the actin cytoskeleton architecture showed no evidence of Lso-induced abnormality in newly Lso-exposed guts. Because each of these approaches has limitations, it cannot be excluded that a few cells undergo apoptosis in response to either Lso.

Because pathogens can manipulate the apoptotic response of their host, we evaluated the expression of apoptosis-related genes during this infection period. Interestingly, analysis of the expression of apoptosis-related genes revealed that the gene IAPP5.2 (survivin-like) was significantly up-regulated in response to both LsoA and LsoB after a 3- and 5-day AAP. We also noted that none of the three caspases was up-regulated during this period; however, the effector caspase 3 had the opposite regulation profiles with IAPP5.2 in response to both LsoA and LsoB. It is possible that LsoA and LsoB suppress caspase activation and the apoptotic response during infection via the up-regulation of the survivin-like IAPP5.2. Indeed, survivin has been shown to prevent the host cellular apoptosis in other infection models. For instance, viral pathogens such as

hepatitis B virus (HBV) and human neurotropic virus JC virus suppress host caspase activation and apoptosis in a survivin-dependent manner (Marusawa et al., 2003; Pina-Oviedo et al., 2007). In addition to virus, during the infection by the intracellular parasite *Cryptosporidium parvum* mRNA levels of survivin increase between 12 and 48 h post infection in gut cells of the mammal host. Moreover, siRNA depletion of survivin significantly increases the effector caspase-3/7 activity and further reduces the parasite growth (Liu et al., 2008). Survivin siRNA depletion also suggested the role of survivin in blocking apoptosis especially more critical after 24 h of *C. parvum* infection. In the present study, we also found that silencing of IAPP5.2 significantly up-regulated the transcriptional expression of the effector caspases 1 and 3 and resulted in the occurrence of TUNEL-positive cells. Therefore, IAPP5.2 could inhibit these caspases and the apoptotic response in the psyllid gut cells. The depletion of IAPP5.2 significantly decreased LsoA and LsoB accumulation in the psyllid gut. Lso ingestion occurred before dsRNA ingestion, therefore any change in Lso accumulation was not linked to a potential behavioral change due to silencing or induced apoptosis, such as a reduction in feeding which could affect Lso ingestion. Therefore, these results indicate that the accumulation of Lso in the psyllid gut could require survivin expression within the infected host cells. This study represents the first report showing that bacterial pathogen represses host caspase activation and apoptosis in a survivin-dependent manner (Fig. 5.8).

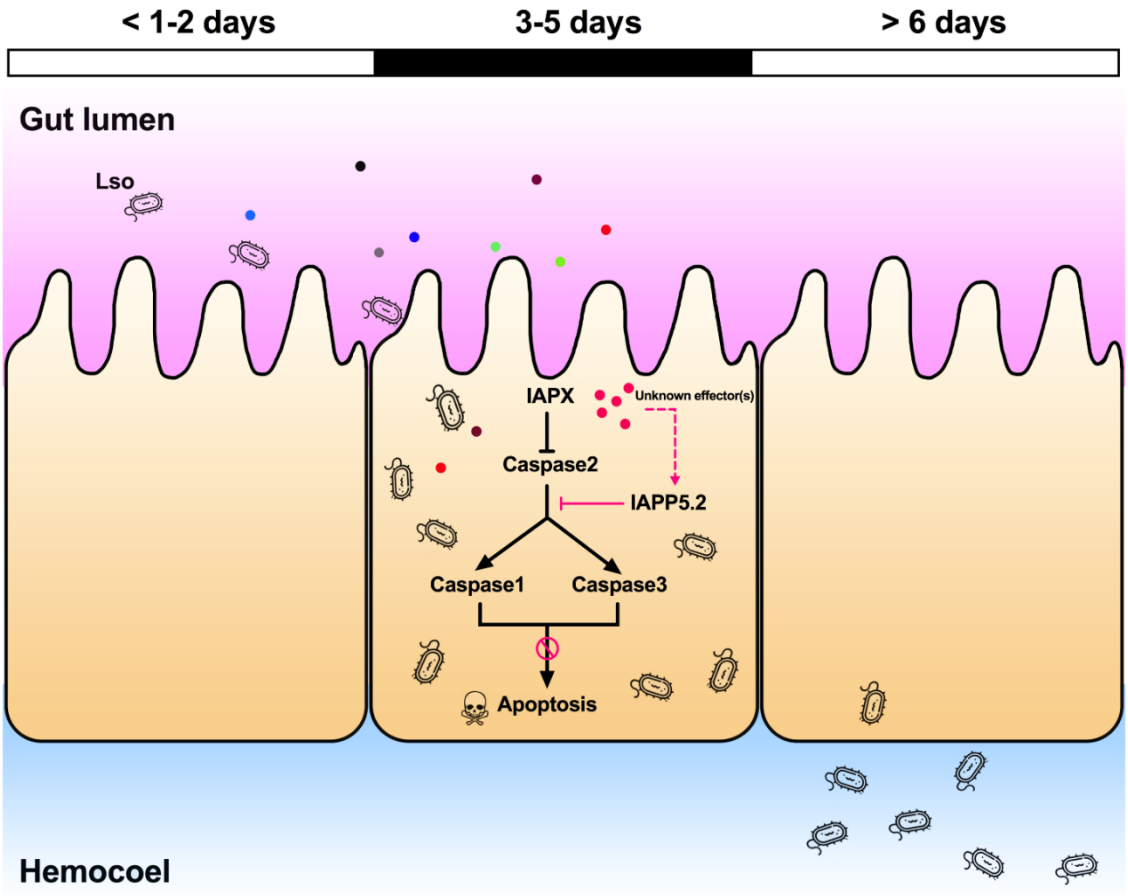

Figure 5.8 Schematic model of the Lso-repressed apoptotic response in the potato psyllid gut by the induction of the anti-apoptotic gene IAPP5.2 (survivin-like) at the early stage of infection. At days 3 and 5 of the infection when Lso first translocate into gut cells, Lso attenuate the psyllid immune responses by up-regulating the inhibitor of apoptosis IAPP5.2 gene via unknown bacterial effectors (pink dots). The up-regulation of IAPP5.2 specifically blocks the activation of effector caspases 1 and 3, which further inhibits the apoptotic response in potato psyllid gut. Other colored dots represent different Lso effectors. IAPX indicates other IAPs in potato psyllid.

In humans, the apoptosis inhibitors XIAP, c-IAP1, and c-IAP2 are able to directly inhibit caspase-3, -7, and -9, while survivin binds specifically to the effector caspase-3 and -7 rather than the initiator caspases (Liu et al., 2008; Shin et al., 2001). Based on our phylogenetic study, caspase 2 is the initiator caspase, while caspases 1 and 3 are effector

caspases (Chapter IV) (Tang & Tamborindeguy, 2019). Thus, in psyllids also, the survivin-like gene could regulate the effector caspases rather than initiator caspase. In addition, we noted that at 7-day infection, the caspase 3 gene was up-regulated; however, we could not observe apoptosis in the psyllid gut. This may reflect the existence of a potato psyllid response to Lso since Lso, in particular LsoB, is detrimental to the vector fitness (Albuquerque Tomilhero Frias et al., 2020; Nachappa et al., 2012b; Yao et al., 2016). Although caspase 3 was up-regulated at day 7 of the infection, it might not have reached or exceeded the threshold to trigger an intracellular apoptotic immune reaction (Maiuri et al., 2007). The fact is that Lso still successfully cross the gut cells, therefore, Lso seems to be preemptive, and has evolved to repress or reduce the apoptotic response in the psyllid gut. This mechanism may help Lso to successfully translocate and colonize the gut cells. How does Lso manipulate the expression of IAPP5.2 is still unknown, however, it is possible that bacterial effector proteins could be involved (Levy et al., 2019).

Quantification of each Lso haplotype following early exposure times to infected plants revealed that LsoA and LsoB population increased with different rates in the psyllid guts. LsoB density increased rapidly after 3 days, while the increase in LsoA relative abundance was much slower. The differences of LsoA and LsoB titer in the gut of adult psyllids could be the result of differences of bacterial pathogenicity or the elicited psyllid immune responses. Indeed, differences in virulence between these two haplotypes were determined in association with their host plants and insect vector: in both cases, LsoB was found to be more pathogenic (Harrison et al., 2019; Mendoza Herrera et al., 2018; Yao et al., 2016). Similarly, the vector immune response could be one factor explaining the

different Lso accumulation profiles. It appears that similar to LsoB, LsoA might stop the apoptotic response in the psyllid gut, as shown in this study, therefore, other immune responses might be differentially elicited in response to each Lso haplotype. It is therefore possible that LsoB is able to better defend itself against the psyllid immunity, or even also manipulate those defenses to its advantage. As a consequence, LsoB could be acquired with higher efficiency than LsoA.

In summary, Lso appears to have evolved the ability to manipulate the cellular apoptotic response in order to establish infection and to permit its life cycle progression. Our study demonstrates for the first time that the manipulation of apoptosis and the suppression of caspase activation observed in the Lso-exposed cells were due to the up-regulation of survivin and was probably mediated by the effector caspases 1 and 3 with unknown bacterial effector(s). This is not only the first study showing that a bacterial pathogen represses the host caspase activation and apoptosis in a survivin-dependent manner, but it is the first report indicating that a plant bacterial pathogen can impede the immune response in its insect vector.

CHAPTER VI

AUTOPHAGIC RESPONSE OF THE POTATO PSYLLID, *BACTERICERA COCKERELLI*, TO '*CANDIDATUS* LIBERIBACTER SOLANACEARUM' AT THE GUT INTERFACE

6.1 INTRODUCTION

Autophagy (or "self-eating") is a conserved cellular degradation process that serves to deliver cytoplasmic proteins and organelles to lysosomes for degradation (Mizushima et al., 2008). It plays important roles in many biological processes, such as maintaining homeostasis and preventing nutritional and metabolic-mediated stresses in eukaryotic organisms ranging from yeast to insects and mammals (Khandia et al., 2019). Autophagy has also been shown to be important in the innate immune defense against infection by viral, bacterial, and fungal pathogens in animals (Yano & Kurata, 2011).

In the last two decades, a series of autophagy-related genes (ATGs) have been characterized from lower (e.g., yeast) to higher eukaryotes (e.g., mammals and insects) (Suzuki et al., 2013; Yang & Klionsky, 2010; Zirin & Perrimon, 2010). Most of but not all ATGs play roles in the canonical autophagy pathway, regulating the formation of autophagosome, a vesicular structure that is the hallmark of autophagy (Levine & Kroemer, 2019). In yeast, more than 30 ATGs were identified, and around 20 of those are required for the efficient formation of sealed autophagosomes that proceed to fuse with lysosomes (Mizushima et al., 2011; Nakatogawa et al., 2009). Under normal conditions, autophagy is kept at a low level, but it can be activated by starvation or other stress signals,

which are known to induce the expression of some ATG genes (He & Klionsky, 2009). Therefore, the identification of genes that participate in autophagy should establish a foundation for furthering our understanding of the molecular mechanism and the potential roles of autophagy in different physiological processes.

In insects, previous studies have revealed that autophagy components are important for *Drosophila* defense against viral infection such as *vesicular stomatitis virus* (Shelly et al., 2009). In addition to virus, autophagy is also required for *Drosophila* to regulate bacterial populations such as the obligate intracellular bacterium *Wolbachia*, which is commonly harbored by insects and nematodes (Voronin et al., 2012). An increasing amount of evidence shows that the autophagy pathway could be induced also by plant pathogens in hemipteran insects, and in particular by vector-borne plant viruses. The induced autophagy may play different roles: it could be a defensive mechanism to protect the insect against the invasion of the pathogens, or it could help the pathogens be acquired or escape specific tissues within the vector. For instance, *Tomato yellow leaf curl virus* (TYLCV) activates the autophagy pathway in its insect vector, the whitefly (*Bemisia tabaci*), and the induction of autophagy results in decreased transmission while the inhibition of this response facilitates virus transmission (Wang et al., 2016). In contrast, Chen et al. (2017) found that autophagy is induced by *Rice gall dwarf virus* (RGDV) in the intestine of its insect vector, the rice leafhopper (*Recilia dorsalis*). Further investigation demonstrated that autophagy activation improves the transmission of RGDV, whereas inhibiting the autophagy pathway blocks viral transmission. However, the

understanding of autophagy induction or inhibition by vector-borne plant pathogenic bacteria and its potential role in bacterial transmission remains largely limited.

'*Candidatus* Liberibacter solanacearum' (Lso) is a phloem-limited, Gram-negative, unculturable bacterium. It is a pathogen that infects members of the Apiaceae and Solanaceae plant families and causes great economic losses. Presently, seven Lso haplotypes have been identified in the world (Glynn et al., 2012; Haapalainen et al., 2018; Lin et al., 2012; Nelson et al., 2013; Swisher Grimm & Garczynski, 2019). Haplotypes LsoA and LsoB are transmitted by the potato psyllid (also known as tomato psyllid), *Bactericera cockerelli*, and infect numerous solanaceous plants (e.g., potatoes and tomatoes) in North America (Liefting et al., 2009a; Tamborindeguy et al., 2017). Both, LsoA and LsoB are associated with potato zebra chip, a disease which has been responsible for millions of dollars losses in potato producing regions (Munyaneza, 2012). Lso is transmitted by psyllids in a circulative and persistent manner (Cicero et al., 2016; Cicero et al., 2017; Cooper et al., 2014). Therefore, the psyllid gut is the first organ that Lso encounters. This organ could act as a barrier for Lso transmission and determine Lso transmission efficiency. Indeed, the ability of the bacteria to infect the gut depends on the insect immune responses as well as the bacterial strategies deployed to disrupt the host immunity.

In this study, we aim to understand whether there might be an association between an autophagic immune response and Lso infection in psyllid gut. Toward this end, we first datamined the potato psyllid transcriptome (Nachappa et al., 2012a) to identify ATGs. Because there is no study thoroughly investigating ATGs in hemipteran insects, we also

annotated ATGs in representative Sternorrhyncha species including the pea aphid (*Acyrthosiphon pisum*), the whitefly (*B. tabaci*), and the Asian citrus psyllid (*Diaphorina citri*) which genomes have been sequenced (Chen et al., 2016a; Gerardo et al., 2010; Hunter et al., 2014; Xie et al., 2017). Second, we evaluated the expression profiles of ATGs in response to LsoA or LsoB infection at the psyllid gut. We focused on the autophagic response of adult psyllids from infected colonies, which most likely acquired the bacteria during the nymphal stages, as well as in the responses that occur in newly infected psyllids adults during the early infection. Third, we conducted pilot experiments to confirm the occurrence of markers of autophagy using western blot assay as well as transmission electron microscopy. This study represents a first step towards understanding the potential role of autophagy in potato psyllid and Lso interactions.

6.2 MATERIALS AND METHODS

6.2.1 Insect colonies and tomato plants

Lso-free, LsoA- and LsoB-infected psyllid colonies were maintained separately on tomato plants (Moneymaker; Victory Seed Company, Molalla, OR) in insect-proof cages (24 × 13.5 × 13.5 cm, BioQuip®, Compton, CA) at room temperature 24 ± 2°C and under a photoperiod of 16: 8 h (L: D), as described in Yao et al. (2016).

To obtain Lso-infected tomato plants, six-week-old tomato plants were infected as described in Nachappa et al. (2014) using three male psyllids harboring LsoA or LsoB, respectively. After one week, the psyllids were removed from the tomato plants. Three weeks after Lso inoculation, the plants were tested for Lso infection using the LsoF/OI2

primers (Li et al., 2009) and the Lso haplotype in the plants was confirmed using the Lso SSR-1 primers (Lin et al., 2012).

6.2.2 Identification and validation of autophagy-related genes

Genes potentially involved in autophagy in hemipteran insects were identified through blast searches of the potato psyllid transcriptome (Nachappa et al., 2012a) and the genome of the pea aphid, the whitefly, and the Asian citrus psyllid (Chen et al., 2016a; Gerardo et al., 2010; Hunter et al., 2014; Xie et al., 2017) using the 20 *D. melanogaster* predicted ATG genes as query (e-value cut off 1e-20) (Érdi et al., 2012). The *D. melanogaster* ATGs sequences are from the FlyBase: https://flybase.org/reports/FBgg0000076.html.

To validate the potato psyllid bioinformatic predictions, primers for each candidate gene were designed (Table A.9). RNA from a pool of 50 adult psyllids was purified using the RNeasy Mini Kit (Qiagen), and genomic DNA was eliminated by DNase I treatment with Turbo DNase (Ambion, Invitrogen). Then, the total RNA was reverse transcribed using the Verso cDNA Synthesis kit (Thermo, Waltham, MA) and anchored-Oligo (dT) primers following the manufacturer's instructions. Candidate genes were amplified by PCR. The PCR conditions were 95 °C for 2 min; followed by 35 cycles of 95 °C for 30 secs, 60 °C for 30 secs, and 72 °C for 30-90 secs (depending of amplicon size); and a final extension at 72 °C for 5 min. Amplicons were visualized in a 1% agarose gel, and amplicons of the expected size were excised from the gel and purified using the PureLink Quick Gel Extraction kit (Invitrogen). Each PCR fragment (150 ng) was cloned into the

pGEM-T easy vector using the pGEM-T easy cloning kit (Promega, Madison, WI) and transformed into NovaBlue Singles Competent Cells (Novagen, Temecula, CA). For each construct, plasmid DNA from at least three colonies was purified using the PureLink Quick Plasmid Miniprep kit (Invitrogen) and sequenced by Eton Bioscience Inc. (San Diego, CA, USA). The obtained sequences were compared to the bioinformatics predictions.

6.2.3 Expression of autophagy-related genes

To investigate the putative autophagic response of the psyllid gut upon Lso infection, approximately seven-day-old Lso-free female adult psyllids were transferred to LsoA- or LsoB-infected plants for 2, 3, 5, and 7 days and are henceforth referred to as LsoA- or LsoB-exposed psyllids (to contrast with psyllids from the LsoA- or LsoB-infected colonies). Insects from the Lso-free colony were used as a control. Three replicates were conducted for each treatment, and each replicate had 200 psyllid individuals. After exposure, the psyllid guts were dissected in 1× PBS with RNAlater (Ambion, Invitrogen) under the stereomicroscope (Olympus) as described in Ibanez et al. (2014a). Similarly, the gut of female adult psyllids from the Lso-free, LsoA- and LsoB-infected colonies were dissected as well. RNA purification and cDNA synthesis from each sample was performed as described above. The expression of autophagy-related genes was evaluated by quantitative real-time PCR (qPCR) using the SensiFAST SYBR Hi-ROX kit (Bioline) according to manufacturer's instructions. Each reaction contained 25 ng of cDNA, 250 nM of each primer (Table A.9), and 1X of SYBR Green Master Mix; the

volume was adjusted with nuclease-free water to 10 µL. The qPCR program was 95 °C for 2 min followed by 40 cycles at 95 °C for 5 sec and 60 °C for 30 sec. qPCR assays were performed using a QuantStudio™ 6 Flex Real-Time PCR System (Applied Biosystems, Foster City, CA). Reactions for all samples were performed in triplicates with a negative control in each run. The relative expression of the candidate genes was estimated with the delta delta CT method (Schmittgen & Livak, 2008), using the two reference genes, elongation factor-1a (GenBank KT185020) and ribosomal protein subunit 18 (GenBank KT279693) (Ibanez & Tamborindeguy, 2016).

6.2.4 Western blot assay

For the western blot analyses, total protein of psyllid gut was isolated using RIPA buffer (Invitrogen, Carlsbad, CA) supplemented with protease inhibitor tablets (Roche Diagnostics, IN). Specifically, approximately seven-day-old Lso-free adult psyllids were transferred to LsoA- or LsoB-infected plants for 1, 2, 3, 5, and 7 days. Insects from the Lso-free colony were used as a control. Proteins from adult psyllids from the Lso-free, LsoA- and LsoB-infected colonies were purified as well. Protein samples were subjected to NuPAGE 4-12% Bis-Tris Protein Gel (Invitrogen, Carlsbad, CA) and then transferred to polyvinylidene fluoride (PVDF) membrane (Biotrace™ PVDF, Gelman Laboratory). The membranes were blocked with 5% nonfat milk in tris-buffered saline (TBS) with 0.1% Tween 20 (Sigma) (TBST) and then incubated overnight with a rabbit polyclonal antibody raised against ATG8 in mammals (Abgent, AP1802a) at a 1:1000 dilution. This antibody has been successfully tested in whiteflies (Wang et al., 2016). The membrane was then

washed three times with TBST and incubated with anti-rabbit IgG secondary antibody (1: 20,000, Sigma) for 1 h. Detection of proteins was performed using the NBT/BCIP substrate solution (Thermo Fisher Scientific). Images were visualized with Azure c400 imaging system (Azure Biosystems).

6.2.5 Transmission electron microscopy

Transmission electron microscopy was used to detect autophagosomes in psyllid gut. The guts from Lso-free and LsoA-infected psyllids were first dissected in 1X phosphate buffered saline (PBS) (Sigma-Aldrich, St. Louis, MO) and fixed with Trumps fixative (McDowell & Trump, 1976) for 2 h, and then postfixed with 1% Osmium tetroxide in water for 20 min in the microwave at 100W. Next, the guts were blocked with 0.5% w/v aqueous uranyl acetate and rinsed with series of acetone (30%, 50%, 70%, 95% and 100%). Gut samples were then transferred to embedding molds and polymerized at 65 °C for 12-24 h. Finally, gut samples were sectioned and observed under JEOL 1200 transmission electron microscope at Texas A&M University Microscopy and Imaging Center.

6.2.7 Data analysis

All data were analyzed with JMP Version 12 (SAS Institute Inc., Cary, NC, USA). Regulation of autophagy-related genes was determined using one-way ANOVA with Tukey's *post hoc* test.

6.3 RESULTS

6.3.1 Autophagy-related genes in potato psyllid and other hemipteran insects

A variable number of autophagy-related genes were identified among the different phloem-feeding species. A total of 23 ATG homologs were identified and their sequences were validated in the potato psyllid via transcriptome search. These genes were classified into 17 ATG gene families. The gene names and abbreviations used hereafter are listed in Table 6.1. In parallel, 28, 26, and 28 ATG homologs were also identified in the genome of the pea aphid, the whitefly, and the Asian citrus psyllid, respectively (Table A.10). For the potato psyllid, we were able to annotate all ATG homologs based on *Drosophila* ATGs annotation, including serine/threonine protein kinase ULK2 (*BcATG1*), *BcATG2*-*BcATG5*, Beclin1 (*BcATG6*), *BcATG7*, gamma-aminobutyric acid receptor-associated protein (*BcATG8*), *BcATG9*, *BcATG10*, *BcATG12*, *BcATG13*, beclin 1-associated autophagy-related key regulator (*BcATG14*), *BcATG16*, RB1-inducible coiled-coil protein 1-like (*BcATG17*), WD repeat domain phosphoinositide-interacting proteins (*BcATG18*), and *ATG101*. The ATGs from all ATG families in *Drosophila* could also be identified in the pea aphid and the whitefly, however, ATG12 and ATG14 were absent in the current Asian citrus psyllid genome.

Table 6.1 Name of *B. cockerelli* autophagy-related genes and their codes used in this study.

Gene name	Code
Serine/threonine-protein kinase ULK2-like isoform 1	*BcATG1*
Autophagy-related protein 2 homolog A-like	*BcATG2A-1*
Autophagy-related protein 2 homolog A	*BcATG2A-2*
Autophagy-related protein 2-like protein A	*BcATG2A-3*

Table 6.1 Continued.

Gene name	Code
Autophagy-related protein 2-like protein B	*BcATG2B*
Autophagy related protein Atg3-like protein	*BcATG3*
Cysteine protease ATG4B-like isoform 1	*BcATG4*
Autophagy protein 5	*BcATG5*
Beclin-1-like protein	*BcATG6*
Ubiquitin-like modifier-activating enzyme ATG7	*BcATG7*
Gamma-aminobutyric acid receptor-associated protein	*BcATG8*
Autophagy-related protein 9A	*BcATG9*
Ubiquitin-like-conjugating enzyme ATG10	*BcATG10*
Autophagy protein 12-like	*BcATG12*
Autophagy-related protein 13 homolog	*BcATG13*
Beclin 1-associated autophagy-related key regulator-like	*BcATG14*
Autophagy-related protein 16-1-like	*BcATG16*
RB1-inducible coiled-coil protein 1-like	*BcATG17*
WD repeat domain phosphoinositide-interacting protein	*BcATG18-1*
WD repeat domain phosphoinositide-interacting protein 2-like	*BcATG18-2*
WD repeat domain phosphoinositide-interacting protein 3	*BcATG18-3*
WD repeat domain phosphoinositide-interacting protein 4-like	*BcATG18-4*
Autophagy-related protein 101-like isoform 1	*BcATG101*

6.3.2 Expression of autophagy-related genes upon Lso infection

The expression pattern of the identified autophagy-related genes was evaluated at specific time points during the early infection period. The ATG genes showed differential expression profiles upon LsoA and LsoB infection.

Upon LsoA infection, variable expression profiles were identified. Nineteen out of the 23 ATGs were regulated in response to LsoA. Among those, *BcATG2A-2*, *BcATG2A-3*, *BcATG2B*, *BcATG6*, and *BcATG16* were only up-regulated at day 2 compared to all other time points or compared to the uninfected guts, while *BcATG1*, *BcATG101*, *BcATG17, BcATG9*, *BcATG18-1*, *BcATG14*, *BcATG5*, and *BcATG3* remained up-regulated longer. *BcATG13*, *BcATG2A-1*, *BcATG18-2*, *BcATG12*, *BcATG7*, and *BcATG8* were expressed at higher levels at days 3 or 5. Four genes (*BcATG18-3*, *BcATG18-4*,

BcATG4, and *BcATG10*) were not significantly regulated upon LsoA infection at all (Fig. 6.1). Overall, genes involved in the events prior to the phagophore formation and elongation showed up-regulated profile upon LsoA infection (Fig. 6.2).

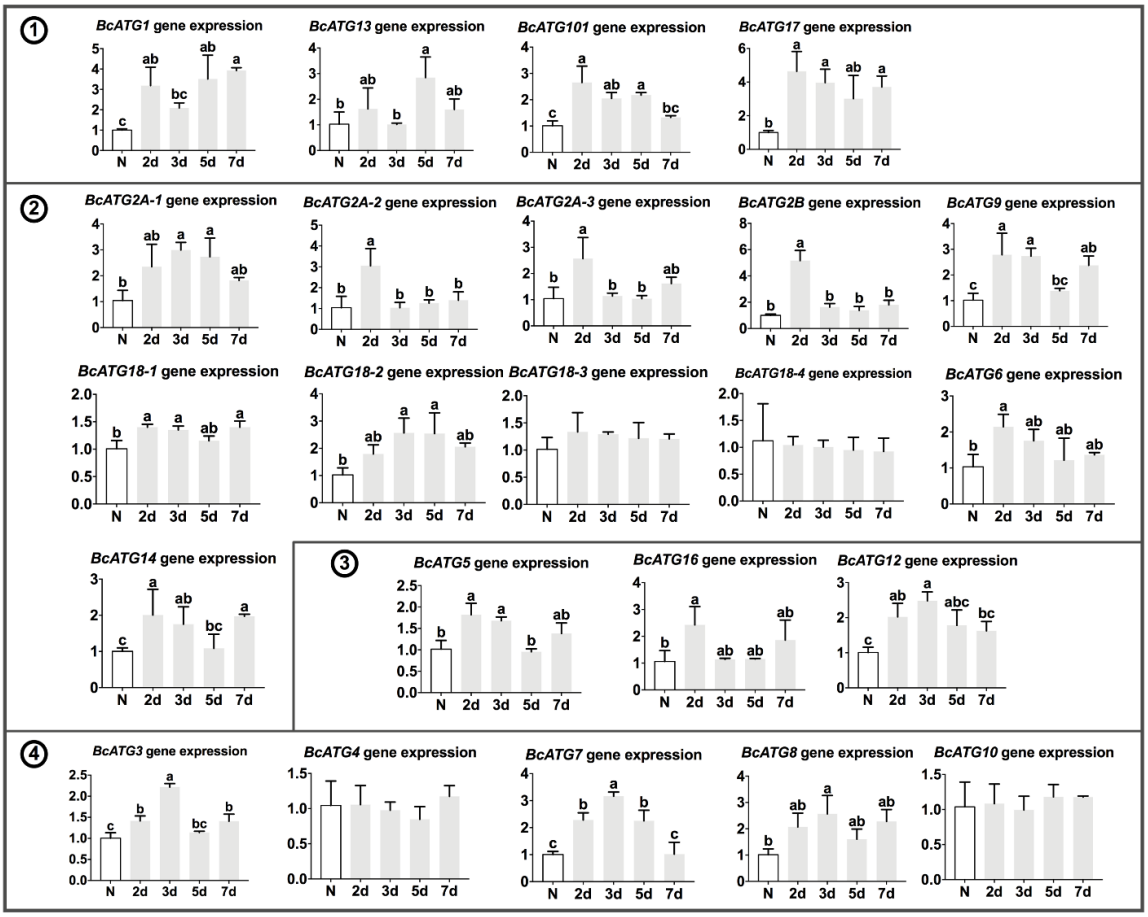

Figure 6.1 Expression of autophagy-related genes (ATGs) in the psyllid gut upon LsoA infection. Data represent means ± SD of three independent experiments. Different letters indicate statistical differences at $P < 0.05$ using one-way ANOVA with Tukey's *post hoc* test. N: Lso-free colonies; A-2d, A-3d, A-5d, and A-7d indicate the psyllids were infected by LsoA for 2, 3, 5, and 7 days, respectively. The enclosed numbers indicate the steps of autophagosome formation: ① autophagy initiation, ② membrane nucleation and phagophore formation, ③ phagophore elongation, and ④ autophagosome completion, respectively.

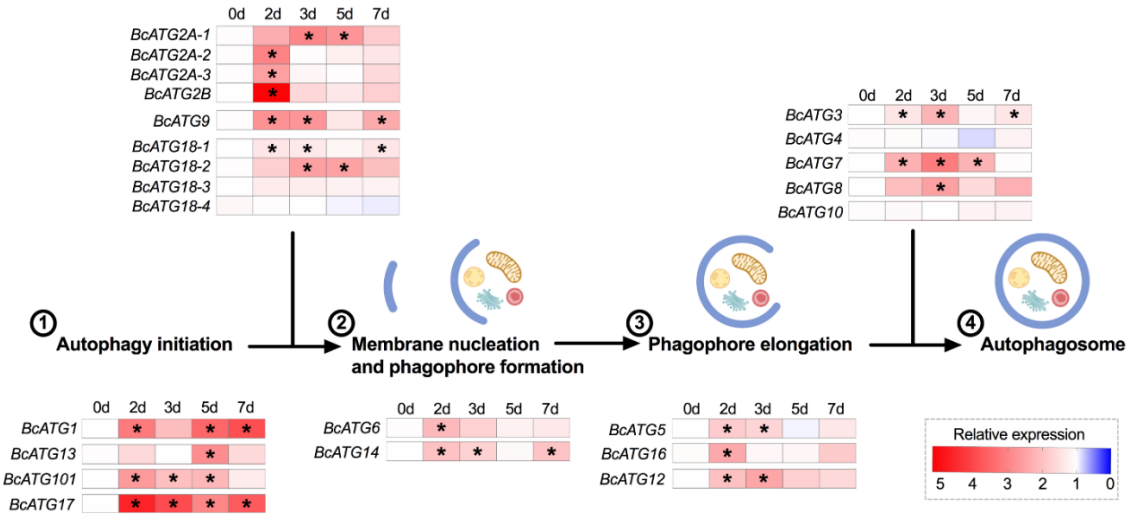

Figure 6.2 Heat map of gene expression profiles of ATGs upon LsoA infection corresponding to the process of autophagosome formation. 0d indicates the control, which are psyllids from the Lso-free colony; 2d, 3d, 5d, and 7d indicate psyllids that were infected by LsoA for 2, 3, 5, and 7 days, respectively. The enclosed numbers indicate the steps of autophagosome formation. * indicates statistical differences between the control (0 day) and the infection (2, 3, 5, or 7 days).

Upon LsoB infection, 13 out of 23 ATGs were regulated and several members had similar expression patterns. First, only *BcATG18-3* was up-regulated at day 2 compared to other time points or compared to the uninfected guts, while four genes (*BcATG1*, *BcATG17*, *BcATG18-2*, and *BcATG8*) remained up-regulated longer. *BcATG101*, *BcATG2A-1*, *BcATG18-1*, *BcATG14*, *BcATG12*, *BcATG4*, *BcATG7* were expressed at higher levels at days 3 or 5, while *BcATG2B* was up-regulated at day 7. Ten genes were not significantly regulated upon LsoB infection (Figs. 6.3 and 6.4).

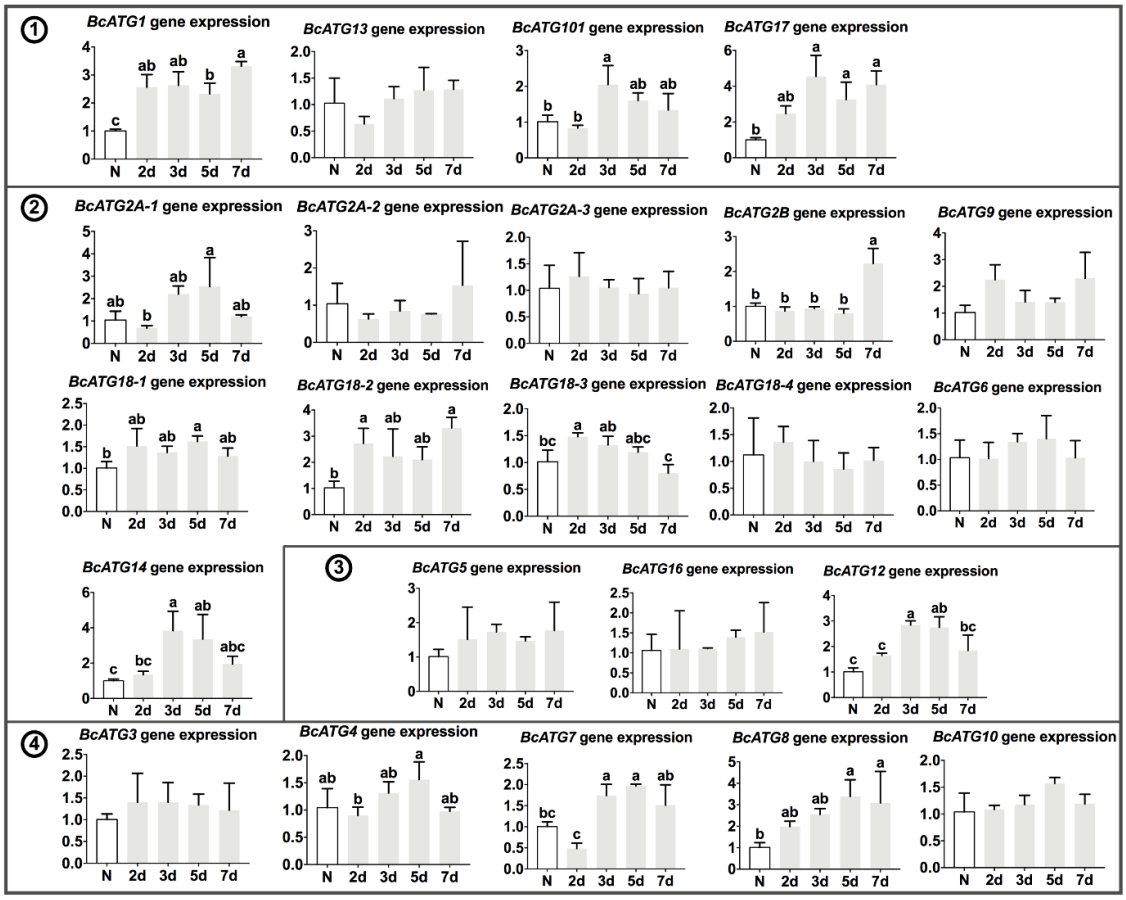

Figure 6.3 Expression of ATGs in the psyllid gut upon LsoB infection. Data represent means ± SD of three independent experiments. Different letters indicate statistical differences at $P < 0.05$ using one-way ANOVA with Tukey's *post hoc* test. N: Lso-free colonies; B-2d, B-3d, B-5d, and B-7d indicate the psyllids were infected by LsoB for 2, 3, 5, and 7 days, respectively. The enclosed numbers indicate the steps of autophagosome formation: ① autophagy initiation, ② membrane nucleation and phagophore formation, ③ phagophore elongation, and ④ autophagosome completion, respectively.

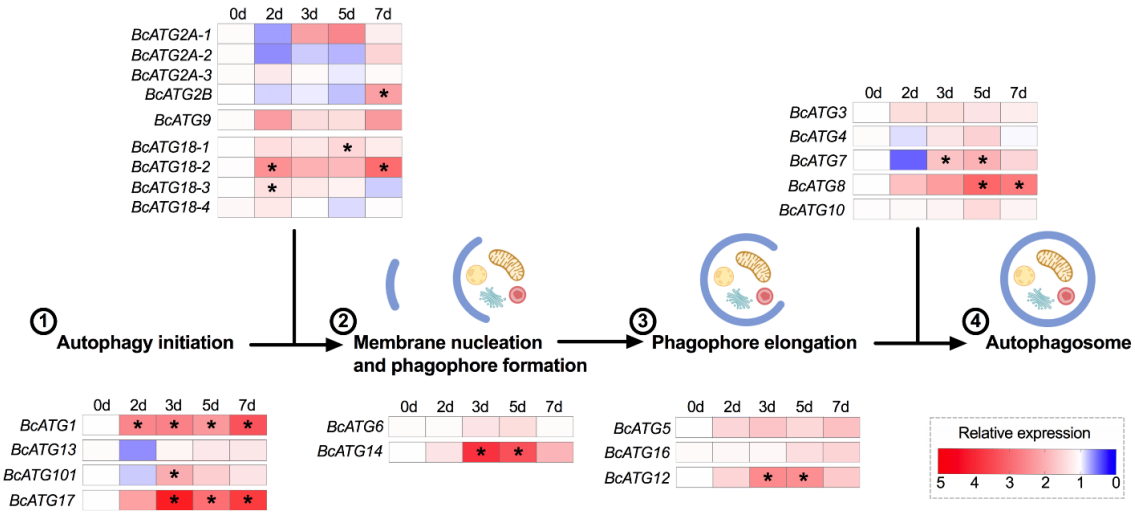

Figure 6.4 Heat map of gene expression profiles of ATGs upon LsoB infection corresponding to the process of autophagosome formation. 0d indicates the control, which are psyllid from the Lso-free colony; 2d, 3d, 5d, and 7d indicate the psyllids that were infected by LsoB for 2, 3, 5, and 7 days, respectively. The enclosed numbers indicate the steps of autophagosome formation. * indicates statistical differences between the control (0 day) and the infection (2, 3, 5, or 7 days).

6.3.3 Expression of autophagy-related genes in response to persistent Lso infection

The expression pattern of the identified autophagy-related genes was also evaluated in adults from the Lso-infected psyllid colonies, which most likely acquired the bacteria during the nymphal stages. We found that approximately half of the ATGs were significantly regulated in response to LsoA or LsoB infection. Ten ATG genes (*BcATG1*, *BcATG2B*, *BcATG9*, *BcATG18-1*, *BcATG18-2*, *BcATG6*, *BcATG16*, *BcATG7*, *BcATG8*, and *BcATG10*) were significantly up-regulated in response to LsoA, while *BcATG17* was down-regulated. However, seven genes (*BcATG1*, *BcATG17*, *BcATG2B*, *BcATG18-1*, *BcATG18-2*, *BcATG14*, and *BcATG8*) were significantly up-regulated in response to LsoB. Taken together, five genes (*BcATG1*, *BcATG2B*, *BcATG18-1*, *BcATG18-2*, and *BcATG8*)

were significantly up-regulated in response to both LsoA and LsoB (Fig. 6.5). Overall, the genes across all the stages of autophagosome formation were significantly regulated (Fig. 6.6).

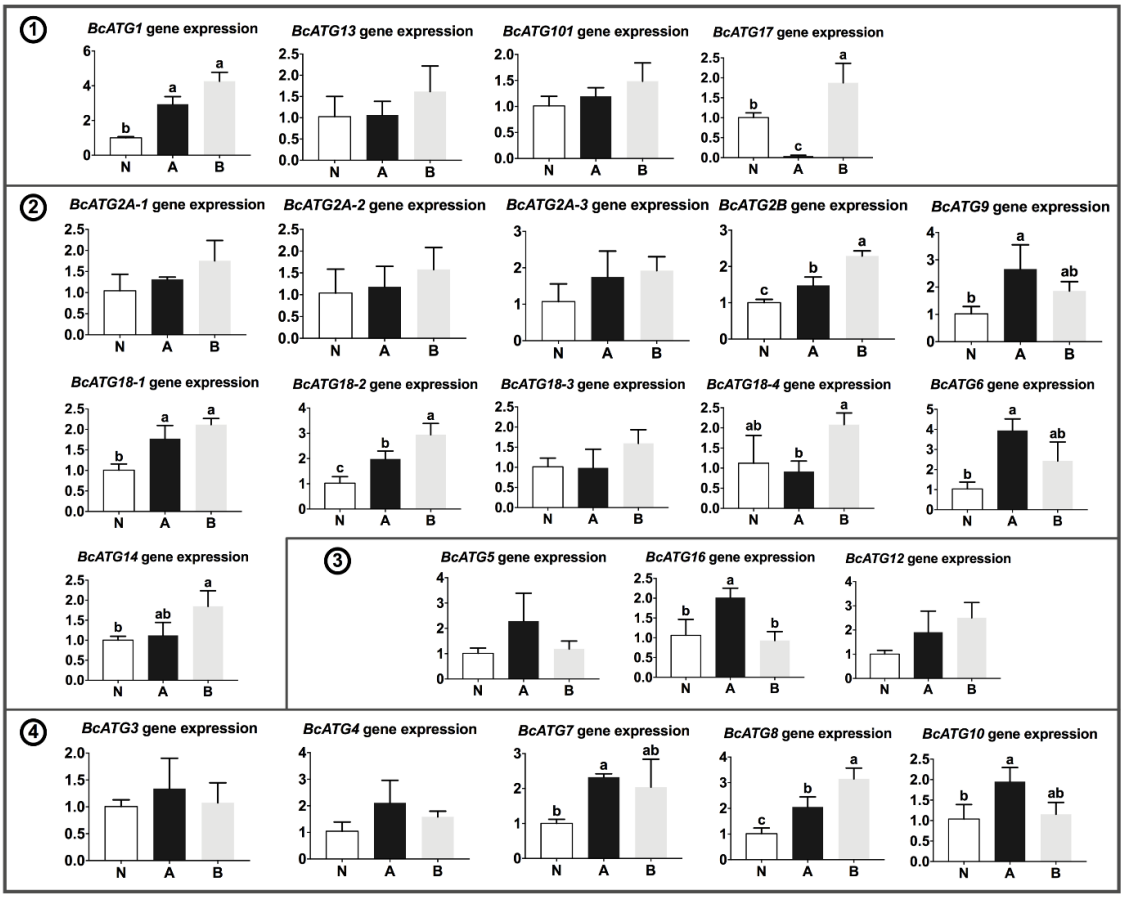

Figure 6.5 Expression of ATGs in the psyllid gut in response to LsoA and LsoB persistent infection. Data represent means ± SD of three independent experiments. Different letters indicate statistical differences at $P < 0.05$ using one-way ANOVA with Tukey's *post hoc* test. N: Lso-free colonies; A and B indicate the psyllids were infected by LsoA and LsoB, respectively. The enclosed numbers indicate the steps of autophagosome formation: ① autophagy initiation, ② membrane nucleation and phagophore formation, ③ phagophore elongation, and ④ autophagosome completion, respectively.

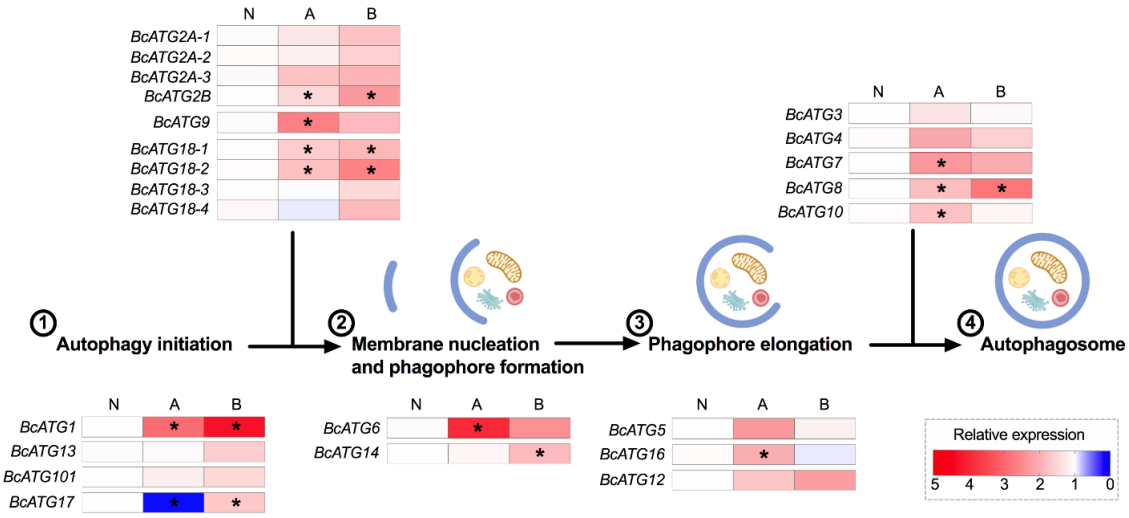

Figure 6.6 Heat map of gene expression profiles of ATGs in response to LsoA and LsoB persistent infection corresponding to the process of autophagosome formation. N: Lso-free colonies; A and B indicate the psyllids were infected by LsoA and LsoB, respectively. The enclosed numbers indicate the steps of autophagosome formation. * indicates statistical differences between the control (0 day) and the infection (2, 3, 5, or 7 days).

6.3.4 Western blot of ATG8 in psyllid guts

To determine whether autophagy is triggered upon Lso exposure or infection, western blot with an antibody recognizing ATG8 was used to analyze the expression of ATG8 protein in Lso-free, Lso-exposed, and Lso-infected psyllids. Our results indicated that only one 16 kDa ATG8-specific band was shown in Lso-free, Lso-exposed and Lso-infected psyllid guts (Fig. 6.7).

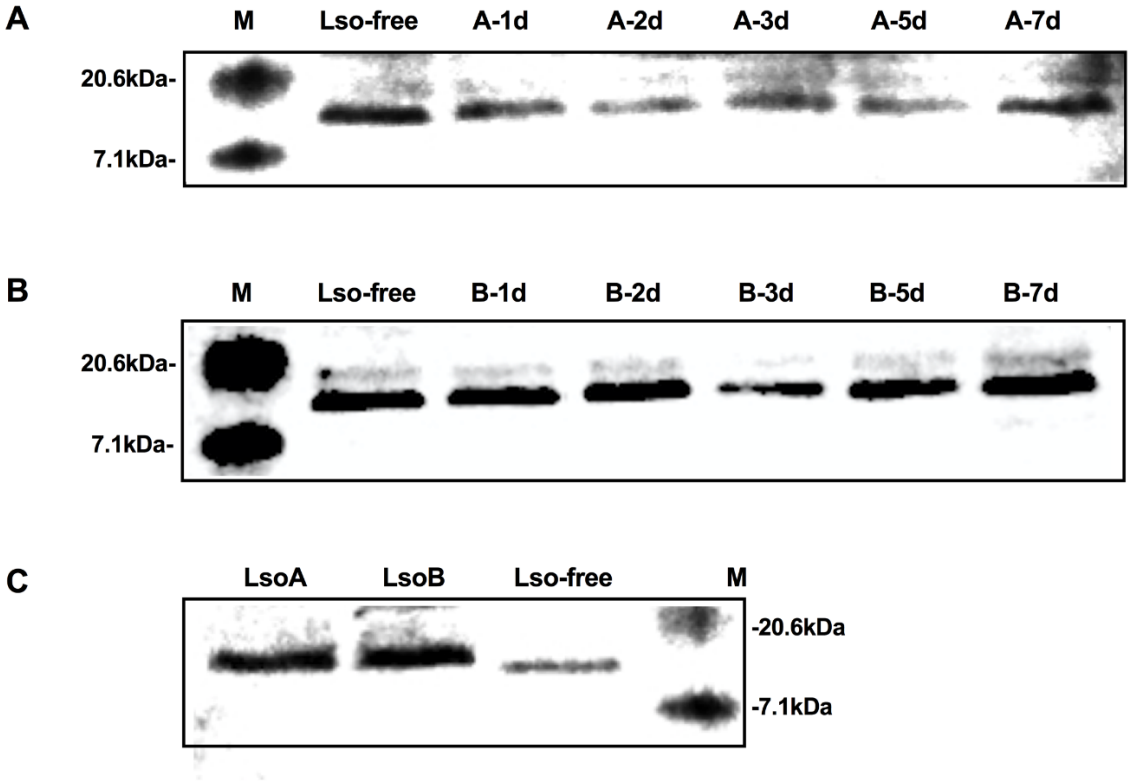

Figure 6.7 Western blot analysis of ATG8 protein in Lso-free, LsoA- and LsoB-exposed and infected psyllids. (A) ATG8 protein in LsoA newly infected psyllids guts; 1d, 2d, 3d, 5d, and 7d indicate 1 day, 2 days, 3 days, 5 days, and 7 days exposure, respectively. (B) ATG8 protein in LsoB newly infected psyllids guts; 1d, 2d, 3d, 5d, and 7d indicate 1 day, 2 days, 3 days, 5 days, and 7 days exposure, respectively. (C) ATG8 protein in LsoA- or LsoB-infected colony psyllids guts. M: protein marker.

6.3.5 Transmission electron microscopy

We performed transmission electron microscopy analysis on guts from Lso-free and LsoA-infected psyllids. The objective was to evaluate whether we could perform transmission electron microscopy in psyllid guts and if we could observe putative autophagosomes in this tissue. In the obtained images specific organelles and structures were observed. Among those structures, putative autophagosomes with double membranes were observed in LsoA-infected psyllid guts (Fig. 6.8).

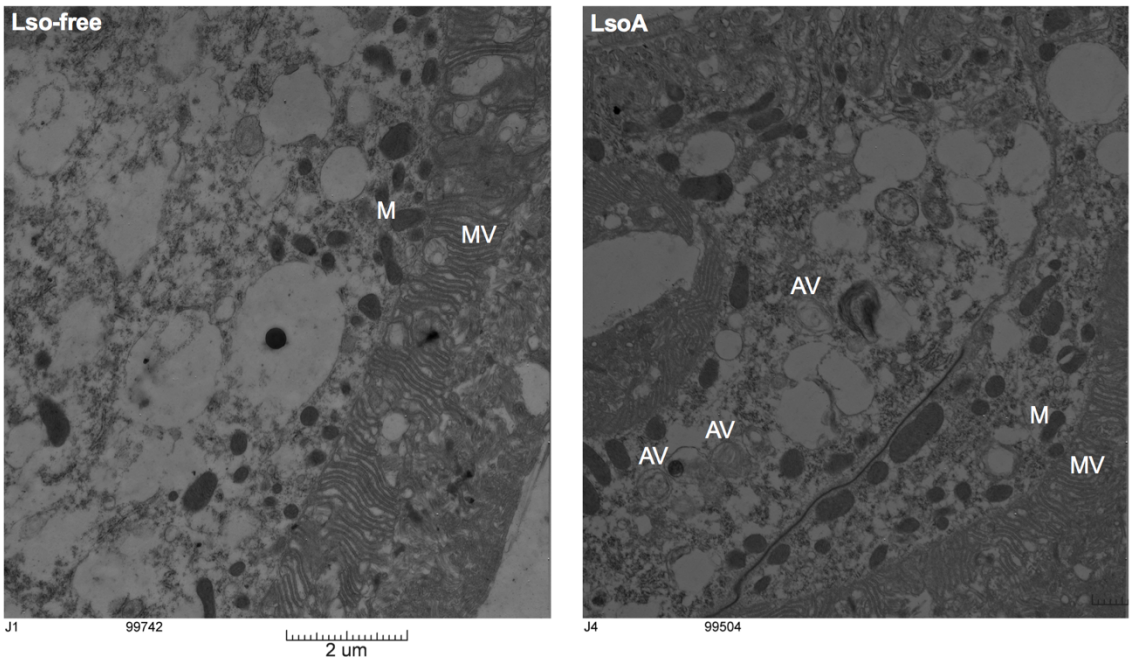

Figure 6.8 Transmission electron micrographs of Lso-free and LsoA-infected psyllid guts. AV: putative autophagic vacuole; M: mitochondria; MV: microvilli.

6.4 DISCUSSION

Autophagy is a self-regulated process and is highly conserved from yeast to mammals (He & Klionsky, 2009). The role of autophagy is not limited to the conditions under the stimulus of starvation. It also has a significant role in the innate immunity. Indeed, autophagy is a cellular degradation process that can capture and eliminate intracellular microbes by delivering them to lysosomes for destruction. In addition to directly degrading pathogens, autophagy can also activate the host immune system (Levine et al., 2011). In mammals, autophagy provides an excellent intracellular defense system against intracellular pathogens such as *Listeria monocytogenes* and *Shigella flexneri* (Krokowski & Mostowy, 2016; Mitchell et al., 2018). Take *S. flexneri* for example, after the bacterial uptake into host cells, the bacterial peptidoglycans can be detected by

nucleotide-binding oligomerization domain (NOD)-like receptors (NLRs), which can further interact with Atg16L1 and recruit other autophagy proteins to initiate autophagosome biogenesis in response to the bacterial invasion (Sorbara et al., 2013).

The core machinery of autophagy can be classified into several functional gene units including: the ATG1/ULK1 (Uncoordinated-51 like kinase) complex (ULK1, ULK2, ATG13, ATG17, ATG101, FIP200 and etc.), the transmembrane protein ATG9 cycling system (ATG2, ATG9, and ATG18), the class III phosphoinositide 3-kinase [PI(3)K] complex (ATG14L, VPS34, Beclin-1, and VPS15), and two ubiquitin-like conjugating systems, ATG12-ATG5 and ATG8/LC3 (light chain 3) (Miller & Celli, 2016). The canonical autophagosome formation process can be subdivided into several phases, including autophagy initiation, membrane nucleation, phagophore formation, phagophore elongation, and autophagosome completion (Gelino & Hansen, 2012; Kuo et al., 2018). First, the ULK/ATG1 and ATG9 complex recruit the autophagy-specific PI(3)K to generate phosphatidylinositol 3-phosphate [PI(3)P] required for membrane nucleation and phagophore formation. To start elongation, the phagophore recruits PI(3)P-binding complex (ATG18/WIPI and ATG2) and then binds ATG5-ATG12/ATG16L1 complex. Finally, the accumulation of those proteins initiates the conjugation of microtubule-associated protein LC3/ATG8 family members to the phagophore, and forms the autophagosome (Gelino & Hansen, 2012; Mizushima et al., 2011).

Here, I determined that the expression of several of the autophagy-related genes in the psyllid gut indeed change significantly after Lso exposure or infection. These genes were regulated in a temporal manner showing different regulation profiles. Upon LsoA

infection, most of the ATGs were significantly up-regulated at 2-day infection, probably at a time when Lso first began to translocate into the gut cells. In particular, the ATGs involved in autophagy initiation and phagophore formation showed more intense up-regulation profile. For instance, *BcATG1* and its subunit *BcATG17*, which control the initiation of autophagosome formation, both were highly upregulated. The induction of six ATGs were delayed until day 3 or day 5 upon exposure to LsoA. Furthermore, eight genes remained induced for a longer period of time. Finally, six genes (*BcATG1*, *BcATG17, BcATG9*, *BcATG18-1*, *BcATG14*, and *BcATG3*) were still up-regulated at day 7. However, the expression of the other tested genes had been reduced to their prior levels. The transcriptional regulation of ATG genes is critical for autophagy. Indeed, the majority of the ATG genes are up-regulated upon stress (Bernard et al., 2015).

The regulation of ATGs upon LsoB infection showed a different pattern compared to LsoA, and approximately half of those genes were regulated during the 7 days analyzed. Specifically, only three genes (*BcATG1*, *BcATG18-2*, and *BcATG18-3*), which contribute to the autophagy initiation and phagophore formation, were significantly up-regulated at the beginning of acquisition (2 days). The other ten genes were induced after 3 days of infection. Overall, the induction of ATGs upon LsoB infection was delayed and/or at a lower level when compared to their expression upon LsoA infection. For instance, *BcATG8*, an ubiquitin-like protein required for the formation of autophagosomal membranes, was significantly up-regulated at day 3 in response to LsoA, while it was induced after day 5 upon LsoB infection. This delayed response probably allows LsoB to be able to replicate and translocate through the gut epithelium faster. Indeed, in Chapter

II, we have shown that LsoB accumulates faster than LsoA and to higher levels in the gut of adult psyllids. Further, this difference in accumulation correlates with a reduced latency and higher transmission efficiency of LsoB than LsoA. We also noted that several genes (e.g., *BcATG13*, *BcATG101*, and *BcATG2*) which function before phagophore formation and elongation showed a down-regulated expression profile (but not significant) upon LsoB infection, probably indicating an early repression of autophagic response by LsoB in the psyllid gut to some extent. Indeed, although bacteria can be targeted and eliminated by autophagy, some of them have evolved strategies to escape this defense system or even hijack the autophagy machinery to promote their intracellular growth (Huang & Brumell, 2014). Importantly, some bacteria inhibit autophagy by directly interfering with the activity of the autophagy components. For instance, *Legionella pneumophila* avoids autophagy using its effector protein by mimicking the function of the host ATG4B-like cysteine protease. ATG4B-like can directly target the amide bond between the tyrosine and the glycine at the C terminus of LC3/ATG8, which is covalently linked to phosphatidylethanolamine (PE) during the autophagy induction to form LC3-PE; therefore further inhibit autophagosome formation (Choy et al., 2012). We hypothesize that probably LsoB can repress (or not induce to the same level) the autophagic response in psyllid gut at the early stages of infection while LsoA could not. Indeed, the early LsoA infection significantly up-regulated all the ATGs involved in autophagy induction in other hemipteran insects by plant viruses. Specifically, three autophagy-related genes (*Ulk1/Atg1*, *Atg5*, and *Atg8*) increased rapidly and significantly after 48 hours post inoculation of RGDV in the rice leafhopper (Chen et al., 2017); furthermore, the

expression of the three ATG genes (*Atg3*, *Atg9* and *Atg12*) increased significantly in TYLCV-infected whiteflies (Wang et al., 2016). In our study, *BcATG1*, *BcATG5*, *BcATG3*, *BcATG9*, and *BcATG12* were significantly regulated after 2 days of LsoA infection, and *BcATG8* was expressed at higher levels at day 3. However, only three of those genes (*BcATG1*, *BcATG12*, and *BcATG8*) were induced upon LsoB infection. Therefore, we hypothesized that autophagy could be induced in the gut of the adult psyllid upon LsoA infection, and this induction may be linked to the reduced increase of LsoA titer in the gut of psyllids compared to LsoB and its delayed transmission. It is unclear whether autophagy is induced in response to LsoB. If induced, this response is probably delayed compared to the induction by LsoA.

In addition, from the ATGs expression profile in response to persistent Lso infection, I also found that several ATGs were up-regulated in response to LsoA or LsoB and that more ATGs were up-regulated in response to LsoA. This observation is consistent with the ATGs induction upon Lso infection. Importantly, differences in virulence between these two haplotypes were determined in association with their host plants and insect vector: in both cases, LsoB was found to be more pathogenic (Harrison et al., 2019; Mendoza Herrera et al., 2018; Yao et al., 2016). It is therefore possible that LsoB is able to better defend itself against the psyllid immunity, or even also manipulate those defenses to its advantage. We also noted that *BcATG17* was significantly down-regulated in response to persistent LsoA infection, indicating a putative repression of the autophagic response. However, both LsoA and LsoB significantly induced the core autophagy gene, *BcATG8*. Therefore, we hypothesized that autophagy could be occurring the gut of the

adult psyllid in response to persistent LsoA and LsoB infection. However, the autophagic immune response cannot be an efficient defense because both LsoA and LsoB can be successfully transmitted by potato psyllids. The plausible explanation is that even if autophagy is induced in response to the pathogen, this defense strategy is not sufficient or not widespread enough to stop Lso.

Several molecular markers of autophagy have been studied to date but the conversion of ATG8 (LC3)-I to ATG8 (LC3)-II via phosphatidylethanolamine (PE) conjugation has been accepted as the gold standard for autophagosome formation. Upon autophagic signal, ATG8 (LC3)-I is conjugated by Atg7, Atg3 and Atg12-Atg5-Atg16L multimers to a PE moiety for the generation of ATG8 (LC3)-II form. Although larger in molecular mass, ATG8 (LC3)-II shows faster electrophoretic mobility in SDS-PAGE gels because of lipidation. The differential mobility of ATG8 (LC3)-I and ATG8 (LC3)-II's helps in their detection/characterization in western blot assay and the conversion of ATG8 (LC3)-I to the lower migrating form ATG8 (LC3)-II has been used as an indicator of autophagy. Therefore, we further verified the autophagy by detecting ATG8 (LC3) protein based on western blot assay. We used the anti-ATG8 (LC3) antibody which has been successfully tested in whiteflies (Wang et al., 2016). However, only one protein band was shown in all the tested samples. In addition, we were unable to determine if the band observed corresponded to ATG8 (LC3)-I or ATG8 (LC3)-II because we did not have a positive control. It is expected that both bands are present in tissues, it is just their relative proportion that changes if autophagy is induced. Therefore, we suspect that this antibody does not work for the potato psyllid. In the future, we will need to include a positive control

to determine which form of ATG8 (LC3) is recognized or test another antibody. Several inducers of autophagy exist, however the amount of the chemical used and the exposure time need to be assessed to properly induce autophagy.

Transmission electron microscopy was also used to assess the formation of autophagic compartments. We indeed found the putative autophagosomes with double membranes structure in LsoA-infected psyllid guts. This was a test to evaluate the dissection, embedding and cutting protocol. Future experiments will need to include the immunelocalization of Lso in the sample to verify that indeed these autophagosomes are enclosing Lso. In addition, LsoB-infected guts need to be analyzed.

In summary, we identified 23 homologs of autophagy-related genes from potato psyllid. Our study suggested that the expression of majority of autophagy-related genes changed significantly after LsoA or LsoB exposure or in the case of established infection of the gut. Importantly, in the case of autophagy, the gene expression correlates with the actual autophagy (He & Klionsky, 2009). However, we cannot conclude if autophagy was really induced by Lso in the present study. Further investigation needs to be conducted to deepen the study of autophagic response of potato psyllid to Lso infection and its role in Lso transmission. The methods such as RNAi-mediated gene silencing to analyze the autophagic response, are recommended.

CHAPTER VII

SUMMARY AND CONCLUSIONS

The gut of potato psyllid is the first organ Lso encounters. It is not only vital for nutrient uptake, but it also plays a key role in immumity and could be a barrier for bacterial transmission. Indeed, examples of strong gut barriers that decrease the efficiency of an insect as vector exist (Burrows et al., 2006; Ohnishi et al., 2009; Tamborindeguy et al., 2013). Thus, a gut barrier is a promising way to disrupt Lso transmission. In this dissertation, I mainly focused on the molecular interactions between Lso and adults of the potato psyllid at the gut interface. This dissertation will be informative to develop sustainable control approaches for the damaging plant diseases based on the disruption of the interactions.

The genes involved in Lso and potato psyllid interactions at the gut interface were investigated by RNA-seq. In general, early ingestion of LsoA or LsoB has a dramatic impact on the physiology of psyllid gut and changes the expression of genes involved in modulation of stress response, immunity, detoxification as well as cell proliferation and epithelial renewal. However, the data also showed that potato psyllid mounts distinct intestinal responses (whether on numbers or categories of genes) upon infection of two Lso haplotypes with most of the distinct genes elicited by LsoB. Indeed, results from our previous studies indicated that LsoB was found to be more pathogenic in association with their host plants and insect vector (Harrison et al., 2019; Mendoza Herrera et al., 2018; Yao et al., 2016). In this study, I also found that LsoA and LsoB have distinct acquisition

and transmission profiles. LsoB titer increased more rapidly in the adult psyllid gut than LsoA. Furthermore, LsoB had a significantly higher transmission efficiency by adult psyllids than LsoA and a shorter latent period between acquisition and inoculation. It is therefore possible that LsoB is able to better defend itself against the psyllid responses, or even also manipulate those defenses to its advantage, allowing LsoB to be able to replicate and translocate through the gut epithelium faster.

It is also well known that the ability of the pathogen to infect the gut and to cross from the gut into the hemocoel could determine the transmission efficiency. For increased transmission, pathogens must exploit their host's cell machinery and avoid host's immune defenses (Vyas et al., 2015). Indeed, the immune response affects the acquisition and transmission of plant pathogens. For instance, apoptosis was observed in the gut of Asian citrus psyllid adults from the CLas-infected colonies, but not in the nymphal gut (Ghanim et al., 2016; Mann et al., 2018). Additionally, CLas titer increased at a faster rate when the bacterium was acquired by nymphs compared to adults (Ammar et al., 2016). Therefore, it is probable that the apoptotic response serves to limit the acquisition or transmission efficiency of CLas by the Asian citrus psyllid. As a parallel study, in this dissertation, I investigated the programmed cell death (apoptosis and autophagy) response of potato psyllid gut to Lso exposure or infection. The results showed that Lso does not induce apoptosis in the gut of the adult potato psyllid. Thus, although the pathogen-vector systems of CLas-Asian citrus psyllid and Lso-potato psyllid are largely similar, the adaptive evolution of the insect vectors with the bacteria might have resulted in different infection strategies. In particular, Asian citrus psyllid might exploit the apoptotic response to limit

the transmission of CLas, while this does not appear to occur in the potato psyllid in response to Lso. However, further investigation showed that Lso appears to have evolved the ability to suppress the cellular apoptotic response in potato psyllid gut to establish infection and to permit its life cycle progression. In detail, the manipulation of apoptosis and the reduction of the caspase expression observed in the Lso-exposed cells correlated to the up-regulation of the apoptosis inhibitor survivin. Silencing of survivin significantly up-regulated the expression of effector caspases and decreased Lso accumulation in the gut of adult psyllid.

Autophagy is another type of programmed cell death. The data indicated that the expression of majority of autophagy-related genes changed significantly after LsoA or LsoB exposure or infection at the gut interface. Transmission electronic microscopy further supported that autophagy probably could be induced in psyllid guts during the persistent Lso infection. However, western blot analysis did not. Therefore, autophagy might be a complicated process in the interactions between Lso and potato psyllid.

In summary, inducing or inhibiting the programmed cell death and other immune responses in the gut of potato psyllid could affect Lso acquisition and could be used as a novel approach to disrupt Lso transmission. Future studies should focus on the role of the autophagic response in Lso acquisition and transmission; in addition, further investigations would seek to identify candidate genes or pathways involved in Lso transmission by potato psyllid based on the existing transcriptome dataset.

REFERENCES

Agarwal, A., Parida, M. and Dash, P.K. (2017) Impact of transmission cycles and vector competence on global expansion and emergence of arboviruses. *Reviews in Medical Virology* **27**: e1941.

Aguilar, R., Jedlicka, A.E., Mintz, M., Mahairaki, V., Scott, A.L. and Dimopoulos, G. (2005) Global gene expression analysis of *Anopheles gambiae* responses to microbial challenge. *Insect Biochemistry and Molecular Biology* **35**: 709-719.

Albuquerque Tomilhero Frias, A., Ibanez, F., Mendoza, A., de Carvalho Nunes, W.M. and Tamborindeguy, C. (2020) Effects of "*Candidatus* Liberibacter solanacearum"(haplotype B) on *Bactericera cockerelli* fitness and vitellogenesis. *Insect Science* **27**: 58-68.

Alfaro-Fernández, A., Siverio, F., Cebrián, M., Villaescusa, F. and Font, M. (2012) '*Candidatus* Liberibacter solanacearum'associated with *Bactericera trigonica*-affected carrots in the Canary Islands. *Plant Disease* **96**: 581-581.

Ammar, E.-D. and Hogenhout, S.A. (2008) A neurotropic route for Maize mosaic virus (Rhabdoviridae) in its planthopper vector *Peregrinus maidis*. *Virus Research* **131**: 77-85.

Ammar, E.-D., Ramos, J.E., Hall, D.G., Dawson, W.O. and Shatters Jr, R.G. (2016) Acquisition, replication and inoculation of *Candidatus* Liberibacter asiaticus following various acquisition periods on huanglongbing-infected citrus by nymphs and adults of the Asian citrus psyllid. *PLoS One* **11**: e0159594.

Ammar, E.-D., Shatters Jr, R.G., Lynch, C. and Hall, D.G. (2011a) Detection and relative titer of *Candidatus* Liberibacter asiaticus in the salivary glands and alimentary canal of *Diaphorina citri* (Hemiptera: Psyllidae) vector of citrus huanglongbing disease. *Annals of the Entomological Society of America* **104**: 526-533.

Ammar, E.-D., Tsai, C.-W., Whitfield, A.E., Redinbaugh, M.G. and Hogenhout, S.A. (2009) Cellular and molecular aspects of rhabdovirus interactions with insect and plant hosts. *Annual Review of Entomology* **54**: 447-468.

Ammar, E.D., Gomez-Luengo, R., Gordon, D. and Hogenhout, S. (2005) Characterization of Maize Iranian mosaic virus and comparison with Hawaiian and other isolates of Maize mosaic virus (Rhabdoviridae). *Journal of Phytopathology* **153**: 129-136.

Ammar, E.D., Shatters, R.G. and Hall, D.G. (2011b) Localization of *Candidatus* Liberibacter asiaticus, associated with citrus Huanglongbing disease, in its psyllid vector using fluorescence in situ hybridization. *Journal of Phytopathology* **159**: 726-734.

Arp, A.P., Hunter, W.B. and Pelz-Stelinski, K.S. (2016) Annotation of the Asian citrus psyllid genome reveals a reduced innate immune system. *Frontiers in Physiology* **7**: 570.

Asai, S. and Shirasu, K. (2015) Plant cells under siege: plant immune system versus pathogen effectors. *Current Opinion in Plant Biology* **28**: 1-8.

Bae, S.J., Kim, M., Kim, S.-H., Kwon, Y.E., Lee, J.-H., Kim, J., Chung, C.H., Lee, W.-J. and Seol, J.H. (2015) NEDD4 controls intestinal stem cell homeostasis by regulating the Hippo signalling pathway. *Nature Communications* **6**: 6314.

Bai, X., Correa, V.R., Toruño, T.Y., Ammar, E.-D., Kamoun, S. and Hogenhout, S.A. (2009) AY-WB phytoplasma secretes a protein that targets plant cell nuclei. *Molecular Plant-Microbe Interactions* **22**: 18-30.

Barreau, F. and Hugot, J. (2014) Intestinal barrier dysfunction triggered by invasive bacteria. *Current Opinion in Microbiology* **17**: 91-98.

Bergmann, A. (2010) The role of ubiquitylation for the control of cell death in *Drosophila*. *Cell Death and Differentiation* **17**: 61.

Bernard, A., Jin, M., Xu, Z. and Klionsky, D.J. (2015) A large-scale analysis of autophagy-related gene expression identifies new regulators of autophagy. *Autophagy* **11**: 2114-2122.

Bové, J.M., Renaudin, J., Saillard, C., Foissac, X. and Garnier, M. (2003) *Spiroplasma citri*, a plant pathogenic mollicute: relationships with its two hosts, the plant and the leafhopper vector. *Annual Review of Phytopathology* **41**: 483-500.

Buchman, J.L., Sengoda, V.G. and Munyaneza, J.E. (2011) Vector transmission efficiency of liberibacter by *Bactericera cockerelli* (Hemiptera: Triozidae) in zebra chip potato disease: effects of psyllid life stage and inoculation access period. *Journal of Economic Entomology* **104**: 1486-1495.

Buchon, N., Broderick, N.A., Poidevin, M., Pradervand, S. and Lemaitre, B. (2009) *Drosophila* intestinal response to bacterial infection: activation of host defense and stem cell proliferation. *Cell Host & Microbe* **5**: 200-211.

Burrows, M., Caillaud, M., Smith, D., Benson, E., Gildow, F. and Gray, S. (2006) Genetic regulation of polerovirus and luteovirus transmission in the aphid *Schizaphis graminum*. *Phytopathology* **96**: 828-837.

Canale, M.C., Tomaseto, A.F., Haddad, M.d.L., Della Coletta-Filho, H. and Lopes, J.R.S. (2016) Latency and persistence of '*Candidatus* Liberibacter asiaticus' in its psyllid vector, *Diaphorina citri* (Hemiptera: Liviidae). *Phytopathology* **107**: 264-272.

Candé, C., Cecconi, F., Dessen, P. and Kroemer, G. (2002) Apoptosis-inducing factor (AIF): key to the conserved caspase-independent pathways of cell death? *Journal of Cell Science* **115**: 4727-4734.

Cao, X., He, Y., Hu, Y., Wang, Y., Chen, Y.-R., Bryant, B., Clem, R.J., Schwartz, L.M., Blissard, G. and Jiang, H. (2015) The immune signaling pathways of *Manduca sexta*. *Insect Biochemistry and Molecular Biology* **62**: 64-74.

Carpane, P., Melcher, U., Wayadande, A., de la Paz Gimenez Pecci, M., Laguna, G., Dolezal, W. and Fletcher, J. (2013) An analysis of the genomic variability of the phytopathogenic mollicute *Spiroplasma kunkelii*. *Phytopathology* **103**: 129-134.

Charroux, B. and Royet, J. (2010) *Drosophila* immune response: From systemic antimicrobial peptide production in fat body cells to local defense in the intestinal tract. *Fly* **4**: 40-47.

Chen, W., Hasegawa, D.K., Kaur, N., Kliot, A., Pinheiro, P.V., Luan, J., Stensmyr, M.C., Zheng, Y., Liu, W. and Sun, H. (2016a) The draft genome of whitefly *Bemisia tabaci* MEAM1, a global crop pest, provides novel insights into virus transmission, host adaptation, and insecticide resistance. *BMC Biology* **14**: 110.

Chen, Y., Chen, Q., Li, M., Mao, Q., Chen, H., Wu, W., Jia, D. and Wei, T. (2017) Autophagy pathway induced by a plant virus facilitates viral spread and transmission by its insect vector. *PLoS Pathogens* **13**: e1006727.

Chen, Y., Lu, C., Li, M., Wu, W., Zhou, G. and Wei, T. (2016b) Adverse effects of rice gall dwarf virus upon its insect vector *Recilia dorsalis* (Hemiptera: Cicadellidae). *Plant Disease* **100**: 784-790.

Choy, A., Dancourt, J., Mugo, B., O'Connor, T.J., Isberg, R.R., Melia, T.J. and Roy, C.R. (2012) The *Legionella* effector RavZ inhibits host autophagy through irreversible Atg8 deconjugation. *Science* **338**: 1072-1076.

Cicero, J., Fisher, T. and Brown, J.K. (2016) Localization of '*Candidatus* Liberibacter solanacearum'and evidence for surface appendages in the potato psyllid vector. *Phytopathology* **106**: 142-154.

Cicero, J.M., Fisher, T.W., Qureshi, J.A., Stansly, P.A. and Brown, J.K. (2017) Colonization and Intrusive Invasion of Potato Psyllid by '*Candidatus* Liberibacter solanacearum'. *Phytopathology* **107**: 36-49.

Cilia, M., Tamborindeguy, C., Fish, T., Howe, K., Thannhauser, T.W. and Gray, S. (2011) Genetics coupled to quantitative intact proteomics links heritable aphid and endosymbiont protein expression to circulative polerovirus transmission. *Journal of Virology* **85**: 2148.

Clarke, T.E. and Clem, R.J. (2003) Insect defenses against virus infection: the role of apoptosis. *International Reviews of Immunology* **22**: 401-424.

Clem, R. (2005) The role of apoptosis in defense against baculovirus infection in insects. In: *Role of apoptosis in infection*. pp. 113-129. Springer.

Cock, P.J., Chilton, J.M., Grüning, B., Johnson, J.E. and Soranzo, N. (2015) NCBI BLAST+ integrated into Galaxy. *Gigascience* **4**: 39.

Cooper, W.R., Sengoda, V.G. and Munyaneza, J.E. (2014) Localization of '*Candidatus* Liberibacter solanacearum'(Rhizobiales: Rhizobiaceae) in *Bactericera cockerelli* (Hemiptera: Triozidae). *Annals of the Entomological Society of America* **107**: 204-210.

Crook, N.E., Clem, R.J. and Miller, L.K. (1993) An apoptosis-inhibiting baculovirus gene with a zinc finger-like motif. *Journal of Virology* **67**: 2168-2174.

Dangl, J.L. and Jones, J.D. (2001) Plant pathogens and integrated defence responses to infection. *Nature* **411**: 826.

Danial, N.N. and Korsmeyer, S.J. (2004) Cell death: critical control points. *Cell* **116**: 205-219.

Diallo, A. and Prigent, C. (2011) The serine/threonine kinases that control cell cycle progression as therapeutic targets. *Bulletin du Cancer* **98**: 1335-1345.

Dietzgen, R., Mann, K. and Johnson, K. (2016) Plant virus–insect vector interactions: current and potential future research directions. *Viruses* **8**: 303.

Dodds, P.N. and Rathjen, J.P. (2010) Plant immunity: towards an integrated view of plant–pathogen interactions. *Nature Reviews Genetics* **11**: 539.

Domingues, C. and Ryoo, H.D. (2012) *Drosophila* BRUCE inhibits apoptosis through non-lysine ubiquitination of the IAP-antagonist REAPER. *Cell Death and Differentiation* **19**: 470.

Dourado, M.N., Santos, D.S., Nunes, L.R., Costa de Oliveira, R.L.B.d., de Oliveira, M.V. and Araújo, W.L. (2015) Differential gene expression in *Xylella fastidiosa* 9a5c during co-cultivation with the endophytic bacterium *Methylobacterium mesophilicum* SR1. 6/6. *Journal of Basic Microbiology* **55**: 1357-1366.

Duan, Y., Zhou, L., Hall, D.G., Li, W., Doddapaneni, H., Lin, H., Liu, L., Vahling, C.M., Gabriel, D.W. and Williams, K.P. (2009) Complete genome sequence of citrus huanglongbing bacterium,'*Candidatus* Liberibacter asiaticus' obtained through metagenomics. *Molecular Plant-Microbe Interactions* **22**: 1011-1020.

Earnshaw, W.C., Martins, L.M. and Kaufmann, S.H. (1999) Mammalian caspases: structure, activation, substrates, and functions during apoptosis. *Annual Review of Biochemistry* **68**: 383-424.

Eigenbrode, S.D., Bosque-Pérez, N.A. and Davis, T.S. (2018) Insect-borne plant pathogens and their vectors: ecology, evolution, and complex interactions. *Annual Review of Entomology* **63**: 169-191.

Elmore, S.J.T.p. (2007) Apoptosis: a review of programmed cell death. *Toxicologic Pathology* **35**: 495-516.

Érdi, B., Nagy, P., Zvara, Á., Varga, Á., Pircs, K., Ménesi, D., Puskás, L.G. and Juhász, G. (2012) Loss of the starvation-induced gene Rack1 leads to glycogen deficiency and impaired autophagic responses in *Drosophila*. *Autophagy* **8**: 1124-1135.

Fan, T., Lu, H., Hu, H., Shi, L., McClarty, G.A., Nance, D.M., Greenberg, A.H. and Zhong, G. (1998) Inhibition of apoptosis in chlamydia-infected cells: blockade of mitochondrial cytochrome c release and caspase activation. *Journal of Experimental Medicine* **187**: 487-496.

Fisher, T.W., Vyas, M., He, R., Nelson, W., Cicero, J.M., Willer, M., Kim, R., Kramer, R., May, G.A. and Crow, J.A. (2014) Comparison of potato and Asian citrus psyllid adult and nymph transcriptomes identified vector transcripts with potential involvement in circulative, propagative Liberibacter transmission. *Pathogens* **3**: 875-907.

Fletcher, J., Wayadande, A., Melcher, U. and Ye, F. (1998) The phytopathogenic mollicute-insect vector interface: a closer look. *Phytopathology* **88**: 1351-1358.

Froissart, R., Michalakis, Y. and Blanc, S. (2002) Helper component-transcomplementation in the vector transmission of plant viruse. *Phytopathology* **92**: 576-579.

Galán, J.E. (1999) Interaction of Salmonella with host cells through the centisome 63 type III secretion system. *Current Opinion in Microbiology* **2**: 46-50.

Gao, L.-Y. and Kwaik, Y.A. (2000) Hijacking of apoptotic pathwaysby bacterial pathogens. *Microbes and Infection* **2**: 1705-1719.

Gasparich, G.E. (2010) Spiroplasmas and phytoplasmas: microbes associated with plant hosts. *Biologicals* **38**: 193-203.

Gelino, S. and Hansen, M. (2012) Autophagy-an emerging anti-aging mechanism. *Journal of Clinical & Experimental Pathology* **S4**: 006.

Geng, L., Qian, L.-X., Shao, R.-X., Liu, Y.-Q., Liu, S.-S. and Wang, X.-W. (2018) Transcriptome profiling of whitefly guts in response to Tomato yellow leaf curl virus infection. *Virology Journal* **15**: 14.

Gerardo, N.M., Altincicek, B., Anselme, C., Atamian, H., Barribeau, S.M., De Vos, M., Duncan, E.J., Evans, J.D., Gabaldón, T. and Ghanim, M.J.G.b. (2010) Immunity and other defenses in pea aphids, *Acyrthosiphon pisum*. *Genome Biology* **11**: R21.

Ghanim, M., Achor, D., Ghosh, S., Kontsedalov, S., Lebedev, G. and Levy, A. (2017) '*Candidatus* Liberibacter asiaticus' accumulates inside endoplasmic reticulum associated vacuoles in the gut cells of *Diaphorina citri*. *Scientific Reports* **7**: 16945.

Ghanim, M., Fattah-Hosseini, S., Levy, A. and Cilia, M. (2016) Morphological abnormalities and cell death in the Asian citrus psyllid (*Diaphorina citri*) midgut associated with *Candidatus* Liberibacter asiaticus. *Scientific Reports* **6**: 33418.

Ghosh, S., Jassar, O., Kontsedalov, S., Lebedev, G., Wang, C., Turner, D., Levy, A. and Ghanim, M. (2019) A transcriptomics approach reveals putative interaction of *Candidatus* Liberibacter solanacearum with the endoplasmic reticulum of its psyllid vector. *Insects* **10**: 279.

Gilbertson, R.L., Batuman, O., Webster, C.G. and Adkins, S. (2015) Role of the insect supervectors *Bemisia tabaci* and *Frankliniella occidentalis* in the emergence and global spread of plant viruses. *Annual Review of Virology* **2**: 67-93.

Gildow, F. (1993) Evidence for receptor-mediated endocytosis regulating luteovirus acquisition by aphids. *Phytopathology* **83**: 270-270.

Girardot, F., Monnier, V. and Tricoire, H. (2004) Genome wide analysis of common and specific stress responses in adult *Drosophila melanogaster*. *BMC Genomics* **5**: 74.

Glynn, J., Islam, M., Bai, Y., Lan, S., Wen, A., Gudmestad, N., Civerolo, E. and Lin, H. (2012) Multilocus sequence typing of '*Candidatus* Liberibacter solanacearum'isolates from North America and New Zealand. *Journal of Plant Pathology* **94**: 223-228.

Gottlieb, Y., Zchori-Fein, E., Mozes-Daube, N., Kontsedalov, S., Skaljac, M., Brumin, M., Sobol, I., Czosnek, H., Vavre, F. and Fleury, F. (2010) The transmission efficiency of tomato yellow leaf curl virus by the whitefly *Bemisia tabaci* is correlated with the presence of a specific symbiotic bacterium species. *Journal of Virology* **84**: 9310-9317.

Götz, M., Popovski, S., Kollenberg, M., Gorovits, R., Brown, J.K., Cicero, J.M., Czosnek, H., Winter, S. and Ghanim, M. (2012) Implication of *Bemisia tabaci* heat shock protein 70 in begomovirus-whitefly interactions. *Journal of Virology* **86**: 13241-13252.

Goyal, L. (2001) Cell death inhibition: keeping caspases in check. *Cell* **104**: 805-808.

Gray, S. and Gildow, F.E. (2003) Luteovirus-aphid interactions. *Annual Review of Phytopathology* **41**: 539-566.

Gray, S.M. and Banerjee, N. (1999) Mechanisms of arthropod transmission of plant and animal viruses. *Microbiol. Mol. Biol. Rev.* **63**: 128-148.

Green, D.R. (2005) Apoptotic pathways: ten minutes to dead. *Cell* **121**: 671-674.

Green, D.R. (2011) *Means to an end: apoptosis and other cell death mechanisms*. Cold Spring Harbor Laboratory Press.

Grimaldi, D., Engel, M.S. and Engel, M.S. (2005) *Evolution of the Insects*. Cambridge University Press.

Gullan, P.J. and Cranston, P.S. (2014) *The insects: an outline of entomology*. John Wiley & Sons.

Haapalainen, M. (2014) Biology and epidemics of *Candidatus* Liberibacter species, psyllid-transmitted plant-pathogenic bacteria. *Annals of Applied Biology* **165**: 172-198.

Haapalainen, M.L., Wang, J., Latvala, S., Lehtonen, M.T., Pirhonen, M. and Nissinen, A.I. (2018) Genetic variation of '*Candidatus* Liberibacter solanacearum' haplotype C and identification of a novel haplotype from *Trioza urticae* and stinging nettle. *Phytopathology* **108**: 925-934.

Hacquard, S., Spaepen, S., Garrido-Oter, R. and Schulze-Lefert, P. (2017) Interplay between innate immunity and the plant microbiota. *Annual Review of Phytopathology* **55**: 565-589.

Haissaguerre, M., Saucisse, N. and Cota, D. (2014) Influence of mTOR in energy and metabolic homeostasis. *Molecular and Cellular Endocrinology* **397**: 67-77.

Hansen, A., Trumble, J., Stouthamer, R. and Paine, T. (2008) A new huanglongbing species,"*Candidatus* Liberibacter psyllaurous", found to infect tomato and potato, is vectored by the psyllid *Bactericera cockerelli* (Sulc). *Applied and Environmental Microbiology* **74**: 5862-5865.

Harrison, K., Tamborindeguy, C., Scheuring, D.C., Herrera, A.M., Silva, A., Badillo-Vargas, I.E., Miller, J.C. and Levy, J.G. (2019) Differences in Zebra Chip severity between '*Candidatus* Liberibacter Solanacearum'haplotypes in Texas. *American Journal of Potato Research* **96**: 86-93.

Hay, B. (2000) Understanding IAP function and regulation: a view from *Drosophila*. *Cell Death and Differentiation* **7**: 1045.

Hay, N. (2011) Interplay between FOXO, TOR, and Akt. *Biochimica et Biophysica Acta (BBA)-Molecular Cell Research* **1813**: 1965-1970.

He, C. and Klionsky, D.J. (2009) Regulation mechanisms and signaling pathways of autophagy. *Annual Review of Genetics* **43**: 67-93.

Heck, M. (2018) Insect transmission of plant pathogens: a systems biology perspective. *mSystems* **3**: e00168-17.

Hengartner, M.O. (2000) The biochemistry of apoptosis. *Nature* **407**: 770-776.

Hill, B. and Purcell, A. (1995) Acquisition and retention of *Xylella fastidiosa* by an efficient vector, *Graphocephala atropunctata*. *Phytopathology* **85**: 209-212.

Hillyer, J.F. (2016) Insect immunology and hematopoiesis. *Developmental & Comparative Immunology* **58**: 102-118.

Hodges, A. and Spreen, T. (2012) Economic impacts of citrus greening (HLB) in Florida, 2006/07-2010/11. *Electronic Data Information Source (EDIS) FE903*: 32611.

Hoffmann, J.A. and Reichhart, J.-M. (2002) *Drosophila* innate immunity: an evolutionary perspective. *Nature Immunology* **3**: 121.

Hogenhout, S.A., Ammar, E.-D., Whitfield, A.E. and Redinbaugh, M.G. (2008a) Insect vector interactions with persistently transmitted viruses. *Annual Review of Phytopathology* **46**: 327-359.

Hogenhout, S.A., Oshima, K., Ammar, E.D., Kakizawa, S., Kingdom, H.N. and Namba, S. (2008b) Phytoplasmas: bacteria that manipulate plants and insects. *Molecular Plant Pathology* **9**: 403-423.

Huang, H.-J., Bao, Y.-Y., Lao, S.-H., Huang, X.-H., Ye, Y.-Z., Wu, J.-X., Xu, H.-J., Zhou, X.-P. and Zhang, C.-X. (2015) Rice ragged stunt virus-induced apoptosis affects virus transmission from its insect vector, the brown planthopper to the rice plant. *Scientific Reports* **5**: 11413.

Huang, J. and Brumell, J.H. (2014) Bacteria–autophagy interplay: a battle for survival. *Nature Reviews Microbiology* **12**: 101.

Hung, C.-M., Garcia-Haro, L., Sparks, C.A. and Guertin, D.A. (2012) mTOR-dependent cell survival mechanisms. *Cold Spring Harbor perspectives in biology* **4**: a008771.

Hunter, W.B., Reese, J. and Consortium, I.P.G. (2014) The Asian citrus psyllid genome (*Diaphorina citri*, Hemiptera). *Journal of Citrus Pathology* **1**: 143.

Ibanez, F., Hancock, J. and Tamborindeguy, C. (2014a) Identification and expression analysis of aquaporins in the potato psyllid, *Bactericera cockerelli*. *PloS One* **9**: e111745.

Ibanez, F., Levy, J. and Tamborindeguy, C. (2014b) Transcriptome analysis of "*Candidatus* Liberibacter solanacearum" in its psyllid vector, *Bactericera cockerelli*. *PloS One* **9**: e100955.

Ibanez, F. and Tamborindeguy, C. (2016) Selection of reference genes for expression analysis in the potato psyllid, *Bactericera cockerelli*. *Insect Molecular Biology* **25**: 227-238.

Imre, G., Berthelet, J., Heering, J., Kehrloesser, S., Melzer, I.M., Lee, B.I., Thiede, B., Dötsch, V. and Rajalingam, K. (2017) Apoptosis inhibitor 5 is an endogenous inhibitor of caspase-2. *EMBO reports* **18**: 733-744.

Inoue, H., Ohnishi, J., Ito, T., Tomimura, K., Miyata, S., Iwanami, T. and Ashihara, W. (2009) Enhanced proliferation and efficient transmission of *Candidatus* Liberibacter asiaticus by adult *Diaphorina citri* after acquisition feeding in the nymphal stage. *Annals of Applied Biology* **155**: 29-36.

Jagoueix, S., Bove, J.-m. and Garnier, M. (1994) The phloem-limited bacterium of greening disease of citrus is a member of the α subdivision of the Proteobacteria. *International Journal of Systematic and Evolutionary Microbiology* **44**: 379-386.

Kakizawa, S., Oshima, K., Kuboyama, T., Nishigawa, H., Jung, H.-y., Sawayanagi, T., Tsuchizaki, T., Miyata, S.-i., Ugaki, M. and Namba, S. (2001) Cloning and expression analysis of Phytoplasma protein translocation genes. *Molecular Plant-Microbe Interactions* **14**: 1043-1050.

Kanga, L.H., Eason, J., Haseeb, M., Qureshi, J. and Stansly, P. (2015) Monitoring for insecticide resistance in Asian citrus psyllid (Hemiptera: Psyllidae) populations in Florida. *Journal of Economic Entomology* **109**: 832-836.

Katsir, L., Ruan, Z., Piasezky, A., Santos-Garcia, D., Jiang, J., Sela, N., Freilich, S. and Bahar, O. (2018) Genome Analysis of Haplotype D of *Candidatus* Liberibacter Solanacearum. *Frontiers in Microbiology* **9**: 2933.

Khandia, R., Dadar, M., Munjal, A., Dhama, K., Karthik, K., Tiwari, R., Yatoo, M., Iqbal, H., Singh, K.P. and Joshi, S.K. (2019) A comprehensive review of autophagy and its various roles in infectious, non-infectious, and lifestyle diseases: current knowledge and prospects for disease prevention, novel drug design, and therapy. *Cells* **8**: 674.

Kingsolver, M.B., Huang, Z. and Hardy, R.W. (2013) Insect antiviral innate immunity: pathways, effectors, and connections. *Journal of Molecular Biology* **425**: 4921-4936.

Klepzig, K., Adams, A., Handelsman, J. and Raffa, K. (2009) Symbioses: a key driver of insect physiological processes, ecological interactions, evolutionary diversification, and impacts on humans. *Environmental Entomology* **38**: 67-77.

Klionsky, D.J., Cregg, J.M., Dunn, W.A., Emr, S.D., Sakai, Y., Sandoval, I.V., Sibirny, A., Subramani, S., Thumm, M. and Veenhuis, M. (2003) A unified nomenclature for yeast autophagy-related genes. *Developmental Cell* **5**: 539-545.

Kornbluth, S. and White, K.J.J.o.c.s. (2005) Apoptosis in *Drosophila*: neither fish nor fowl (nor man, nor worm). *Journal of Cell Science* **118**: 1779-1787.

Krokowski, S. and Mostowy, S. (2016) Interactions between *Shigella flexneri* and the autophagy machinery. *Frontiers in Cellular and Infection Microbiology* **6**: 17.

Kruse, A., Fattah-Hosseini, S., Saha, S., Johnson, R., Warwick, E., Sturgeon, K., Mueller, L., MacCoss, M.J., Shatters Jr, R.G. and Heck, M.C. (2017) Combining'omics and microscopy to visualize interactions between the Asian citrus psyllid vector and the Huanglongbing pathogen *Candidatus* Liberibacter asiaticus in the insect gut. *PloS One* **12**: e0179531.

Kumar, S. and Doumanis, J. (2000) The fly caspases. *Cell Death And Differentiation* **7**: 1039-1044.

Kunta, M., Zheng, Z., Wu, F., da Graca, J.V., Park, J.-W., Deng, X. and Chen, J. (2017) Draft whole-genome sequence of "*Candidatus* Liberibacter asiaticus" strain TX2351 isolated from Asian citrus psyllids in Texas, USA. *Genome Announc.* **5**: e00170-17.

Kuo, C.-J., Hansen, M. and Troemel, E. (2018) Autophagy and innate immunity: Insights from invertebrate model organisms. *Autophagy* **14**: 233-242.

Lalaoui, N., Lindqvist, L.M., Sandow, J.J. and Ekert, P.G. (2015) The molecular relationships between apoptosis, autophagy and necroptosis. *Seminarsin Cell and Developmental Biology* **39**: 63-69.

Lamason, R.L. and Welch, M.D. (2017) Actin-based motility and cell-to-cell spread of bacterial pathogens. *Current Opinion in Microbiology* **35**: 48-57.

Lamkanfi, M., Declercq, W., Kalai, M., Saelens, X. and Vandenabeele, P. (2002) Alice in caspase land. A phylogenetic analysis of caspases from worm to man. *Cell Death and Differentiation* **9**: 358-361.

Lan, H., Zhang, L., Liu, Y., Chen, H., Jia, D., Chen, Q. and Wei, T. (2015) An RNA interference pathway modulates the persistent infection of Southern rice black-streaked dwarf virus in insect vector, *Sogatella furcifera*. *Chinese Science Bulletin* **60**: 1361-1369.

Lannan, E., Vandergaast, R. and Friesen, P.D. (2007) Baculovirus caspase inhibitors P49 and P35 block virus-induced apoptosis downstream of effector caspase DrICE activation in *Drosophila melanogaster* cells. *Journal of Virology* **81**: 9319-9330.

Lasithiotakis, K.G., Sinnberg, T.W., Schittek, B., Flaherty, K.T., Kulms, D., Maczey, E., Garbe, C. and Meier, F.E. (2008) Combined inhibition of MAPK and mTOR signaling inhibits growth, induces cell death, and abrogates invasive growth of melanoma cells. *Journal of Investigative Dermatology* **128**: 2013-2023.

Leclerc, V. and Reichhart, J.M. (2004) The immune response of *Drosophila melanogaster*. *Immunological Reviews* **198**: 59-71.

Leger, R.J.S. and Wang, C. (2010) Genetic engineering of fungal biocontrol agents to achieve greater efficacy against insect pests. *Applied Microbiology and Biotechnology* **85**: 901-907.

Leonard, M.T., Fagen, J.R., Davis-Richardson, A.G., Davis, M.J. and Triplett, E.W. (2012) Complete genome sequence of *Liberibacter crescens* BT-1. *Standards in Genomic Sciences* **7**: 271.

Leulier, F., Lhocine, N., Lemaitre, B. and Meier, P. (2006a) The *Drosophila* inhibitor of apoptosis protein DIAP2 functions in innate immunity and is essential to resist gram-negative bacterial infection. *Molecular and Cellular Biology* **26**: 7821-7831.

Leulier, F., Ribeiro, P., Palmer, E., Tenev, T., Takahashi, K., Robertson, D., Zachariou, A., Pichaud, F., Ueda, R. and Meier, P. (2006b) Systematic in vivo RNAi analysis of putative components of the *Drosophila* cell death machinery. *Cell Death and Differentiation* **13**: 1663-1674.

Leulier, F., Rodriguez, A., Khush, R.S., Abrams, J.M. and Lemaitre, B. (2000) The *Drosophila* caspase Dredd is required to resist gram-negative bacterial infection. *EMBO Reports* **1**: 353-358.

Levine, B. and Kroemer, G. (2019) Biological functions of autophagy genes: a disease perspective. *Cell* **176**: 11-42.

Levine, B., Mizushima, N. and Virgin, H.W. (2011) Autophagy in immunity and inflammation. *Nature* **469**: 323.

Levy, J., Ravindran, A., Gross, D., Tamborindeguy, C. and Pierson, E. (2011) Translocation of'*Candidatus* Liberibacter solanacearum', the Zebra Chip pathogen, in potato and tomato. *Phytopathology* **101**: 1285-1291.

Levy, J.G., Gross, R., Mendoza Herrera, M.A., Tang, X., Babilonia, K., Shan, L., Kuhl, J., Dibble, M., Xiao, F. and Tamborindeguy, C. (2019) Lso-HPE1, an effector of '*Candidatus* Liberibacter solanacearum'can repress plant immune response. *Phytopathology* **110**: 648-655.

Li, W., Abad, J.A., French-Monar, R.D., Rascoe, J., Wen, A., Gudmestad, N.C., Secor, G.A., Lee, M., Duan, Y. and Levy, L. (2009) Multiplex real-time PCR for detection, identification and quantification of '*Candidatus* Liberibacter

solanacearum'in potato plants with zebra chip. *Journal of Microbiological Methods* **78**: 59-65.

Li, W., Hartung, J.S. and Levy, L. (2006) Quantitative real-time PCR for detection and identification of *Candidatus* Liberibacter species associated with citrus huanglongbing. *Journal of Microbiological Methods* **66**: 104-115.

Liefting, L.W., Sutherland, P.W., Ward, L.I., Paice, K.L., Weir, B.S. and Clover, G.R. (2009a) A new '*Candidatus* Liberibacter'species associated with diseases of solanaceous crops. *Plant Disease* **93**: 208-214.

Liefting, L.W., Weir, B.S., Pennycook, S.R. and Clover, G.R. (2009b) '*Candidatus* Liberibacter solanacearum', associated with plants in the family Solanaceae. *International Journal of Systematic and Evolutionary Microbiology* **59**: 2274-2276.

Lin, H., Islam, M.S., Bai, Y., Wen, A., Lan, S., Gudmestad, N.C. and Civerolo, E.L. (2012) Genetic diversity of '*Cadidatus* Liberibacter solanacearum'strains in the United States and Mexico revealed by simple sequence repeat markers. *European Journal of Plant Pathology* **132**: 297-308.

Lin, H., Lou, B., Glynn, J.M., Doddapaneni, H., Civerolo, E.L., Chen, C., Duan, Y., Zhou, L. and Vahling, C.M. (2011) The complete genome sequence of '*Candidatus* Liberibacter solanacearum', the bacterium associated with potato zebra chip disease. *PLoS One* **6**: e19135.

Liu, J., Enomoto, S., Lancto, C.A., Abrahamsen, M.S. and Rutherford, M.S. (2008) Inhibition of apoptosis in *Cryptosporidium parvum*-infected intestinal epithelial cells is dependent on survivin. *Infection and Immunity* **76**: 3784-3792.

Lo, W.-S., Huang, Y.-Y. and Kuo, C.-H. (2016) Winding paths to simplicity: genome evolution in facultative insect symbionts. *FEMS Microbiology Reviews* **40**: 855-874.

Maiuri, M.C., Zalckvar, E., Kimchi, A. and Kroemer, G. (2007) Self-eating and self-killing: crosstalk between autophagy and apoptosis. *Nature Reviews Molecular Cell Biology* **8**: 741-752.

Mann, M., Fattah-Hosseini, S., Ammar, E.-D., Stange, R., Warrick, E., Sturgeon, K., Shatters, R. and Heck, M. (2018) *Diaphorina citri* nymphs are resistant to morphological changes induced by "*Candidatus* Liberibacter asiaticus" in midgut epithelial cells. *Infection and Immunity* **86**: 00889-17.

Marino, G., Niso-Santano, M., Baehrecke, E.H. and Kroemer, G. (2014) Self-consumption: the interplay of autophagy and apoptosis. *Nature Reviews. Molecular Cell Biology* **15**: 81.

Martini, X., Hoffmann, M., Coy, M.R., Stelinski, L.L. and Pelz-Stelinski, K.S. (2015) Infection of an insect vector with a bacterial plant pathogen increases its propensity for dispersal. *PLoS One* **10**: e0129373.

Marusawa, H., Matsuzawa, S.i., Welsh, K., Zou, H., Armstrong, R., Tamm, I. and Reed, J.C. (2003) HBXIP functions as a cofactor of survivin in apoptosis suppression. *The EMBO Journal* **22**: 2729-2740.

McDowell, E. and Trump, B. (1976) Histologic fixatives suitable for diagnostic light and electron microscopy. *Archives of Pathology & Laboratory Medicine* **100**: 405-414.

Meier, P., Silke, J., Leevers, S.J. and Evan, G.I. (2000) The *Drosophila* caspase DRONC is regulated by DIAP1. *EMBO Journal* **19**: 598-611.

Mendoza Herrera, A., Levy, J., Harrison, K., Yao, J., Ibanez, F. and Tamborindeguy, C. (2018) Infection by *Candidatus* Liberibacter solanacearum'haplotypes A and B in Solanum lycopersicum'Moneymaker'. *Plant Disease* **102**: 2009-2015.

Michel, T., Reichhart, J.-M., Hoffmann, J.A. and Royet, J. (2001) *Drosophila* Toll is activated by Gram-positive bacteria through a circulating peptidoglycan recognition protein. *Nature* **414**: 756.

Miller, C. and Celli, J. (2016) Avoidance and subversion of eukaryotic homeostatic autophagy mechanisms by bacterial pathogens. *Journal of Molecular Biology* **428**: 3387-3398.

Mitchell, G., Cheng, M.I., Chen, C., Nguyen, B.N., Whiteley, A.T., Kianian, S., Cox, J.S., Green, D.R., McDonald, K.L. and Portnoy, D.A. (2018) *Listeria monocytogenes* triggers noncanonical autophagy upon phagocytosis, but avoids subsequent growth-restricting xenophagy. *Proceedings of the National Academy of Sciences* **115**: E210-E217.

Mizushima, N., Levine, B., Cuervo, A.M. and Klionsky, D.J. (2008) Autophagy fights disease through cellular self-digestion. *Nature* **451**: 1069.

Mizushima, N., Yoshimori, T. and Ohsumi, Y. (2011) The role of Atg proteins in autophagosome formation. *Annual Review of Cell and Developmental Biology* **27**: 107-132.

Munyaneza, J., Fisher, T., Sengoda, V., Garczynski, S., Nissinen, A. and Lemmetty, A. (2010) First Report of" *Candidatus* Liberibacter solanacearum" Associated with Psyllid-Affected Carrots in Europe. *Plant Disease* **94**: 639.

Munyaneza, J.E. (2012) Zebra chip disease of potato: biology, epidemiology, and management. *American Journal of Potato Research* **89**: 329-350.

Myllymäki, H., Valanne, S. and Rämet, M. (2014) The *Drosophila* imd signaling pathway. *The Journal of Immunology* **192**: 3455-3462.

Nachappa, P., Levy, J., Pierson, E. and Tamborindeguy, C. (2014) Correlation between "*Candidatus* Liberibacter solanacearum" infection levels and fecundity in its psyllid vector. *Journal of Invertebrate Pathology* **115**: 55-61.

Nachappa, P., Levy, J. and Tamborindeguy, C. (2012a) Transcriptome analyses of *Bactericera cockerelli* adults in response to "*Candidatus* Liberibacter solanacearum" infection. *Molecular Genetics and Genomics* **287**: 803-817.

Nachappa, P., Shapiro, A.A. and Tamborindeguy, C. (2012b) Effect of '*Candidatus* Liberibacter solanacearum' on fitness of its insect vector, *Bactericera cockerelli* (hemiptera: Triozidae), on tomato. *Phytopathology* **102**: 41-46.

Nakatogawa, H., Suzuki, K., Kamada, Y. and Ohsumi, Y. (2009) Dynamics and diversity in autophagy mechanisms: lessons from yeast. *Nature reviews Molecular Cell Biology* **10**: 458.

Nelson, W.R., Sengoda, V.G., Alfaro-Fernandez, A.O., Font, M.I., Crosslin, J.M. and Munyaneza, J.E. (2013) A new haplotype of "*Candidatus* Liberibacter solanacearum" identified in the Mediterranean region. *European Journal of Plant Pathology* **135**: 633-639.

Ng, J.C. and Falk, B.W. (2006) Virus-vector interactions mediating nonpersistent and semipersistent transmission of plant viruses. *Annual Review Phytopathology* **44**: 183-212.

Ocampo, C.B., Caicedo, P.A., Jaramillo, G., Bedoya, R.U., Baron, O., Serrato, I.M., Cooper, D.M. and Lowenberger, C. (2013) Differential expression of apoptosis related genes in selected strains of *Aedes aegypti* with different susceptibilities to dengue virus. *PLoS One* **8**: e61187.

Ohnishi, J., Kitamura, T., Terami, F. and Honda, K.-i. (2009) A selective barrier in the midgut epithelial cell membrane of the nonvector whitefly *Trialeurodes vaporariorum* to Tomato yellow leaf curl virus uptake. *Journal of General Plant Pathology* **75**: 131-139.

Orlovskis, Z., Canale, M.C., Thole, V., Pecher, P., Lopes, J.R. and Hogenhout, S.A. (2015) Insect-borne plant pathogenic bacteria: getting a ride goes beyond physical contact. *Current Opinion in Insect Science* **9**: 16-23.

Park, W.-R. and Nakamura, Y. (2005) p53CSV, a novel p53-inducible gene involved in the p53-dependent cell-survival pathway. *Cancer Research* **65**: 1197-1206.

Pedersen, J., LaCasse, E.C., Seidelin, J.B., Coskun, M. and Nielsen, O.H. (2014) Inhibitors of apoptosis (IAPs) regulate intestinal immunity and inflammatory bowel disease (IBD) inflammation. *Trends in Molecular Medicine* **20**: 652-665.

Pelz-Stelinski, K., Brlansky, R., Ebert, T. and Rogers, M. (2010) Transmission parameters for *Candidatus* Liberibacter asiaticus by Asian citrus psyllid (Hemiptera: Psyllidae). *Journal of Economic Entomology* **103**: 1531-1541.

Pelz-Stelinski, K. and Killiny, N. (2016) Better together: association with '*Candidatus* Liberibacter asiaticus' increases the reproductive fitness of its insect vector, *Diaphorina citri* (Hemiptera: Liviidae). *Annals of the Entomological Society of America* **109**: 371-376.

Perilla-Henao, L.M. and Casteel, C.L. (2016) Vector-borne bacterial plant pathogens: interactions with hemipteran insects and plants. *Frontiers in Plant Science* **7**: 1163.

Pina-Oviedo, S., Urbanska, K., Radhakrishnan, S., Sweet, T., Reiss, K., Khalili, K. and Del Valle, L. (2007) Effects of JC virus infection on anti-apoptotic protein survivin in progressive multifocal leukoencephalopathy. *The American Journal of Pathology* **170**: 1291-1304.

Prager, S.M., Vindiola, B., Kund, G.S., Byrne, F.J. and Trumble, J.T. (2013) Considerations for the use of neonicotinoid pesticides in management of *Bactericera cockerelli* (Šulk)(Hemiptera: Triozidae). *Crop Protection* **54**: 84-91.

Prins, M. and Goldbach, R. (1998) The emerging problem of tospovirus infection and nonconventional methods of control. *Trends in Microbiology* **6**: 31-35.

Purcell, A.H. (1982) Insect vector relationships with procaryotic plant pathogens. *Annual Review of Phytopathology* **20**: 397-417.

Ramphul, U.N., Garver, L.S., Molina-Cruz, A., Canepa, G.E. and Barillas-Mury, C. (2015) *Plasmodium falciparum* evades mosquito immunity by disrupting JNK-mediated apoptosis of invaded midgut cells. *Proceedings of the National Academy of Sciences* **112**: 1273-1280.

Rankin, S. (2005) Sororin, the cell cycle and sister chromatid cohesion. *Cell Cycle* **4**: 1039-1042.

Ravindran, A., Saenkham, P., Levy, J., Tamborindeguy, C., Lin, H., Gross, D.C. and Pierson, E. (2018) Characterization of the serralysin-like gene of '*Candidatus* Liberibacter solanacearum'associated with potato zebra chip disease. *Phytopathology* **108**: 327-335.

Ren, S.L., Li, Y.H., Zhou, Y.T., Xu, W.M., Cuthbertson, A.G., Guo, Y.J. and Qiu, B.L. (2016) Effects of *Candidatus* Liberibacter asiaticus on the fitness of the vector *Diaphorina citri*. *Journal of Applied Microbiology* **121**: 1718-1726.

Renaudin, J., Béven, L., Batailler, B., Duret, S., Desqué, D., Arricau-Bouvery, N., Malembic-Maher, S. and Foissac, X. (2015) Heterologous expression and processing of the flavescence dorée phytoplasma variable membrane protein VmpA in *Spiroplasma citri*. *BMC Microbiology* **15**: 82.

Ribet, D. and Cossart, P. (2015) How bacterial pathogens colonize their hosts and invade deeper tissues. *Microbes and Infection* **17**: 173-183.

Rivero, A., Vezilier, J., Weill, M., Read, A.F. and Gandon, S. (2010) Insecticide control of vector-borne diseases: when is insecticide resistance a problem? *PLoS Pathogens* **6**: e1001000.

Ronquist, F., Teslenko, M., Van Der Mark, P., Ayres, D.L., Darling, A., Höhna, S., Larget, B., Liu, L., Suchard, M.A. and Huelsenbeck, J.P. (2012) MrBayes 3.2: efficient Bayesian phylogenetic inference and model choice across a large model space. *Systematic Biology* **61**: 539-542.

Salvesen, G.S. and Duckett, C.S. (2002) Apoptosis: IAP proteins: blocking the road to death's door. *Nature Reviews Molecular Cell Biology* **3**: 401.

Schmittgen, T.D. and Livak, K.J. (2008) Analyzing real-time PCR data by the comparative C T method. *Nature Protocols* **3**: 1101.

Schneider, D.S. and Ayres, J.S. (2008) Two ways to survive infection: what resistance and tolerance can teach us about treating infectious diseases. *Nature Reviews Immunology* **8**: 889.

Sengoda, V.G., Buchman, J.L., Henne, D.C., Pappu, H.R. and Munyaneza, J.E. (2013) "*Candidatus* Liberibacter solanacearum" titer over time in *Bactericera cockerelli* (Hemiptera: Triozidae) after acquisition from infected potato and tomato plants. *Journal of Economic Entomology* **106**: 1964-1972.

Sengoda, V.G., Cooper, W.R., Swisher, K.D., Henne, D.C. and Munyaneza, J.E. (2014) Latent period and transmission of "*Candidatus* Liberibacter solanacearum" by the potato psyllid *Bactericera cockerelli* (Hemiptera: Triozidae). *PLoS One* **9**: e93475.

Shelly, S., Lukinova, N., Bambina, S., Berman, A. and Cherry, S. (2009) Autophagy is an essential component of *Drosophila* immunity against vesicular stomatitis virus. *Immunity* **30**: 588-598.

Shi, Y. (2004) Caspase activation: revisiting the induced proximity model. *Cell* **117**: 855-858.

Shin, S., Sung, B.-J., Cho, Y.-S., Kim, H.-J., Ha, N.-C., Hwang, J.-I., Chung, C.-W., Jung, Y.-K. and Oh, B.-H. (2001) An anti-apoptotic protein human survivin is a direct inhibitor of caspase-3 and-7. *Biochemistry* **40**: 1117-1123.

Silke, J. and Vaux, D.L. (2001) Two kinds of BIR-containing protein-inhibitors of apoptosis, or required for mitosis. *Journal of Cell Science* **114**: 1821-1827.

Sorbara, M.T., Ellison, L.K., Ramjeet, M., Travassos, L.H., Jones, N.L., Girardin, S.E. and Philpott, D.J. (2013) The protein ATG16L1 suppresses inflammatory cytokines induced by the intracellular sensors Nod1 and Nod2 in an autophagy-independent manner. *Immunity* **39**: 858-873.

Sprawka, I., Goławska, S., Parzych, T., Sytykiewicz, H. and Czerniewicz, P. (2015) Apoptosis induction by concanavalin A in gut cells of grain aphid. *Arthropod-Plant Interactions* **9**: 133-140.

Suzuki, K., Akioka, M., Kondo-Kakuta, C., Yamamoto, H. and Ohsumi, Y. (2013) Fine mapping of autophagy-related proteins during autophagosome formation in *Saccharomyces cerevisiae*. *Journal of Cell Science* **126**: 2534-2544.

Swisher Grimm, K. and Garczynski, S. (2019) Identification of a New Haplotype of '*Candidatus* Liberibacter solanacearum' in *Solanum tuberosum*. *Plant disease* **103**: 468-474.

Swisher, K.D., Henne, D.C. and Crosslin, J.M. (2014) Identification of a fourth haplotype of *Bactericera cockerelli* (Hemiptera: Triozidae) in the United States. *Journal of Insect Science* **14**: 161.

Swisher, K.D., Munyaneza, J.E. and Crosslin, J.M. (2012) High resolution melting analysis of the cytochrome oxidase I gene identifies three haplotypes of the potato psyllid in the United States. *Environmental Entomology* **41**: 1019-1028.

Tahzima, R., Maes, M., Achbani, E., Swisher, K., Munyaneza, J. and De Jonghe, K. (2014) First report of '*Candidatus* Liberibacter solanacearum' on carrot in Africa. *Plant Disease* **98**: 1426.

Tamborindeguy, C., Bereman, M.S., DeBlasio, S., Igwe, D., Smith, D.M., White, F., MacCoss, M.J., Gray, S.M. and Cilia, M. (2013) Genomic and proteomic analysis of *Schizaphis graminum* reveals cyclophilin proteins are involved in the transmission of cereal yellow dwarf virus. *PLoS One* **8**: e71620.

Tamborindeguy, C., Huot, O.B., Ibanez, F. and Levy, J. (2017) The influence of bacteria on multi-trophic interactions among plants, psyllids, and pathogen. *Insect Science* **24**: 961-974.

Tamura, K., Stecher, G., Peterson, D., Filipski, A. and Kumar, S. (2013) MEGA6: molecular evolutionary genetics analysis version 6.0. *Molecular Biology and Evolution* **30**: 2725-2729.

Tang, X.-T. and Tamborindeguy, C. (2019) No evidence of apoptotic response of the potato psyllid, *Bactericera cockerelli*, to "*Candidatus* Liberibacter solanacearum" at the gut interface. *Infection and Immunity*: DOI: 10.1128/IAI.00242-19.

Tang, X.T., Ibanez, F. and Tamborindeguy, C. (2019) Quenching autofluorescence in the alimentary canal tissues of *Bactericera cockerelli* (Hemiptera: Triozidae) for immunofluorescence labeling. *Insect Science* doi: 10.1111/1744-7917.12660.

Teresani, G.R., Bertolini, E., Alfaro-Fernández, A., Martínez, C., Tanaka, F.A.O., Kitajima, E.W., Roselló, M., Sanjuán, S., Ferrándiz, J.C. and López, M.M. (2014) Association of '*Candidatus* Liberibacter solanacearum'with a vegetative disorder of celery in Spain and development of a real-time PCR method for its detection. *Phytopathology* **104**: 804-811.

Tewari, M., Yu, M., Ross, B., Dean, C., Giordano, A. and Rubin, R. (1997) AAC-11, a novel cDNA that inhibits apoptosis after growth factor withdrawal. *Cancer Research* **57**: 4063-4069.

Thompson, S.M., Johnson, C.P., Lu, A.Y., Frampton, R.A., Sullivan, K.L., Fiers, M.W., Crowhurst, R.N., Pitman, A.R., Scott, I.A. and Wen, A. (2015) Genomes of '*Candidatus* Liberibacter solanacearum'haplotype A from New Zealand and the United States suggest significant genome plasticity in the species. *Phytopathology* **105**: 863-871.

Tian, L., Song, T., He, R., Zeng, Y., Xie, W., Wu, Q., Wang, S., Zhou, X. and Zhang, Y. (2017) Genome-wide analysis of ATP-binding cassette (ABC) transporters in the sweetpotato whitefly, *Bemisia tabaci*. *BMC genomics* **18**: 330.

Trapnell, C., Roberts, A., Goff, L., Pertea, G., Kim, D., Kelley, D.R., Pimentel, H., Salzberg, S.L., Rinn, J.L. and Pachter, L. (2012) Differential gene and transcript expression analysis of RNA-seq experiments with TopHat and Cufflinks. *Nature Protocols* **7**: 562.

Valanne, S., Wang, J.-H. and Rämet, M. (2011) The *Drosophila* toll signaling pathway. *The Journal of Immunology* **186**: 649-656.

Voronin, D., Cook, D.A., Steven, A. and Taylor, M.J. (2012) Autophagy regulates *Wolbachia* populations across diverse symbiotic associations. *Proceedings of the National Academy of Sciences* **109**: E1638-E1646.

Vyas, M., Fisher, T.W., He, R., Nelson, W., Yin, G., Cicero, J.M., Willer, M., Kim, R., Kramer, R. and May, G.A. (2015) Asian citrus psyllid expression profiles suggest *Candidatus* Liberibacter asiaticus-mediated alteration of adult nutrition and metabolism, and of nymphal development and immunity. *PLoS One* **10**: e0130328.

Wang, J., Haapalainen, M., Schott, T., Thompson, S.M., Smith, G.R., Nissinen, A.I. and Pirhonen, M. (2017) Genomic sequence of *'Candidatus* Liberibacter solanacearum' haplotype C and its comparison with haplotype A and B genomes. *PLoS One* **12**: e0171531.

Wang, L.-L., Wang, X.-R., Wei, X.-M., Huang, H., Wu, J.-X., Chen, X.-X., Liu, S.-S. and Wang, X.-W. (2016) The autophagy pathway participates in resistance to tomato yellow leaf curl virus infection in whiteflies. *Autophagy* **12**: 1560-1574.

Wang, X.R., Wang, C., Wang, X.W., Qian, L.X., Chi, Y., Liu, S.S., Liu, Y.Q. and Wang, X.W.J.I.m.b. (2018) The functions of caspase in whitefly *Bemisia tabaci* apoptosis in response to UV irradiation. *Insect Molecular Biology* **27**: 739-751.

Wang, Z., Gerstein, M. and Snyder, M. (2009) RNA-Seq: a revolutionary tool for transcriptomics. *Nature Reviews Genetics* **10**: 57.

Wayadande, A.C. and Fletcher, J. (1998) Development and Use of an Established Cell Line of the Leafhopper*Circulifer tenellusto* Characterize*Spiroplasma citri*–Vector Interactions. *Journal of Invertebrate Pathology* **72**: 126-131.

Weiberg, A., Wang, M., Lin, F.-M., Zhao, H., Zhang, Z., Kaloshian, I., Huang, H.-D. and Jin, H. (2013) Fungal small RNAs suppress plant immunity by hijacking host RNA interference pathways. *Science* **342**: 118-123.

Whitfield, A.E., Falk, B.W. and Rotenberg, D.J.V. (2015) Insect vector-mediated transmission of plant viruses. **479**: 278-289.

Wilson, R., Goyal, L., Ditzel, M., Zachariou, A., Baker, D.A., Agapite, J., Steller, H. and Meier, P. (2002) The DIAP1 RING finger mediates ubiquitination of Dronc and is indispensable for regulating apoptosis. *Nature Cell Biology* **4**: 445-450.

Wulff, N.A., Zhang, S., Setubal, J.C., Almeida, N.F., Martins, E.C., Harakava, R., Kumar, D., Rangel, L.T., Foissac, X. and Bové, J.M. (2014) The complete genome sequence of *'Candidatus* Liberibacter americanus', associated with Citrus huanglongbing. *Molecular Plant-Microbe Interactions* **27**: 163-176.

Wuriyanghan, H. and Falk, B.W. (2013) RNA interference towards the potato psyllid, *Bactericera cockerelli*, is induced in plants infected with recombinant Tobacco mosaic virus (TMV). *PloS One* **8**: e66050.

Wuriyanghan, H., Rosa, C. and Falk, B.W. (2011) Oral delivery of double-stranded RNAs and siRNAs induces RNAi effects in the potato/tomato psyllid, *Bactericerca cockerelli*. *PloS One* **6**: e27736.

Xie, W., Chen, C., Yang, Z., Guo, L., Yang, X., Wang, D., Chen, M., Huang, J., Wen, Y. and Zeng, Y. (2017) Genome sequencing of the sweetpotato whitefly *Bemisia tabaci* MED/Q. *GigaScience* **6**: gix018.

Xu, C., Xia, Y., Li, K. and Ke, C. (1988) Further study of the transmission of citrus huanglungbin by a psyllid, *Diaphorina citri* Kuwayama. *International Organization of Citrus Virologists Conference Proceedings* **10**: 243-248.

Xu, D., Wang, Y., Willecke, R., Chen, Z., Ding, T. and Bergmann, A. (2006) The effector caspases drICE and dcp-1 have partially overlapping functions in the apoptotic pathway in *Drosophila*. *Cell Death and Differentiation* **13**: 1697-1706.

Xu, D., Woodfield, S.E., Lee, T.V., Fan, Y., Antonio, C. and Bergmann, A. (2009) Genetic control of programmed cell death (apoptosis) in *Drosophila*. *Fly* **3**: 78-90.

Yam, P.T. and Theriot, J.A. (2004) Repeated cycles of rapid actin assembly and disassembly on epithelial cell phagosomes. *Molecular Biology of the Cell* **15**: 5647-5658.

Yang, Z. and Klionsky, D.J. (2010) Mammalian autophagy: core molecular machinery and signaling regulation. *Current Opinion in Cell Biology* **22**: 124-131.

Yano, T. and Kurata, S. (2011) Intracellular recognition of pathogens and autophagy as an innate immune host defence. *The Journal of Biochemistry* **150**: 143-149.

Yao, J., Saenkham, P., Levy, J., Ibanez, F., Noroy, C., Mendoza, A., Huot, O., Meyer, D.F. and Tamborindeguy, C. (2016) Interactions '*Candidatus* Liberibacter solanacearum'–*Bactericera cockerelli*: haplotype effect on vector fitness and gene expression analyses. *Frontiers in Cellular and Infection Microbiology* **6**: 62.

Ye, J., Fang, L., Zheng, H., Zhang, Y., Chen, J., Zhang, Z., Wang, J., Li, S., Li, R. and Bolund, L. (2006) WEGO: a web tool for plotting GO annotations. *Nucleic Acids Research* **34**: W293-W297.

Ye, J., Zhang, Y., Cui, H., Liu, J., Wu, Y., Cheng, Y., Xu, H., Huang, X., Li, S. and Zhou, A. (2018) WEGO 2.0: a web tool for analyzing and plotting GO annotations, 2018 update. *Nucleic Acids Research* **46**: W71-W75.

Zachariou, A., Tenev, T., Goyal, L., Agapite, J., Steller, H. and Meier, P. (2003) IAP-antagonists exhibit non-redundant modes of action through differential DIAP1 binding. *EMBO Journal* **22**: 6642-6652.

Zhang, X., Tang, N., Hadden, T.J. and Rishi, A.K. (2011) Akt, FoxO and regulation of apoptosis. *Biochimica et Biophysica Acta (BBA)-Molecular Cell Research* **1813**: 1978-1986.

Zhou, D., Chen, L.M., Hernandez, L., Shears, S.B. and Galán, J.E. (2001) A *Salmonella* inositol polyphosphatase acts in conjunction with other bacterial effectors to promote host cell actin cytoskeleton rearrangements and bacterial internalization. *Molecular Microbiology* **39**: 248-260.

Zimmermann, K.C., Bonzon, C. and Green, D.R. (2001) The machinery of programmed cell death. *Pharmacology and Therapeutics* **92**: 57-70.

Zirin, J. and Perrimon, N. (2010) *Drosophila* as a model system to study autophagy. *Seminars in Immunopathology* **32**: 363-372.

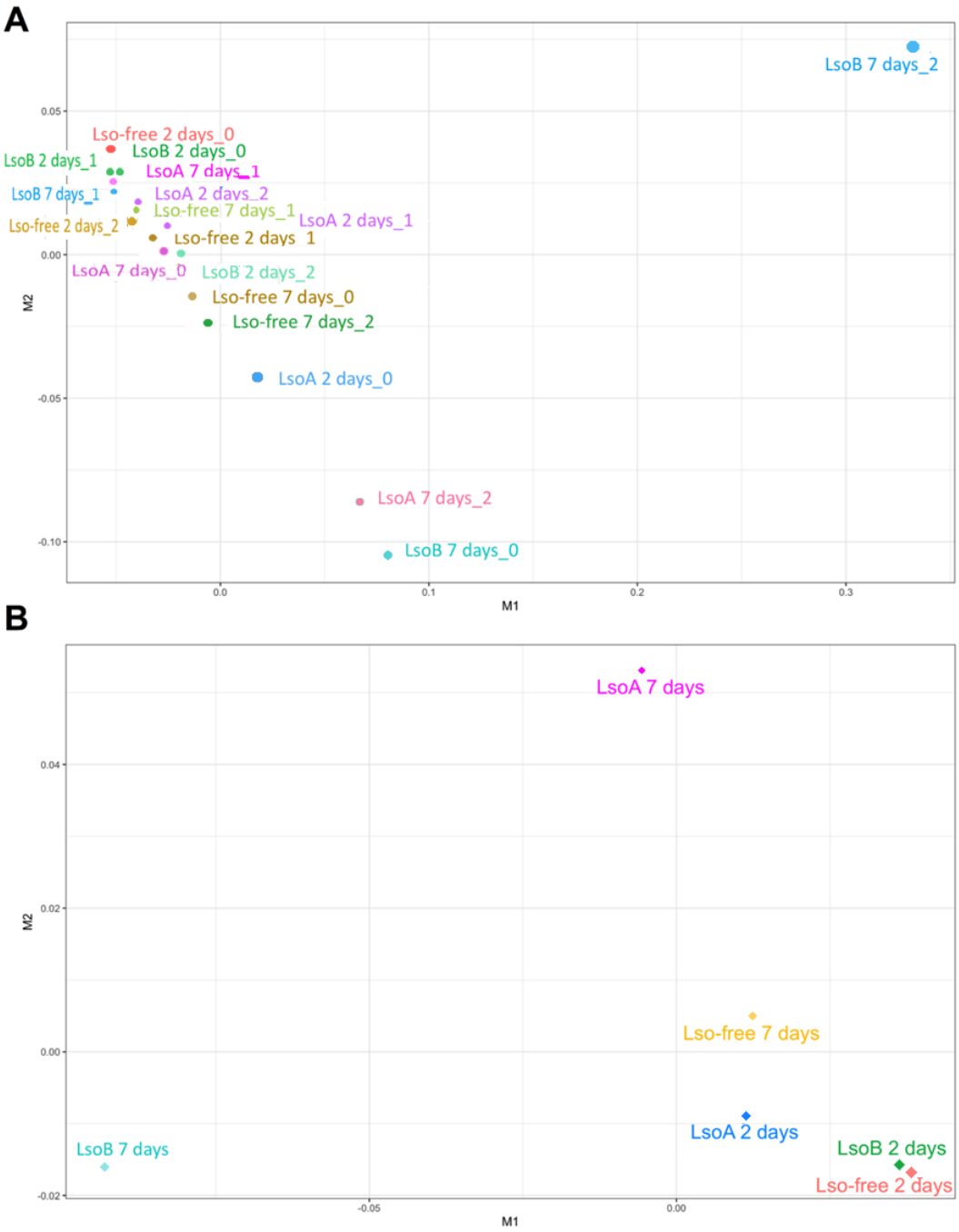

Figure A.1 Multidimensional scaling (MDS) plot of 18 libraries across six treatments samples. (A) MDS of 18 libraries. (B) MDS of six treatments samples.

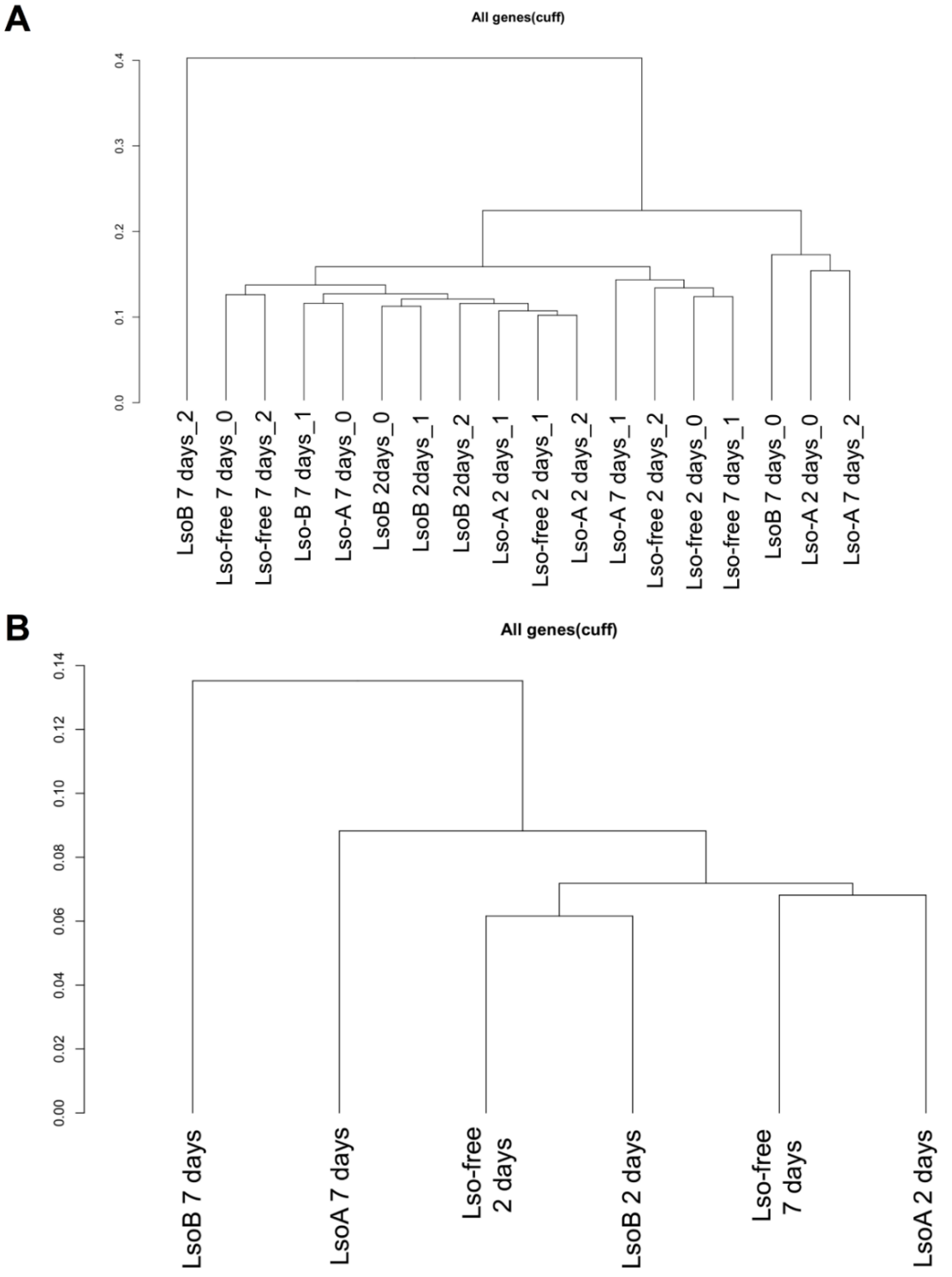

Figure A.2 Cluster dendrogram of 18 libraries across six treatments samples. (A) Dendrogram of 18 libraries. (B) dendrogram of six treatments samples.

```
                10        20        30        40        50        60        70        80        90
1       ATGGAAAACACGCGTACTCTATCCTCTCTACGAGACCTACTCACGCCGTATCTGAGCGGGACTCAGAAGAAAACCCTGCGCATGACTTTC
1        M  E  N  T  R  T  L  S  S  L  R  D  L  L  T  P  Y  L  S  G  T  Q  K  K  T  L  R  M  T  F

              100       110       120       130       140       150       160       170       180
91      TATCGGAACAGGCTGAAGTCTTTCATCAGCTGGCCGTTCACTTCGGCCGGCGACGTGTGTTCGGCCGAGAGCATGGCCGCGGCCGGCTTC
31       Y  R  N  R  L  K  S  F  I  S  W  P  F  T  S  A  G  D  V  C  S  A  E  S  M  A  A  A  G  F

              190       200       210       220       230       240       250       260       270
181     TATTCCATTTCCAAGCGGAAGAATGACACCTCGGTCAAGTGTTTCGTGTGCCTGAAGGAGCTGGATGGGTGGGAGGCGAGGGATGACCCC
61       Y  S  I  S  K  R  K  N  D  T  S  V  K  C  F  V  C  L  K  E  L  D  G  W  E  A  R  D  D  P

              280       290       300       310       320       330       340       350       360
271     TGGGAGGAGCATAGGAGACACCAGGGGGCGTGTCCTTACGTCCAGCTGGGCAAGAGGGAGGACCAGTGGACGCTGGAGGACTGGGTGGCG
91       W  E  E  H  R  R  H  Q  G  A  C  P  Y  V  Q  L  G  K  R  E  D  Q  W  T  L  E  D  W  V  A

              370       380       390       400       410       420       430       440       450
361     CTGCAGGAGGGCGTGGCCGTGAGGCTCTTGGAGGAAAAACAGAACATGGATTTGGAAAATTTGGAAGAACAACTCAAAACTAATGAGAGG
121      L  Q  E  G  V  A  V  R  L  L  E  E  K  Q  N  M  D  L  E  N  L  E  E  Q  L  K  T  N  E  R

              460       470       480
451     AAGCTGCAGAAAGAAAGAAAGAGGAAGCGAAAATGA
151      K  L  Q  K  E  R  K  R  K  R  K  *
```

Figure A.3 DNA and protein sequence of IAPP5.2 gene. The highlight indicates the Baculovirus IAP Repeat (BIR) domain.

Table A.1 Primers for RT-qPCR validation.

Genes	Primers
Nedd4	F: GCGCATCTTCTTCATAGACCA R: CGGCTATTTGAGGATTGGAT
Hsp	F: TGAGAGAGATAGCCGAGGTG R: TCTGGGAATCGTTGAAGTAGG
Patj	F: CACTACATCCGGTCCATCCT R: GTGCTCATTCACCTCAAGCA
RASSF2	F: TACGAGACAATGGCGAACAG R: TGAGGACCCAGCATCACAC
HIGD2A	F: AGAAGGAACAGGATGAGTTGG R: GAAGATCCACTCTCTGGGGTAA
Tret1	F: CGTGTCTCATCCTGTTCGTC R: ATCCCTTCCTCGTCCTCATT
UBE4A	F: TGAAACAACCTGGGCTCTATG R: ACGATGTGGGAGAAGAAGGA
ZN728	F: ACCGTATTGCTGCCACATCT R: AAGGGTCTTTCGCCTGTATG
ZN91	F: CGAGCGACTCAACAAACTGA R: TGATGCAGTAGGGACACTGG
TRIP12	F: GCAAGAGGTGCTAAAGAACGA R: ATGAGGATCTCCGCCATCT

Table A.2 Summary statistics of transcriptome libraries.

Samples	Reads number	Mapped reads	Mapped rate (%)
Lso-free 2-day rep1	46,373,575	19,940,637	43.0
Lso-free 2-day rep2	49,049,463	21,630,813	44.1
Lso-free 2-day rep3	42,454,067	18,000,524	42.4
Lso-free 7-day rep1	40,597,962	16,117,391	39.7
Lso-free 7-day rep2	47,157,120	20,088,933	42.6
Lso-free 7-day rep3	39,518,942	16,479,399	41.7
LsoA 2-day rep1	38,985,733	15,906,179	40.8
LsoA 2-day rep2	40,627,811	16,291,752	40.1
LsoA 2-day rep3	54,515,788	22,078,894	40.5
LsoA 7-day rep1	48,360,594	20,118,007	41.6
LsoA 7-day rep2	51,770,107	20,915,123	40.4
LsoA 7-day rep3	47,470,121	18,655,758	39.3
LsoB 2-day rep1	41,224,598	17,973,925	43.6
LsoB 2-day rep2	38,599,255	15,902,893	41.2
LsoB 2-day rep3	41,368,602	17,498,919	42.3
LsoB 7-day rep1	36,623,405	15,857,934	43.3
LsoB 7-day rep2	47,253,373	20,224,444	42.8
LsoB 7-day rep3	46,148,068	19,059,152	41.3

Table A.3 Summary statistics of transcriptome libraries of Lso.

Samples	Reads number	Mapped reads	Mapped rate (%)
Lso-free 7-day rep1	87,529,560	6	0.00
Lso-free 7-day rep2	79,987,406	448	0.00
Lso-free 7-day rep3	63,155,715	9	0.00
LsoA 7-day rep1	69,997,837	20,220	0.03
LsoA 7-day rep2	74,472,502	1,085	0.00
LsoA 7-day rep3	85,983,994	15,295	0.02
LsoB 7-day rep1	58,265,732	42,340	0.07
LsoB 7-day rep2	65,114,401	50,980	0.08
LsoB 7-day rep3	57,486,131	28,168	0.05

Table A.4 DEGs associated with zinc fingers.

	GI number	Annotation	Fold change
Objective1: Haplotype	**Lso-free (7d) vs LsoB (7d)**		
	gi|1041535729	probable helicase with zinc finger domain	11.74
	gi|1041551763	zinc finger protein 91-like	9.3
	gi|1062680758	zinc finger CCHC domain-containing protein 8 homolog	8.69
	gi|1041534625	GATA zinc finger domain-containing protein 14-like	6.48
	gi|662220554	zinc finger protein 64 homolog, isoforms 3 and 4-like	5.4
	gi|1041552204	gastrula zinc finger protein XlCGF49.1-like, partial	6.08
	gi|1041545616	zinc finger protein Xfin-like	6.91
Objective2: Time	**LsoA (2d) vs LsoA (7d)**		
	gi|662200707	AN1-type zinc finger protein 2A-like	2.87
	gi|662193469	zinc finger protein OZF-like	5.41
	gi|662224129	zinc finger protein 761-like	3.46
	gi|1189056580	AN1-type zinc finger protein 6 isoform X2	3.13
	gi|662220364	zinc finger protein 91-like	3.07
	gi|1041531946	zinc finger protein 271 isoform X2	-6.05
	LsoB (2d) vs LsoB (7d)		
	gi|1041532471	zinc finger protein 271-like	14.39
	gi|1041535729	probable helicase with zinc finger domain	16.86
	gi|1041535320	zinc finger and BTB domain-containing protein 24-like	6.18
	gi|1041545447	zinc finger protein 64 homolog, isoforms 1 and 2-like	3.89
	gi|662187921	zinc finger protein 808-like	5.52
	gi|1041545439	zinc finger protein 711-like	4.61
	gi|1041545447	zinc finger protein 64 homolog, isoforms 1 and 2-like	7.8
	gi|1041551763	zinc finger protein 91-like	12.01
	gi|1041533950	zinc finger protein 84-like	4.65
	gi|1041546623	zinc finger protein 26-like	2.96
	gi|1062680758	zinc finger CCHC domain-containing protein 8 homolog	5.97
	gi|662188588	zinc finger protein 728-like	5.09

Table A.4 Continued.

	GI number	Annotation	Fold change
Objective2: Time	gi|1041534625	GATA zinc finger domain-containing protein 14-like	8.29
	gi|1041545437	zinc finger protein 107-like	5.17
	gi|1041548843	zinc finger protein OZF-like	10.33
	gi|1041546007	zinc finger protein 467-like	6.38
	gi|1041548927	zinc finger MYM-type protein 4-like	5.64
	gi|1059385947	zinc finger FYVE domain-containing protein 26 homolog isoform X2	4.3
	gi|1041533950	zinc finger protein 84-like	6.31
	gi|1041550280	zinc finger protein 681-like	4.04
	gi|1041537714	zinc finger protein ZFAT-like	3.77
	gi|662186483	zinc finger protein OZF-like	4.51
	gi|662188672	zinc finger CCCH-type with G patch domain-containing protein	4.16
	gi|1041533950	zinc finger protein 84-like	4.15
	gi|1060152124	zinc finger matrin-type protein CG9776 isoform X2	5.43
	gi|1101366102	zinc finger SWIM domain-containing protein 5-like	6.88
	gi|1228358716	centrosome-associated zinc finger protein CP190-like isoform X1	6.08
	gi|961138841	zinc finger protein 62 homolog	3.95
	gi|1040686930	gastrula zinc finger protein XlCGF57.1-like	3.38
	gi|1041545449	gastrula zinc finger protein XlCGF17.1-like	2.79
	gi|662220554	zinc finger protein 64 homolog, isoforms 3 and 4-like	7.61
	gi|1041553783	zinc finger protein 605-like	6.36
	gi|662221164	zinc finger protein 702	5.36
	gi|1041552204	gastrula zinc finger protein XlCGF49.1-like	8.89
	gi|1041545457	zinc finger protein 513-like	5.13
	gi|1041545457	zinc finger protein 513-like	4.85

Table A.4 Continued.

	GI number	Annotation	Fold change
Objective2: Time	gi|1041530329	zinc finger protein 64 homolog, isoforms 3 and 4-like	5.71
	gi|662183487	zinc finger MYND domain-containing protein 10	6.67
	gi|1041545616	zinc finger protein Xfin-like	8.57
	LsoA&LsoB (2d) vs LsoA&LsoB (7d)		
	gi|1041533694	zinc finger protein-like 1 homolog isoform X1	3.34/3.82

For LsoA&LsoB, the value beside "/" indicates Lso-free vs. LsoA, and Lso-free vs. LsoB, respectively. "-" indicates down-regulation in the second condition (on the right side of "vs").

Table A.5 Down-regulated DEGs in response to Lso.

	GI number	Annotation	Fold change
Objective1: Haplotype	**Lso-free (2d) vs LsoB (2d)**		
	gi|662205492	pleckstrin homology domain-containing family J member 1-like	-4.71
	gi|662199817	uncharacterized protein LOC103510220	-4.74
	gi|1036730840	alanine aminotransferase 1	-4.11
	gi|662207585	N-alpha-acetyltransferase 35, NatC auxiliary subunit-like	-4.54
	gi|662202860	uncharacterized protein LOC103511784 isoform X1	-5.67
	gi|662196843	RNA pseudouridylate synthase domain-containing protein 3-like	-10
	gi|1060208525	conserved oligomeric Golgi complex subunit 3	-12
	gi|662212760	protein wntless	-17.56
	Lso-free (2d) vs LsoA&LsoB (2d)		
	gi|1314956304	beta-ureidopropionase	-11.97/-12.29
	gi|1041545896	tudor domain-containing protein 1-like	-9.92/-19.92

Table A.5 Continued.

	GI number	Annotation	Fold change
Objective1: Haplotype	**Lso-free (7d) vs LsoA (7d)**		
	gi|646706993	Laminin subunit alpha	-5.77
	gi|1041539257	uncharacterized protein LOC103508912	-7.01
	gi|662204427	probable small nuclear ribonucleoprotein E	-3.17
	Lso-free vs (7d) LsoB (7d)		
	gi|1101361217	shootin-1	-7.28
	gi|662220628	uncharacterized protein LOC103521131	-5.33
	Lso-free (7d) vs LsoA&LsoB (7d)		
	gi|1314956304	beta-ureidopropionase	-5.18/-8.6
	gi|662196843	RNA pseudouridylate synthase domain-containing protein 3-like	-10.78/-8.34
Objective2: Time	**LsoA (2d) vs LsoA (7d)**		
	gi|1060228182	laminin subunit alpha	-4.55
	gi|1041539257	uncharacterized protein LOC103508912	-8.26
	gi|1041545157	facilitated trehalose transporter Tret1-like	-2.72
	gi|1041547585	galactokinase-like	-2.94
	gi|1036851719	AP-3 complex subunit sigma-2	-3.28
	gi|1101398038	huntingtin	-4.31
	gi|1189055661	amidophosphoribosyltransferase	-4.07
	gi|1041539029	uncharacterized protein LOC103508705	-3.77
	gi|1041531946	zinc finger protein 271 isoform X2	-6.05
	gi|1041537311	poly(rC)-binding protein 3-like	-12.17
	LsoB (2d) vs LsoB (7d)		
	gi|662190957	39S ribosomal protein L30, mitochondrial	-3.57
	gi|1036953778	peptidyl-prolyl cis-trans isomerase-like 2	-2.83
	gi|1041538717	lipid storage droplets surface-binding protein 1-like	-8.26
	gi|1101361217	shootin-1	-14.75
	gi|662219729	ATP-binding cassette sub-family F member 1	-3.86

For LsoA&LsoB, the value beside "/" indicates Lso-free vs. LsoA, and Lso-free vs. LsoB, respectively. "-" indicates down-regulation in the second condition (on the right side of "vs").

Table A.6 Primers for bioinformatics validation and gene expression analyses by qPCR of apoptosis-related genes.

Gene Code	Validation Primers (5'-3')	qPCR primers (5'-3')
IAP1	F: CGATTGGAAATTGGTGT	F: AACAAGTACAGCGGTGACGA
	R: GGGAATGTGTAGTAGGCT	R: TTTACACAGGCGACCATCAG
IAPP2	F: TTTATCTGTCCAGGATAGTG	F: AGCAGAACACAGGAGGCAAA
	R: ACAACTACAACATTCACCTC	R: TGATTAGGCAGTCCACCATTC
IAP5	F: TTCCTTCCTATTGCTAC	F: GAGTTCTTCCACAATCCACCA
	R: CCATCTGCTTGTCTCTTT	R: CTGAGTTGCCGTTCTCTTCC
TRIAP1	F: CCTACAGATTGGTTGTTC	F: CCTTTTTCAGGTAGCCCTCA
	R: CTCCACTGCTACTACTTTT	R: AGCTGTGTGCATTCCTTGCT
IAPP5	F: GTACCTATTGAGAGCATAA	F: AAAAGGGTTCTTGCACACCA
	R: TCATAAATCCTAGACACAG	R: CAGAATATGCACTTGGCACA
IAPP5.2	F: GGATGGAAGAGAAAGCAAAA	F: CTCGGTCAAGTGTTTCGTGT
	R: CCACATTCAAACAACACTGG	R: TGGTGTCTCCTATGCTCCTC
IAP6		F: ATGGGAACAGCCAGACAGA
		R: TACCACATCAGCAAGGCAAG
AIF3	F: GCCCGCTGTTCTAATTG	F: TGGCTCCTGCTTCAGTCTTT
	R: AAGGGGATGTTGGTGTTG	R: CAGTTTCCCCATCAACATCC
AIF1	F: CGAACTCATACCGAAAAAG	F: GATAGCAAGAAGAAGCCCAAAC
	R: TGCTACTCAAATCACCTCA	R: CCCCCAATGAGAAGATAAGGA
Caspase1	F: AAAATCGTCTCCAGGCTTCA	F: CAAGGAGATGGTCTGGATGG
	R: TCAGAGTGGTCAAGTTCCTTTC	R: ATGAGGAAGTCAGCGTGGAG
Caspase2	F: TTTGATGCTTTGTGGGA	F: ATGTCCCCAGCAATGGTATC
	R: AACTTGGGAATGTTGGC	R: CACAGGGTGTTGACTTCTTCA
Caspase3	F: GTAAGCAACAATACGACACC	F: AAGCTGGATGGTGGAGTACG
	R: CATAGGAGGGGATCTTGTAG	R: CAGCATAGGAGGGGATCTTG

Table A.7 Comparison of inhibitors of apoptosis in *D. melanogaster, A. pisum, B. tabaci, D. citri* and *B. cockerelli*.

D. melanogaster **(conserved domains, protein length in AA)**	***A. pisum*** **(protein length in AA)**	***B. tabaci*** **(protein length in AA)**	***D. citri*** **(protein length in AA)**	***B. cockerelli*** **(most similar protein, conserved domains, E-value, protein length in AA)**
Deterin (1 BIR domain, 153 AA)	LOC103310572 baculoviral IAP repeat-containing protein 2-like (132 AA)	LOC109040487 baculoviral IAP repeat-containing protein 5.2 (144 AA)	LOC103516527 baculoviral IAP repeat-containing protein 5 (162 AA)	Bc-IAPP5 (*D. citri* baculoviral IAP repeat-containing protein 5, 1 BIR domain, 4e-059, 168 AA)
	LOC100570215 baculoviral IAP repeat-containing protein 3 (128 AA)		LOC103523747 baculoviral IAP repeat-containing protein 5-like, partial (107 AA)	Bc-IAPP5.2 (*D. citri* baculoviral IAP repeat-containing protein 5.2-like, 1 BIR domain, 7e-059, 161 AA)
	LOC103309101 baculoviral IAP repeat-containing protein 3-like (227 AA)		LOC103508457 baculoviral IAP repeat-containing protein 5.2-like (160 AA)	
	LOC100569400 baculoviral IAP repeat-containing protein 5-like (157 AA)		LOC103522644 baculoviral IAP repeat-containing protein 5.2-like (160 AA)	
DIAP1 (2 BIR, 1 RING_Ubox domains, 438 AA)	LOC103310098 baculoviral IAP repeat-containing protein 7 (466 AA)	LOC109044806 death-associated inhibitor of apoptosis 1-like (424 AA)	LOC103506717 putative inhibitor of apoptosis (376 AA)	Bc-IAP1 (*D. citri* putative inhibitor of apoptosis isoform X1, 2 BIR and 1 Ring_Ubox domains, e-177, 419 AA)
	LOC100159034 baculoviral IAP repeat-containing protein 7-B (530 AA)	LOC109035520 putative inhibitor of apoptosis (342 AA)		

Table A.7 Continued.

D. melanogaster **(conserved domains, protein length in AA)**	***A. pisum*** **(protein length in AA)**	***B. tabaci*** **(protein length in AA)**	***D. citri*** **(protein length in AA)**	***B. cockerelli*** **(most similar protein, conserved domains, E-value, protein length in AA)**
	LOC100168361 baculoviral IAP repeat-containing protein 7-B-like (410 AA)			
	LOC100168556 baculoviral IAP repeat-containing protein 7-B (482 AA)			
	LOC100159652 baculoviral IAP repeat-containing protein 3 (282 AA)			
DIAP2 (3 BIR, 1 RING-HC_Birc2_3_7, 1 UBA_IAPs domains, 498 AA)			LOC103508496 death-associated inhibitor of apoptosis 2 (734 AA)	Bc-IAP2 (*D. citri* death-associated inhibitor of apoptosis 2, 3 BIR, 1 RING-HC_Birc2_3_7, 1 UBA_IAPs domains, 1e-041, 551AA)
DBRUCE (1 BIR, 1 UQ_con) domains, 4876 AA)		LOC109033757 baculoviral IAP repeat-containing protein 6-like (UBCc, 1338 AA)	LOC103519068[1] baculoviral IAP repeat-containing protein 6-like (886 AA)	Bc-IAP6 (*B. tabaci* baculoviral IAP repeat-containing protein 6-like, 1 BIR and 1 UQ_con/UBCc domains, 0.0, 4367 AA)*
		LOC109034999 baculoviral IAP repeat-containing protein 6-like (4519 AA)	LOC103519067[1] baculoviral IAP repeat-containing protein 6-like, partial (286 AA)	

Table A.7 Continued.

D. melanogaster **(conserved domains, protein length in AA)**	***A. pisum*** **(protein length in AA)**	***B. tabaci*** **(protein length in AA)**	***D. citri*** **(protein length in AA)**	***B. cockerelli*** **(most similar protein, conserved domains, E-value, protein length in AA)**
			LOC103511215[2] uncharacterized protein LOC103511215 (257 AA)	
			LOC113468273[2] uncharacterized protein LOC113468273 (359 AA)	
			LOC103511214[2] baculoviral IAP repeat-containing protein 6-like (432 AA)	
			LOC113468270[2] baculoviral IAP repeat-containing protein 6-like (316 AA)	
			LOC103520833[3] baculoviral IAP repeat-containing protein 6-like, partial (181 AA)	
			LOC103520832[3] baculoviral IAP repeat-containing protein 6-like (550 AA)	

Table A.7 Continued.

D. melanogaster **(conserved domains, protein length in AA)**	***A. pisum*** **(protein length in AA)**	***B. tabaci*** **(protein length in AA)**	***D. citri*** **(protein length in AA)**	***B. cockerelli*** **(most similar protein, conserved domains, E-value, protein length in AA)**
			LOC103506354[4] baculoviral IAP repeat-containing protein 6 (260 AA)	
			LOC103506343[4] baculoviral IAP repeat-containing protein 6-like (113 AA)	
AAC11 (1 API5 domain, 536 AA)	LOC100159875 apoptosis inhibitor 5 (524 AA)	LOC109036946 apoptosis inhibitor 5 (543 AA)	LOC103505580 apoptosis inhibitor 5-like (393 AA)	Bc-IAP5 (*D. citri* apoptosis inhibitor 5-like, 1 API5 domain, e-172, 539 AA)
			LOC103505581 apoptosis inhibitor 5 homolog (120 AA)	
			LOC103520736 apoptosis inhibitor 5 (452 AA)	
Uncharacterized protein Dmel_CG30108 (UPF0203, 88 AA)		LOC109038919 TP53-regulated inhibitor of apoptosis 1-like (79 AA)	LOC103505407 TP53-regulated inhibitor of apoptosis 1-like (102 AA)	Bc-TRIAP1 (*D. citri* TP53-regulated inhibitor of apoptosis 1-like, 3e-045, 1 UPF0203 domain, 102 AA)
Uncharacterized protein Dmel_CG30109 (UPF0203, 88 AA)				

* Not verified by sequencing. [1,2,3,4] Loci number with similar superscript are located in the same contig.

Table A.8 The qPCR and RNAi primers used in this study.

Gene Code	qPCR primers (5'-3')
IAP1	F: AACAAGTACAGCGGTGACGA
	R: TTTACACAGGCGACCATCAG
IAP2	F: AGCAGAACACAGGAGGCAAA
	R: TGATTAGGCAGTCCACCATTC
IAPP5	F: AAAAGGGTTCTTGCACACCA
	R: CAGAATATGCACTTGGCACA
IAPP5.2	F: GACCTACTCACGCCGTATCTG
	R: CTTCAGCCTGTTCCGATAGAA
Caspase1	F: CAAGGAGATGGTCTGGATGG
	R: ATGAGGAAGTCAGCGTGGAG
Caspase2	F: ATGTCCCCAGCAATGGTATC
	R: CACAGGGTGTTGACTTCTTCA
Caspase3	F: AAGCTGGATGGTGGAGTACG
	R: CAGCATAGGAGGGGATCTTG
RNAi	**PCR primers (5'-3')**
dsIAPP5.2	F*: *TAATACGACTCACTATAGGGAGA*GCTTCTATTCCATTTCCAAG
	R*: *TAATACGACTCACTATAGGGAGA*CGCTTCCTCTTTCTTTCTTT

*The italic sequences are T7 promoter sequences.

Table A.9 Primers for bioinformatics validation and gene expression analyses by qPCR of autophagy-related genes.

Gene Code	Validation Primers (5'-3')	qPCR primers (5'-3')
BcATG1	F: AACTCTCCCCTCACCCTCAT	F: CGACCCACAACAACAACAAC
	R: GTCTACATGGCGGAGGTGTT	R: ATTTAGCCAGCGTTTCACAG
BcATG2A-1	F: GGCACTTTGTCCTGGTCTTC	F: CTTTCCGTTTTCCGACAGTT
	R: CGAAGTCTGCCTTCTCCATC	R: GGTCAAGGGTCAGTTTCTCC
BcATG2A-2	F: TAAAACACCACCGGAGGAAG	F: CAAGGACAGTGAAGGAGCAG
	R: GCTCACGCTAGGAATCGAAC	R: TACCTGGACACGGAGAACAC
BcATG2A-3	F: TTCCAGAGGCTTTCGTTGTT	F: TTAGATGAGCGCGACAACAC
	R: GGATGGGAAACCTCAGTTTG	R: CTCCACCAGACACTCCAACA
BcATG2B	F: CGGCGAGTACATTCACGAT	F: GTGATACCGGGAGACAAGGA
	R: CCTCCTCTTCTTCCTCAGA	R: GTAGATATGCGGTGGGCAGT
BcATG3	F: AGTTTGTGGCAGCAGGAGAT	F: CTCAAGACGCTGCAAACAAA
	R: AAAGCGGTTTAGAACCGAAA	R: GTGTCAACCCAACCCTCATC
BcATG4	F: TTAGCCCTTTGGTATTGTGA	F: TCCAAGACATCAACCCTGTG
	R: GCGAAGAGGCTGTAAGTATC	R: GCTTTCCCCCTATCACTCCT
BcATG5	F: CACCGAGAGATCACACGAAA	F: ATGTGACCGACCATCAGCTT
	R: GGTGTTGGAGTTGCCTTCAT	R: TCCACAGCTTCTCTGCTAGGAC
BcATG6	F: CACTACCCCACACTCAATAACA	F: ATTCACCATCTCCTCTCCA
	R: CATCTGGAAGAGGAAAGCAT	R: TGACTCTCTGCTTCTACACTGA
BcATG7	F: CGGTTCTTTCACCAGCTCTC	F: ATGACGGGGACACAAAGTTC
	R: GAGACTGACGAGCAGGGTTC	R: GATCCATAGACTCCCGCAAG
BcATG8	F: ATCAACGTTAAGAGCTCAAG	F: GTTGAAAAAGCCCCCAAAG
	R: CAGGGTCCAGGGTAGAAAGA	R: GCGGATGAGGAAATAGAACTG
BcATG9	F: TCCTCAGGAAGGAGGAGTGA	F: GACAAGCACACACATCCAGAG
	R: AGGAGGACTTGGGAGCTAGG	R: GAGTTACAAGTGGCGAGCATAA

Table A.9 Continued.

Gene Code	Validation Primers (5'-3')	qPCR primers (5'-3')
BcATG10	F: CTACATGAAACCCCATAAGA	F: CACCCCTATCTGAGGAAACC
	R: TCTCTGCCTCTTAACCCATA	R: CTTGACCCTTGTTGGTAACG
BcATG12	F: GTACCGATTGACTTGCATTC	F: TTTGCACCTTCTCCTGACAC
	R: ATCCACTTCCTCCATGATTG	R: CCATGCTTGTGTTTTGCAGT
BcATG13	F: TATTGTGCGTCCCATGTGTT	F: GGATGGCTTCAACAAGGTTC
	R: GATGGTCAGGTCCGTTCTGT	R: GATGGTCAGGTCCGTTCTGT
BcATG14	F: AACAGCTTCGAGCTAAGCAAA	F: TAAATTCAGCAAGCGTGTGG
	R: GCTCTCCTCCTCCTCATCCT	R: ATGCAAAGGCAGGTCAGTGT
BcATG16	F: TGGATGTGTAGAGGCAGGAA	F: GCTGTGATAGAACCCCCAAG
	R: AGCAAGACTGCTGGAGAAGG	R: CGTCGTATGTCACCAGATCG
BcATG17	F:	F: CAGAAGGCACTGATACGGAAG
	R:	R: AATGTTCGTCCTCACGGTCT
BcATG18-1	F: TGTCTTCATCTAGTTCTCCAG	F: GTCGGTCCACATTTTCTTCA
	R: CCAGTGTATCTGTGAGTGGTT	R: TCAGGAGGCAGTGTAAAGTTG
BcATG18-2	F: TTTCAAGTGCTGCTGTAGAT	F: GCATAGGTTGGATGGTCGTAA
	R: AGGCGAGATGTTTGTTGCTT	R: TCGGAAGTTTTGAGAGAGCA
BcATG18-3	F: CACAAGTCTGAAAGTGGAAAGC	F: CTAGGCCATGTGGAAATGCT
	R: GGGAATGCGAGGAGAGAGT	R: TGTTGGGGTACTTTGGGTGT
BcATG18-4	F: ACCTTTGCCTTCTAAATGAG	F: CAAGCAACATGAGCAAAGGA
	R: TGTCTCTTCTCAATCTTACAGC	R: GCCATTATCCATGCAACAAG
BcATG101	F: GGTCACCAAATCGACGAAGT	F: CTCAAGCCTCTTTCACACGA
	R: TAGTTGATGGGGTCGTAGGC	R: AGGGTGCCAACGGAGTATTT

Table A.10 Comparison of autophagy-related genes in *D. melanogaster*, *A. pisum*, *B. tabaci*, *D. citri*, and *B. cockerelli*.

D. melanogaster **(conserved domains, protein length in AA)**	***A. pisum*** **(protein length in AA)**	***B. tabaci*** **(protein length in AA)**	***D. citri*** **(protein length in AA)**	***B. cockerelli*** **(most similar protein, E-value, protein length in AA)**
Autophagy-related 1 (Atg1) (855 AA)	LOC100159542 serine/threonine-protein kinase unc-51 (663 AA)	LOC109038743 serine/threonine-protein kinase ULK2 (664 AA)	LOC103514260 serine/threonine-protein kinase ULK1 (567 AA)	serine/threonine-protein kinase ULK2-like isoform 1 (2.72112E-39, 226 AA)
Autophagy-related 2 (Atg2) (1906 AA)	LOC100169298 autophagy-related protein 2 homolog B (1983 AA)	LOC109044529 autophagy-related protein 2 homolog B isoform X1 (1993 AA) / LOC109044529 autophagy-related protein 2 homolog B isoform X2 (1964 AA)	LOC103519534 autophagy-related protein 2 homolog B (340 AA)	autophagy-related protein 2 homolog A-like (9.975E-115, 443 AA)
			LOC113465363 autophagy-related protein 2 homolog A-like (361 AA)	autophagy-related protein 2 homolog A (1.2937E-110, 1025 AA)
			LOC103509283 autophagy-related protein 2 homolog A-like (137 AA)	Autophagy-related protein 2-like protein A (8.18151E-39, 192 AA)
			LOC113471576 autophagy-related protein 2 homolog B-like (95 AA)	Autophagy-related protein 2-like protein B (4.6835E-28, 158 AA)
Autophagy-related 3 (Atg3) (330 AA)	LOC100168321 autophagy related protein Aut1-like (339 AA)	LOC109031323 ubiquitin-like-conjugating enzyme ATG3 (316 AA)	LOC103517262 ubiquitin-like-conjugating enzyme ATG3 (140 AA)	autophagy related protein Atg3-like protein (4.03526E-132, 326 AA)
	LOC100159720 ubiquitin-like-conjugating enzyme ATG3 (335 AA)		LOC113470558 ubiquitin-like-conjugating enzyme ATG3 (119 AA)	
			LOC103517272 ubiquitin-like-conjugating enzyme ATG3 (89 AA)	

Table A.10 Continued.

D. melanogaster **(conserved domains, protein length in AA)**	***A. pisum*** **(protein length in AA)**	***B. tabaci*** **(protein length in AA)**	***D. citri*** **(protein length in AA)**	***B. cockerelli*** **(most similar protein, E-value, protein length in AA)**
Autophagy-related 4a (Atg4a) (410 AA)		LOC109042782 cysteine protease ATG4A (396 AA)	LOC103520402 cysteine protease ATG4A-like (170 AA)	
			LOC103520210 cysteine protease ATG4A-like (117 AA)	
Autophagy-related 4b (Atg4b) (668 AA)	LOC100160112 cysteine protease ATG4B (402 AA)		LOC103520393 cysteine protease ATG4B-like (124 AA)	cysteine protease ATG4B-like isoform 1 (3.00685E-158, 395 AA)
	LOC100571688 cysteine protease ATG4B (252 AA)			
Autophagy-related 5 (Atg5) (269 AA)	Autophagy-specific gene 5 (266 AA)	LOC109038543 autophagy protein 5 isoform X1 (289 AA)/ LOC109038543 autophagy protein 5 isoform X2 (252 AA)	LOC103512211 autophagy protein 5 (270 AA)	Autophagy protein 5 (1.11789E-124, 267 A)
Autophagy-related 6 (Atg6) (422 AA)	LOC100162879 beclin-1-like protein (420 AA)	LOC109036018 beclin-1-like protein (429 AA)	LOC103511670 beclin-1-like protein (497 AA)	Beclin-1-like protein (1.26527E-75, 519 AA)
Autophagy-related 7 (Atg7) (510 AA)	LOC100168214 ubiquitin-like modifier-activating enzyme ATG7 (680 AA)	LOC109037754 ubiquitin-like modifier-activating enzyme ATG7 (654 AA)	LOC103514245 ubiquitin-like modifier-activating enzyme ATG7 (626 AA)	Ubiquitin-like modifier-activating enzyme ATG7 (1.55145E-145, 536 AA)
Autophagy-related 8a (Atg8a) (121 AA)	LOC100163628 gamma-aminobutyric acid receptor-associated protein-like (118 AA)	LOC109035081 gamma-aminobutyric acid receptor-associated protein (120 AA)	LOC103508318 gamma-aminobutyric acid receptor-associated protein isoform X3 (120 AA)	gamma-aminobutyric acid receptor-associated protein (3E-114, 119 AA)

Table A.10 Continued.

D. melanogaster **(conserved domains, protein length in AA)**	***A. pisum*** **(protein length in AA)**	***B. tabaci*** **(protein length in AA)**	***D. citri*** **(protein length in AA)**	***B. cockerelli*** **(most similar protein, E-value, protein length in AA)**
Autophagy-related 8b (Atg8b) (120 AA)			LOC103521693 gamma-aminobutyric acid receptor-associated protein-like (109 AA)	
Autophagy-related 9 (Atg9) (845 AA)	LOC100159271 autophagy-related protein 9A (712 AA)	LOC109034026 autophagy-related protein 9A (730 AA)	LOC103522855 autophagy-related protein 9A (606 AA)	Autophagy-related protein 9A (6.45637E-174, 717 AA)
	LOC100167077 autophagy-related protein 9A (615 AA)			
Autophagy-related 10 (Atg10) (172 AA)	LOC100575896 ubiquitin-like-conjugating enzyme ATG10 (165 AA)	LOC109040219 ubiquitin-like-conjugating enzyme ATG10 (203 AA)	LOC103523617 ubiquitin-like-conjugating enzyme ATG10 (206 AA)	ubiquitin-like-conjugating enzyme ATG10 (4E-53, 222 AA)
Autophagy-related 12 (Atg12) (111 AA)	LOC100159402 ubiquitin-like protein ATG12 (107 AA)	LOC109033666 autophagy protein 12-like (118 AA)		autophagy protein 12-like (5E-38, 113 AA)
Autophagy-related 13 (Atg13) (523 AA)	LOC100573619 autophagy-related protein 13 homolog isoform X3 (472 AA) / LOC100573619 autophagy-related protein 13 homolog isoform X1 (517 AA) / LOC100573619 autophagy-related protein 13 homolog isoform X2 (514 AA)	LOC109038021 autophagy-related protein 13 homolog isoform X1 (420 AA) / LOC109038021 autophagy-related protein 13 homolog isoform X2 (417 AA)	LOC103506104 autophagy-related protein 13-like (219 AA)	autophagy-related protein 13 homolog (3.03445E-79, 298 AA)

Table A.10 Continued.

D. melanogaster **(conserved domains, protein length in AA)**	***A. pisum*** **(protein length in AA)**	***B. tabaci*** **(protein length in AA)**	***D. citri*** **(protein length in AA)**	***B. cockerelli*** **(most similar protein, E-value, protein length in AA)**
			LOC103515171 autophagy-related protein 13 homolog (292 AA)	
Autophagy-related 14 (Atg14) (503 AA)	LOC100164156 beclin 1-associated autophagy-related key regulator isoform X2 (483 AA) / LOC100164156 beclin 1-associated autophagy-related key regulator isoform X1 (487 AA)	LOC109042483 beclin 1-associated autophagy-related key regulator isoform X1 (477 AA) / LOC109042483 beclin 1-associated autophagy-related key regulator isoform X2 (476 AA)		beclin 1-associated autophagy-related key regulator-like (1.86016E-81, 416AA)
Autophagy-related 16 (Atg16) (612 AA)	LOC100167285 autophagy-related protein 16-1 (541 AA)	LOC109034579 autophagy-related protein 16-1 (549 AA)	LOC103513712 autophagy-related protein 16-1-like isoform X2 (344 AA) / LOC103513712 autophagy-related protein 16-1-like isoform X1 (425 AA)	Autophagy-related protein 16-1-like (0.0, 550 AA)
Autophagy-related 17 (Atg17) (1357 AA)	LOC100573296 RB1-inducible coiled-coil protein 1 isoform X1 (1039 AA) / LOC100573296 RB1-inducible coiled-coil protein 1 isoform X2 (1037 AA)	LOC109034605 RB1-inducible coiled-coil protein 1 isoform X2 (1113 AA) / LOC109034605 RB1-inducible coiled-coil protein 1 isoform X1 (1114 AA)	LOC103507010 RB1-inducible coiled-coil protein 1-like (441 AA)	RB1-inducible coiled-coil protein 1-like (0.0, 1033 AA) *
			LOC103520418 RB1-inducible coiled-coil protein 1-like (462 AA)	

Table A.10 Continued.

D. melanogaster **(conserved domains, protein length in AA)**	***A. pisum*** **(protein length in AA)**	***B. tabaci*** **(protein length in AA)**	***D. citri*** **(protein length in AA)**	***B. cockerelli*** **(most similar protein, E-value, protein length in AA)**
			LOC103515171 autophagy-related protein 13 homolog (292 AA)	
Autophagy-related 14 (Atg14) (503 AA)	LOC100164156 beclin 1-associated autophagy-related key regulator isoform X2 (483 AA) / LOC100164156 beclin 1-associated autophagy-related key regulator isoform X1 (487 AA)	LOC109042483 beclin 1-associated autophagy-related key regulator isoform X1 (477 AA) / LOC109042483 beclin 1-associated autophagy-related key regulator isoform X2 (476 AA)		beclin 1-associated autophagy-related key regulator-like (1.86016E-81, 416AA)
Autophagy-related 16 (Atg16) (612 AA)	LOC100167285 autophagy-related protein 16-1 (541 AA)	LOC109034579 autophagy-related protein 16-1 (549 AA)	LOC103513712 autophagy-related protein 16-1-like isoform X2 (344 AA) / LOC103513712 autophagy-related protein 16-1-like isoform X1 (425 AA)	Autophagy-related protein 16-1-like (0.0, 550 AA)
Autophagy-related 17 (Atg17) (1357 AA)	LOC100573296 RB1-inducible coiled-coil protein 1 isoform X1 (1039 AA) / LOC100573296 RB1-inducible coiled-coil protein 1 isoform X2 (1037 AA)	LOC109034605 RB1-inducible coiled-coil protein 1 isoform X2 (1113 AA) / LOC109034605 RB1-inducible coiled-coil protein 1 isoform X1 (1114 AA)	LOC103507010 RB1-inducible coiled-coil protein 1-like (441 AA)	RB1-inducible coiled-coil protein 1-like (0.0, 1033 AA) *
			LOC103520418 RB1-inducible coiled-coil protein 1-like (462 AA)	

Table A.10 Continued.

D. melanogaster **(conserved domains, protein length in AA)**	***A. pisum*** **(protein length in AA)**	***B. tabaci*** **(protein length in AA)**	***D. citri*** **(protein length in AA)**	***B. cockerelli*** **(most similar protein, E-value, protein length in AA)**
Autophagy-related 18b (Atg18b) (471 AA)	LOC100165258 WD repeat domain phosphoinositide-interacting protein 2 isoform X3 (463 AA) / LOC100165258 WD repeat domain phosphoinositide-interacting protein 2 isoform X5 (422 AA) / LOC100165258 WD repeat domain phosphoinositide-interacting protein 2 isoform X4 (445 AA) / LOC100165258 WD repeat domain phosphoinositide-interacting protein 2 isoform X2 (464 AA)	LOC109043586 WD repeat domain phosphoinositide-interacting protein 2 isoform X2 (425 AA) / LOC109043586 WD repeat domain phosphoinositide-interacting protein 2 isoform X1 (446 AA)		WD repeat domain phosphoinositide-interacting protein 2-like (0, 465 AA)
Autophagy-related 101 (Atg101) (218 AA)	LOC100164875 autophagy-related protein 101 isoform X3 (219 AA)	LOC109034734 autophagy-related protein 101 isoform X2 (218 AA) / LOC109034734 autophagy-related protein 101 isoform X1 (232 AA)	LOC103509748 autophagy-related protein 101 (244 AA)	autophagy-related protein 101-like isoform 1 (5.64157E-82, 244 AA)
			LOC103509752 autophagy-related protein 101 (211 AA)	

* Not verified by sequencing.